LBL-424
Preprint c.1

LIGHT SCATTERING FROM LIQUIDS AND LIQUID CRYSTALS

Hal J. Rosen
(Ph. D. Thesis)

November 1971

AEC Contract No. W-7405-eng-48

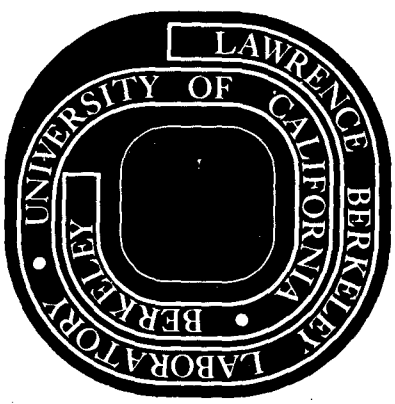

LBL-424
c.1

DISCLAIMER

LIGHT SCATTERING FROM LIQUIDS AND LIQUID CRYSTALS

Contents

LIGHT SCATTERING FROM LIQUIDS AND LIQUID CRYSTALS

Hal J. Rosen

Department of Physics, University of California
and
Inorganic Materials Research Division
Lawrence Berkeley Laboratory
Berkeley, California 94720

ABSTRACT

In this thesis three separate investigations using the light scattering technique will be presented. In Section II results of Raman measurements on I_2 complexes in various solutions are reported. Emphasis is on the variation of the Raman spectrum of I_2 in mixtures of n-hexane and benzene or methylated benzenes. Our results indicate that each I_2 molecule can probably interact with more than one donor and the effect of inert molecules in the solution should be taken into account. In Section III we present a Raman study of the phase transitions of the nematic liquid crystal, Para-Azoxydianisole. The intensities of several Raman modes were shown to change abruptly at the phase transitions, but no detectable frequency shift of any mode was observed. Our results suggest that the Raman spectrum of Para-Azoxydianisole is only affected by short range ordering. Qualitative interpretation of the results is given. Finally, in Section IV, we present our Brillouin scattering measurements of the

propagation of hypersonic waves in a cholesteric medium at the liquid-to-liquid-crystal transition. Contrary to the results obtained by others, we have found no anomalous change in either the velocity or the attenuation of the hypersonic waves at the transition.

I. INTRODUCTION

Light scattering is a spectroscopic technique for investigating low frequency excitations. Although this technique has been known for almost 60 years most of the work in this field has been done since 1961 when the laser was invented. Such diverse excitations as: rotational, vibrational and electronic energy levels, phonons (acoustic and optic), entropy and pressure fluctuations, magnons, plasmons, polaritons and rotons have been studied. These excitations range in frequency from a few Hertz to 10^{14} Hertz.

It is instructive to make a comparison between the light scattering technique and the infra-red absorption technique. First consider an absorption process. One can cause transitions between two energy levels a and b by shining in radiation whose frequency matches the energy spacing, Ω. The cross-section for this process is calculated from first order perturbation theory and is typically 10^{-21} cm^2. In a light scattering experiment one causes transitions by a second order or Raman process. For such a process a photon of frequency ω is absorbed and a scattered photon of frequency $\omega-\Omega$ is emitted with the material system making a transition from a to b. By detecting the scattered radiation one can determine the energy spacing Ω of the two levels of the system. Of course, the cross-section for this second order process is much smaller than the absorption cross-section and is typically 10^{-30} cm^2. However, with a laser source one can easily detect such modes. The light scattering technique has a major advantage over the infra-red absorption technique in that one does not have to match the frequency of the source to the energy spacing. In principle, one can measure any low frequency

excitation with a single frequency source. Actually the two techniques are complementary in the sense that the two processes have complementary selection rules. Some modes can be detected via Raman processes (tensor selection rules) while others are only infra-red active (vector selection rules).

In this thesis I will report on three separate investigations using the light scattering technique. In the first investigation the interaction between iodine and benzene (methytated benzenes) was studied by carefully monitoring the vibrational frequency of I_2 as the benzene (methylated benzene) concentration was changed. The results of this investigation are presented in Sec. II. In Sec. III a Raman study of the nematic liquid crystal Para-Azoxydianisole at its phase transitions is presented. Finally, in Sec. IV an investigation of the propagation of sound at the liquid crystal-liquid phase transition using the Brillouin scattering technique will be presented.

SECTION II

RAMAN STUDY OF IODINE COMPLEXES IN SOLUTIONS*

1. Introduction

For the past two decades, the subject of charge-transfer interaction between molecules has attracted much attention. In particular, charge-transfer complexes of iodine have been investigated by many research workers.[1] Among the many properties of charge-transfer complexes, the uv absorptivity has been investigated most thoroughly. Results are often analyzed using the Benesi-Hildebrand equation.[2] They are generally in qualitative agreement with the charge-transfer theory proposed by Mulliken.[3] However, for weak complexes, the results often show anomalous behavior.[4] For example, since the charge-transfer interaction between I_2 and methylated benzenes increases with methylation, one would expect the uv extinction coefficient of the complex also to increase with methylation, but the opposite was found.[5]

In order to explain the anomalies, various authors have modified the Benesi-Hildebrand theory[2] in a variety of ways.[6-10] In particular, Orgel and Mulliken[10] pointed out that there is no á priori reason to assume the existence of only 1:1 stable complexes in solution. The observed properties of complexes in solution should be statistical averages over all attainable complex configurations in thermal equilibrium.[10] This is particularly true for weak I_2 complexes in which the charge-transfer interaction is of fairly long range.[11]

There has also been criticism on the uv absorption measurements. The measurements were usually carried out at a single frequency in the charge-transfer band, ignoring the possible shift and change of profile

*To be published in J. Molecular Physics

of the absorption band. As Mulliken and Person[12] pointed out, the extinction coefficient which goes into any theory of complexes should be the one integrated over the entire charge-transfer band. Unfortunately, there are technical difficulties in making absorption measurements over the whole band to a good degree of accuracy. It is therefore important to perform measurements on other properties of complexes to offer an independent test of the theories. Infrared and Raman studies serve this purpose.

There have been several reports of infrared[13] and Raman[14,15] experiments on charge-transfer complexes. Raman measurements on I_2 complexes,[14] however, have been limited to the case of I_2 in pure donor solution. No systematic investigation of the changes in the Raman spectrum of I_2 complexes as a function of donor concentration has been reported yet.

In this paper,[16] we would like to report our recent experimental studies on I_2 complexes in solution with modern Raman spectroscopic technique. Emphasis is on the change of the Raman spectrum of I_2 due to charge-transfer interaction between I_2 and various donors. The results indicate that I_2 can simultaneously interact with more than one donor. In Section II, a brief theoretical discussion on the average properties of complexes in solution is given. Then in Section III, we describe the experimental setup and procedure briefly. Finally, in Section IV, the experimental results are presented and interpreted.

II. Theoretical Discussion

Properties of a molecule are generally affected by molecular interaction with its surrounding molecules. For complexes in solution, the observed properties of the complexes should correspond to statistical averages over all possible complex configurations, as suggested by Orgel and Mulliken.[10] Consider a solution of complexes, with a small amount of acceptors dissolved in a mixture of donors and inert solvent molecules. The concentration of acceptors is so low that the interaction between acceptors can be neglected. Therefore, the properties of an acceptor in the solution are affected only by its interactions with the neighboring donors and inert molecules. We shall not make any prejudgment on what types of interactions they are, although it is believed that the interaction between acceptors and donors is mainly due to charge-transfer interaction. Let $\rho(\underset{\sim}{R})$ be the statistical distribution function for a particular configuration (denoted by $\underset{\sim}{R}$) of donors and inert molecules around the acceptor. Then, for a certain property X of the acceptors, such as the uv absorption coefficient, Raman scattering cross-section, etc., the corresponding observed quantity is given by

$$\langle X \rangle = \int_{V_o} X(\underset{\sim}{R})\rho(\underset{\sim}{R})\, d\underset{\sim}{R}. \qquad (1)$$

where the volume of integration V_o is chosen large enough to include all molecules interacting with the acceptor. The expression for $\rho(\underset{\sim}{R})$ can be obtained from simple statistical mechanics.

If we allow an acceptor to interact simultaneously with several surrounding molecules, then we can show from statistical treatment (see Appendix I for details) that Eq. (1) takes the form

$$\langle X \rangle = \frac{a_o + a_1\rho_B + a_2\rho_B^2 + \cdots}{1 + b_1\rho_B + b_2\rho_B^2 + \cdots} \qquad (2)$$

where ρ_B is the donor concentration in the solution, and a_n and b_n are constant coefficients.

In experimental investigation, it is more interesting to compare the observed property of acceptors at finite donor concentrations with the same property at zero donor concentration (corresponding to pure inert solvent). Therefore, the quantity of interest is

$$\langle \Delta X \rangle \equiv \langle X \rangle - \langle X \rangle_{\rho_B=0}. \tag{3}$$

From Eq. (2), we obtain

$$\langle \Delta X \rangle = \frac{c_1\rho_B+c_2\rho_B^2+\ldots}{1+b_1\rho_B+b_2\rho_B^2+\ldots}. \tag{4}$$

where c_n and b_n are constant coefficients.

When only the linear terms are kept in both the numerator and the denominator, the above equation reduces to the well-known Benesi-Hildebrand equation,[2]

$$1/\langle \Delta X \rangle = (1/\Delta X_o)(1+1/K\rho_B). \tag{5}$$

where ΔX_o and K are constants depending on the properties of the complexes. In the Benesi-Hildebrand model, K represents the equilibrium constant, but this is not true here as is seen from the derivation of Eq. (5).

If the terms quadratic in ρ_B are also kept, then the equation has the form derived by Deranleau.[9]

We now consider the case of Raman scattering from complexes in solution. Because of interaction between donors and acceptors (mainly due to charge-transfer interaction), Raman scattering from a vibrational mode of the acceptor is changed through changes of energies and wave functions of the eigenstates of the acceptor. The scattering cross-section could either increase or decrease, but if the newly created, strong charge-transfer band happens to be near the frequency of the exciting field, it is likely to have a noticeable enhancement.[18] With X replaced by $(d\sigma/d\Omega)$ in the above equations, we then have the functional dependence of the observed differential scattering cross-section $(d\sigma/d\Omega)$ on the donor concentration ρ_B.

Interaction between donors and acceptors also loosens up the interatomic bonding in an acceptor. As a result, the vibrational frequencies of the acceptor usually shift to lower values.[19,20] For complexes in solution, the observed spectral distribution for a Raman mode is given by

$$S(\omega) = \int_{V_o} g(\omega-\omega_v(\underset{\sim}{R}))\ (d\sigma(\underset{\sim}{R})/d\Omega)\ \rho(\underset{\sim}{R})\ d\underset{\sim}{R} \qquad (6)$$

where $g(\omega-\omega_v)$ is the lineshape function. Normally, the distribution of donors and inert molecules has a few most favorable configurations $\underset{\sim}{R}_1$, $\underset{\sim}{R}_2$, etc. If the corresponding $\omega_v(\underset{\sim}{R}_1)$, $\omega_v(\underset{\sim}{R}_2)$, etc. are separated by more than a linewidth, then several distinct peaks would be observed for the same mode in the spectrum. This happens, for example, in the

case of strong 1:1 complexes in solution. There, two well-separated Raman lines could be observed for an acceptor mode, one for complexed and one for uncomplexed acceptor molecules.

We can also measure the mean vibrational frequency defined as

$$\langle \omega_v \rangle = \int_{-\infty}^{\infty} S(\omega)\omega\, d\omega / \int_{-\infty}^{\infty} S(\omega)d\omega. \tag{7}$$

From Eq. (6), we can readily find

$$\langle \omega_v \rangle = \int_{V_o} \omega_v(\underset{\sim}{R})(d\sigma(\underset{\sim}{R})/d\Omega)\, \rho(\underset{\sim}{R})d\underset{\sim}{R} / \int_{V_o} (d\sigma(\underset{\sim}{R})/d\Omega)\, \rho(\underset{\sim}{R})d\underset{\sim}{R} \tag{8}$$

which can also be expressed in the form of Eq. (2). The mean vibrational frequency shift is then given by

$$\langle \Delta\omega_v \rangle \equiv \langle \omega_v \rangle - \langle \omega_v \rangle_{\rho_B=0} = \frac{c_1\rho_B + c_2\rho_B^2 + \ldots}{1 + b_1\rho_B + b_2\rho_B^2 + \ldots}. \tag{9}$$

where b_n and c_n are constants. Again, in special cases, the above equation reduces to the simple form of the Benesi-Hildebrand equation, Eq. (5), although the physical meanings of the coefficients would be different.

We shall apply these results to the case of Raman scattering from I_2 complexes in solution in Section IV.

III. Experimental Arrangement

The construction of the Raman spectrometer was the same as that of Landon and Porto.[21] The output of a He-Ne laser (Spectra Physics Model 125), after passing through an interference filter, was focused on the sample with a microscope objective. Scattered radiation from the sample in a direction perpendicular to the incoming beam was collected with a projector lens and focused on the entrance slit of a double monochromator. (Spex Model 1400) For detection, the photon counting technique was adopted. (See Appendix II for details). A photomultiplier (EMI 9558 QA), cooled to -70°C with dry nitrogen, was used to detect single photons in the form of current pulses. These pulses were then amplified, shaped, and finally registered on a multichannel analyzer.

This setup proved to be both convenient and sensitive. Excellent Raman spectra of I_2 in solutions were obtained with little effort. For example, with a scan speed of 1.Å/min and a slit width of 4 cm^{-1} on the monochromator, the fundamental Raman line of I_2 in a 0.06 molar solution appeared with a signal-to-noise ratio greater than 50. A typical spectrum is shown in Fig. 1. Iodine absorbs rather strongly at the laser frequency (6328 Å). To avoid heating effects, it is necessary not to focus the laser beam too strongly into the I_2 solution. One must also properly choose the concentration of I_2 and the distance the scattered radiation travels through the solution in order to optimize the signal-to-noise ratio. In our experiments, the I_2 concentration was usually taken to be 0.06 M, and the laser was focused at approximately 1 mm away from the cell window through which the scattered radiation was collected. For frequency calibration, spectral lines from a Ne lamp were used.

A major difficulty in our Raman studies on I_2 complexes is that the Raman lines of I_2 sometimes overlap with Raman lines of the solvent molecules. Decomposition of the lines introduces error and makes the experimental data much less accurate. For examples, the I_2 fundamental overlaps slightly with a toluene line at 214 cm^{-1}, and the first overtone of I_2 overlaps with a weak benzene line at 404 cm^{-1}. In principle, the above difficulty can be avoided by measurements at two different I_2 concentrations so that the part due to solvent molecules in the observed spectrum can be subtracted out. No such correction procedure was made in our experiments.

The chemicals used were all of the Reagent grade. High purity of the solvents is not important here, since the effect of impurities on iodine should be small. We saw no observable effects from the small quantities of impurities in our experiments. Solutions were prepared the same day they were measured. Errors in the concentrations of solutions were estimated to be ± 2%. Unless specified, all measurements were made at 25°C.

IV. Experimental Results and Discussion

A. Raman Spectra of I_2 in Various Solvents

In an iodine solution, interaction of I_2 with solvent molecules always leads to a shift in the frequency of the I_2 stretching vibration. We can usually divide the intermolecular interaction into two types: the long-range van der Waals interaction[22] and the short-range chemical interaction.[23] In the case of I_2 complexes, the chemical interaction is presumably dominated by the charge-transfer interaction. In many cases, it is important to separate the effect of the charge-transfer interaction from that of the van der Waals interaction.

In order to estimate the effect of van der Waals interaction, we have measured the Raman spectra of I_2 dissolved in various solvents. While a true microscopic theory for the vibrational frequency shifts due to van der Waals interaction is not available, it is generally assumed, from Onsager's reaction field model, that the frequency shift $\Delta\omega_V$ for a solute molecule is a function of n^2 where n is the refractive index of the solvent.[24] For a narrow range of n^2, we would then expect that $\Delta\omega_V(n^2)$ can be approximated by a straight line. The results of our Raman measurements on the fundamental vibration of I_2 in various solvents are given in Table I. Here, the mean vibrational frequency $\langle\omega_V\rangle$ is defined as the center of gravity of the Raman line with respect to the exciting laser frequency. Our measurements on this mean frequency could be as accurate as $\pm$ .1 cm^{-1}. In Fig. 2, the mean frequency shifts, defined as $\langle\Delta\omega_V^o\rangle \equiv \omega_{Vo} - \langle\omega_V\rangle$ where ω_{Vo}=213.3 cm^{-1} is the vibrational frequency of I_2 in the vapor phase,[25] are plotted against $(n^2 - 1)$.[26] From uv absorption measurements, we know that I_2 has essentially no charge-transfer interaction with n-hexane, n-heptane, and CCl_4.[27] Figure 2 shows that the frequency shifts for I_2 in these three solvents are small, and the three respective points indeed fall on a straight line. The frequency shifts in the other solvents are partly due to charge-transfer interaction, and Fig. 2 indicates that the charge-transfer interaction between I_2 and solvent molecules increases in the following order: chloroform, cyclohexane, nitrobenzene, chlorobenzene, bromobenzene, benzene, toluene, m-xylene, and mesitylene. This result on the relative strengths of the charge-transfer interaction between I_2 and different donors is consistent with the uv measurements.[5,27]

B. Raman Spectra of I_2 in Mixtures of n-hexane and Benzene or Methylated Benzenes

For a better understanding of charge-transfer complexes in solution, we have made a systematic investigation of the Raman spectrum of I_2 in mixtures of n-hexane and benzene or methylated benzenes. In pure n-hexane, the I_2 Raman line has a mean vibrational frequency of 210.1 cm^{-1}, and an apparent full width at half maximum of 6.0 cm^{-1}. (The corresponding true full width is 5.1 cm^{-1}, obtained from deconvolution of the line with the slit function.) With increasing benzene concentration in the mixture, the line gradually shifts to lower frequencies (see Fig. 3) with little change in the line profile, and finally reaches a mean frequency of 204.6 cm^{-1} in pure benzene. This shift is primarily due to charge-transfer interaction between I_2 and benzene, since we recall that there is no charge-transfer interaction between I_2 and n-hexane and that the van der Waals shifts estimated for I_2 in pure n-hexane and in pure benzene differ only by 0.4 cm^{-1} as seen from Fig. 2.[28]

This observation cannot be explained by the model of I_2 and benzene forming 1:1 complexes[2] (allowing each I_2 to interact with only one donor). Such a model would predict two discrete Raman lines of I_2 in the mixed solution, one for I_2 unassociated with benzene, and the other for I_2 complexed with benzene. As the benzene concentration increases, the frequencies of the two lines would remain unchanged, but their relative intensity would change. Even for I_2 in pure benzene, only 60% of I_2 would have formed 1:1 complexes,[2] and the uncomplexed I_2 line would be easily detectable. Our spectra show that, with increasing benzene concentration, the I_2 line shifts as a whole to lower frequencies. The shift from pure n-hexane to pure benzene is greater than the half width of the line. It is impossible to decompose the line into two lines, one for

complexed I_2 and one for uncomplexed I_2, as required by the above model. We did observe a small change (< 25%) in the linewidth as shown in Fig. 4, but it does not affect our conclusion. Similar results were obtained for I_2 in mixtures of n-hexane and toluene or m-xylene. Our results suggest that the charge-transfer interaction between I_2 and the donors is weak, and each I_2 molecule can interact simultaneously with more than one donor. The observed spectrum $S(\omega)$ is a statistical average over all complex configurations as indicated by Eq. (6).

Microscopic pictures also seem to suggest that an I_2 molecule could interact effectively with more than one donor. Mulliken has discussed various models of a 1:1 I_2-benzene complex.[3] According to him, the most compact and most probable model has the iodine molecule resting on the benzene molecule with its axis parallel to the plane of the benzene ring and its center on the sixfold axis of the benzene. In all the models, it seems obvious that we cannot rule out the possibility of having a second benzene molecule interacting with the iodine from the other side, although the interaction could be shielded considerably by the interaction of the iodine with the first benzene molecule. This shielding should be more effective for stronger charge-transfer interaction, since the I_2 molecule is more negatively charged in the complex formation with the first donor, and therefore reduces its

ability to interact with other donors. We then expect that for sufficiently strong I_2 complexes, I_2 and donor molecules would actually form 1:1 complexes with a more or less definite configuration at low donor concentrations. Correspondingly, two Raman lines should appear with their relative intensity changing with donor concentration. This is indeed the case for I_2 in mixutres of n-hexane and mesitylene.[29] At low concentrations of mesitylene, two lines at 210.1 cm^{-1} and 202.5 cm^{-1} can be observed. With increasing mesitylene concentration, the complexed I_2 line (202.5 cm^{-1}) increases in intensity and the uncomplexed line (210.1 cm^{-1}) diminishes. For mesitylene concentration higher than 40%, only the complex line remains and gradually shifts as a whole to lower frequencies with increasing mesitylene concentration. This gradual shift again indicates that each I_2 molecule now starts interacting effectively with more than one donor although the interaction is shielded to some extent by the charge-transfer interaction between I_2 and the first donor. One can also regard the I_2-mesitylene complex as a unit which now interacts weakly with surrounding donors to form higher-order complexes in various attainable configurations.

Since the charge-transfer interaction between I_2 and pyridine is supposed to be even stronger, we would expect to observe the same phenomenon for I_2 in mixtures of n-hexane and pryidine. We found that there are indeed two lines at 210.1 cm^{-1} and 185 cm^{-1} for pyridine concentrations less than 0.2%. With increasing pyridine concentration above 0.2%, the uncomplexed line disappears and the complexed line gradually shifts to lower frequencies with increasing linewidth.

Finally, in pure pyridine, the line appears at 174 cm^{-1} with a linewidth of 15 cm^{-1}. Infrared measurements on I_2-pyridine (Py I_2) complexes in inert solvents with small concentrations of I_2 and pyridine have also revealed an absorption band around 184 cm^{-1}.[13] In addition, Plyler and Mulliken[13] have observed two infrared absorption bands for I_2 and pyridine in benzene, one at 204 cm^{-1} and one at 174 cm^{-1}. they identify the 204 cm^{-1} line as due to I_2-benzene complexes. They also suggest that the 174 cm^{-1} line could be due to the formation of double complexes Benzene-PyI_2 of donor-acceptor character, or due to PyI_2 in "contact" donor-acceptor interaction with the benzene molecules around it. Our observation of a gradual shift of the complexed I_2 line from 185 cm^{-1} to 174 cm^{-1}, which has also been observed in the infrared-work of Ginn and Wood,[13] leads us to believe that the shift is the result of interaction between the PyI_2 complex and neighboring molecules in the statistical sense. The interaction could be of donor-acceptor character, but since the PyI_2 complex has a large permanent dipole moment, van der Waals interaction between PyI_2 and surrounding molecules could also be appreciable. Further studies of the PyI_2 complex in different solvents could help determine which type of interaction is more important. Our remark here also applies to the case of PyI_2 in benzene.

As we mentioned earlier, measurements of the mean vibrational frequency shift $\langle \Delta\omega_v \rangle$ in the Raman spectrum can be very accurate, and can be used to test quantitatively the theories on complexes in solution. In Fig. 3, $1/\langle \Delta\omega_v \rangle$, the inverse of the mean frequency shift of the I_2 fundamental vibration from its value in pure n-hexane, is plotted against $1/(\rho_B/\rho_{BO})$, the inverse of the normalized concentration of benzene or methylated benzene, where ρ_B is the concentration of benzene

or methylated benzene in the mixture, and ρ_{B0} the concentration of pure benzene or methylated benzene. The results look very much the same as those obtained from the uv measurements with the extinction coefficient replaced by the mean frequency shift. This is not unexpected since both the average uv extinction coefficient (integrated over the entire charge-transfer band) and the mean frequency shift should have the form of Eq. (4) in Section II. In fact, if we use the Benesi-Hildebrand equation, or Eq. (5), to fit the experimental data by the least-square method, we find that the constant K deduced from our measurements is within 25% of the value of K_{uv} deduced from uv absorption measurements[5, 30,31] (see Table II). This gives us further assurance that the vibrational frequency shifts of I_2 in these mixtures from its value in pure n-hexane is primarily due to charge-transfer interaction.

In Fig. 3, while the Benesi-Hildebrand equation yields a straight line, the experimental data show some evidence of curvature. From Eq. (9), we realize that a better approximation should be

$$1/\langle \Delta\omega \rangle = (1+\alpha_1 X+\alpha_2 X^2)/(\beta_1 X+\beta_2 X^2) \qquad (10)$$

where $X = \rho_B/\rho_{B0}$ and α_1, α_2, β_1, and β_2 are constant parameters. In Fig. 3, the theoretical curves obtained from a least-square fit of both Eq. (10) and the Benesi-Hildebrand equation are shown. It is seen that Eq. (10) appears to give a better description of the experimental data. The values of

α_1, α_2, β_1, and β_2 are given in Table III. However, the uncertainty in determining these parameters is quite large,[32] as suggested by the small difference between the two sets of curves in Fig. 3. (The parameter β_1 can, however, be determined quite accurately from the asymptotic slope of $1/\langle \Delta\omega_v \rangle$ vs ρ_{B0}/ρ_B at small ρ_B).[32] The least-square error in the fitting could of course be greatly improved if more experimental data points are available.

C. Temperature Dependence of Raman Spectra of I_2 in Mixtures of Benzene and n-Hexane

Generally, thermal agitation decreases the probability of interaction between molecules. Therefore, the vibrational frequency shift of I_2 in solution should be smaller at higher temperatures. In Fig. 5, we show the variation of the frequency shift as a function of the benzene concentration in mixtures of benzene and n-hexane at 25°C and 55°C. For a given benzene concentration, the shift is indeed smaller at the higher temperature.

D. Variation of Raman Scattering Intensity with Benzene Concentration in Mixtures of Benzene and CCl_4

For complexes in solution, the variation of the Raman scattering cross-section I_2 should have the same functional dependence on the

donor concentration as the extinction coefficient for charge-transfer absorption.[15] Thus, measurements of Raman scattering intensity of I_2 as a function of the donor concentration should provide another test on the theories of complexes in solution. Bahnick and Person[15] have in fact made such measurements on several charge-transfer complexes. The equilibrium constants deduced from their results by assuming 1:1 complexes agree with those obtained from uv measurements. We have measured the integrated Raman cross-section of I_2 in mixtures of benzene and CCl_4. In order to eliminate possible variations of collection efficiency, change of absorptivity with benzene concentration, long-term instability of the Raman spectrometer, etc., we need an internal intensity calibration for scattering cross-section measurements. This is provided by the strong Raman line of CCl_4 at 217 cm^{-1}. We always measured the Raman line of I_2 together with the 217 cm^{-1} line of CCl_4. We then considered only the relative scattering cross-section of the I_2 line with respect to the CCl_4 line. We found experimentally that in the absence of I_2, the scattering intensity of the 217 cm^{-1} CCl_4 line is proportional to the concentration of CCl_4 in agreement with the results of Bahnick and Person.[15] Therefore, within experimental error, the scattering cross-section of the CCl_4 line should be unaffected by the CCl_4-benzene interaction. Our experimental results in Fig. 6 show that the relative Raman cross-section of I_2 increases with the benzene concentration. This behavior agrees qualitatively with what we would predict since a strong charge-transfer band appears in the near uv (see Section II). Unfortunately, there is inherent inaccuracy in the measurements of integrated intensity. The same difficulty clearly exists also in the measurements of Bahnick and Person.[15]

In our case, the accuracy is worse since the CCl_4 line overlaps slightly with the I_2 line. Consequently, the results in Fig. 6 cannot be used for a quantitative test on the different theories of complexes in solution.

E. First Raman Overtone of I_2 in Mixtures of Benzene and n-hexane.

We have also measured the relative scattering cross-section of the I_2 first overtone with respect to the fundamental as a function of benzene concentration. Usually, one would expect the overtones to be much weaker than the fundamental. However, we found in pure n-hexane that the first overtone is only 4 times less intense than the fundamental. This anomaly is probably due to resonance enhancement, since the exciting laser frequency is at the lower edge of the visible absorption band of I_2. Because of this resonance Raman effect, the I_2 Raman line is exceptionally strong (100 times more intense than the 217 cm^{-1} CCl_4 line), and it would not be surprising even if the first overtone happened to be more intense than the fundamental.[33] As the benzene concentration increases, the relative cross-section becomes smaller, and finally in pure benzene, the overtone is approximately 8 times weaker than the fundamental. This is presumably because the visible absorption band of I_2 has a blue shift resulting from the charge-transfer interaction between I_2 and benzene.[2,34] Here again, the results are not accurate enough for a more detailed quantitative discussion.

Anharmonicity in a molecular vibration should be reflected in the overtone spectrum of the vibration. Thus, measurements of the overtone spectrum of I_2 complexes in solution should yield information

about how the anharmonicity of the I-I intramolecular potential is changed by the charge-transfer interaction. We have measured the first Raman overtone of I_2 in mixtures of benzene and n-hexane. Just as for the fundamental, the mean frequency of the overtone shifts to lower frequencies as the benzene concentration is increased (see Fig. 7). The overtone line is roughly symmetric, with a linewidth of about 18 cm^{-1} which increases slightly with higher benzene concentrations. Qualitatively, these results are expected if we take into account the statistical distribution of complex configurations in solution, and consider the fact that the overtone line is usually broader than the fundamental.

To show explicitly the change of anharmonicity, we have plotted in Fig. 8 the difference between twice the mean fundamental frequency and the mean-overtone frequency as a function of the benzene concentration. In pure n-hexane the anharmonicity is 2.5 times greater than the value found in vapor[25] and as the benzene concentration increases, the "average" anharmonicity of the vibration decreases, approaching zero for benzene concentrations greater than 50%. The difference between the anharmonicity in pure n-hexane and in vapor is presumably due to van der Waals interaction between I_2 and n-hexane which enhances the anharmonicity. On the other hand, the charge-transfer interaction apparently tends to make the I_2 vibration more harmonic.

F. Intermolecular Mode of I_2 Complexes

In addition to a change in the Raman spectrum of I_2, the charge-transfer interaction between I_2 and the donor could also induce a new intermolecular mode. Frequencies of intermolecular modes are generally low, higher for stronger interaction. The charge-transfer interaction

between I_2 and pyridine is exceptionally strong. From the infrared absorption spectrum, Lake and Thompson[13] have indeed found the intermolecular mode at 94 cm^{-1} in the I_2-pyridine complex. We have tried to observe the same intermolecular mode from the Raman spectrum. However, from the charge configuration of the I_2-pyridine complex, this intermolecular mode is probably more infrared-active than Raman-active. Because of this and also because of the relatively large scattering background near the exciting laser line, we have not been successful in detecting this intermolecular mode.

V. Conclusions

It is demonstrated that Raman spectroscopy can be used to investigate charge-transfer complexes in solution. By measuring the mean frequencies of the I_2 stretching vibration in various solvents, the frequency shift due to van der Waals interaction can be separated from that due to charge-transfer interaction. Investigation of the I_2 Raman spectrum in mixtures of n-hexane and benzene or methylated benzene shows that each I_2 molecule can probably interact simultaneously with more than one donor in the statistical sense. We have also measured, for various donor concentrations, the temperature variation, the linewidth, and the scattering cross-section of the I_2-fundamental and, in addition, the I_2 overtone spectrum. Results agree qualitatively with what the theory would predict.

References

1. See, for example, G. Briegleb, Elektronen-Donator-Acceptor-Komplexe (Springer-Verlag, Berlin, 1961);
   L. J. Andrews and R. M. Keefer, Molecular Complexes in Organic Chemistry (Holden-Day, Inc., San Francisco, Calif. 1964).
2. H. A. Benesi and J. H. Hildebrand, J. Am. Chem. Soc. 71, 2703 (1949).
3. R. S. Mulliken, J. Am. Chem. Soc. 72, 600 (1950); 74, 811 (1952).
4. See, for example, L. J. Andrews and R. M. Keefer, Molecular Complexes in Organic Chemistry (Holden-Day, Inc., San Francisco, Calif., 1964) p. 28.
5. L. J. Andrews and R. M. Keefer, J. Am. Chem. Soc. 74, 4500 (1952).
6. G. D. Johnson and R. E. Bowen, J. Am. Chem. Soc. 87, 1655 (1965).
7. S. Carter, J. N. Murrell, and E. J. Rosch, J. Chem. Soc. 2048 (1965).
8. P. H. Emslie, R. Foster, C. A. Fyfe, and I. Horman, Tetrahedron 21, 2843 (1965).
9. D. A. Deranleau, J. Am. Chem. Soc. 91, 4050 (1969).
10. L. E. Orgel and R. S. Mulliken, J. Am. Chem. Soc. 79, 4839 (1957).
11. R. S. Mulliken, Rec. Trav. Chim. 75, 845 (1956).
12. R. S. Mulliken and W. B. Person, Ann. Rev. Phys. Chem. 13, 107 (1962).
13. J. Yarwood and W. B. Person, J. Am. Chem. Soc. 90, 594 (1968);
    E. K. Plyler and R. S. Mulliken, J. Am. Chem. Soc. 81, 823 (1959);
    R. F. Lake and H. W. Thompson, Proc. Roy. Soc. (London) A297, 440 (1967);
    H. Yada, J. Tanaka, and S. Nagakura, J. Mol. Spectry. 9, 461 (1962);
    S. G. W. Ginn and J. L. Wood, Trans. Faraday Soc. 62, 777 (1966).

14. P. Klaboe, J. Am. Chem. Soc. 89, 3667 (1967);
H. Stammreich, R. Forneris, and Y. Tavares, Spectrochim. Acta 17, 1173 (1961).

15. D. A. Bahnick and W. B. Person, J. Chem. Phys. 48, 1251 (1968); 48, 5637 (1968); J. Phys. Chem. 73, 2309 (1969).

16. Preliminary results of the experiments were reported in Y. R. Shen, H. Rosen, and F. Stenman, Chem. Phys. Letters 1, 671 (1968).

17. See, for example, J. O. Hirschfelder, C. F. Curtiss, and B. B. Bird, Molecular Theory of Gases and Liquids (John Wiley and Sons, Inc., New York, 1954).

18. See, for example, G. Placzek, Marx's Handbuch der Radiologie VI, 2, 209 (1934).

19. H. B. Friedrich and W. B. Person, J. Chem. Phys. 44, 2161 (1966).

20. W. B. Person, J. Chem. Phys. 38, 109 (1963).

21. D. Landon and S. P. S. Porto, Appl. Opt. 4, 762 (1965).

22. We define the van der Waals interaction here to include electrostatic, induction and dispersion forces between molecules. See Ref. 23.

23. This classification is somewhat arbitrary; See J. O. Hirschfelder, C. F. Curtiss, and R. B. Bird, Molecular Theory of Gases and Liquids (John Wiley and Sons, Inc., New York, 1954) p. 917.

24. See, for example, A. D. Buckingham, Proc. Roy. Soc. (London), A248, 169 (1958).
L. H. Jones and R. M. Badger, J. Am. Chem. Soc. 73, 3132 (1951).

25. G. Herzberg, Molecular Spectra and Molecular Structure. I. Spectra of Diatomic Molecules (Prentice-Hall, Inc., New York 1939) p. 488.

26. Indices of refraction for the solvents are obtained from Handbook of Chemistry and Physics (Chemical Rubber Co., Cleveland, 1963) p. 766.

27. S. H. Hastings, J. L. Franklin, J. C. Schiller, and F. A. Matsen, J. Am. Chem. Soc. 75, 2900 (1953).

28. If CCl_4 were used instead of n-hexane, then since CCl_4 and benzene have roughly the same refractive index, the van der Waals shift would presumably remain unchanged with benzene concentration in the CCl_4-benzene mixtures. Unfortunately, the 217 cm^{-1} CCl_4 line overlaps slightly with the I_2 line, making accurate frequency measurements more difficult.

29. The same phenomenon was observed by Bahnick and Person for ICN forming charge-transfer complexes with tetrahydrofuran in a mixed solvent of CH_2Cl_2 and $CHCl_2$. See Ref. 15.

30. R. M. Keefer and L. J. Andrews, J. Am. Chem. Soc. 77, 2164 (1955).

31. The values of K_{uv} obtained by different authors are usually different. Our values of K fall within the spread of values of K_{uv} tabulated in G. Briegleb, Electronen-Donor-Acceptor-Komplexes (Springer-Verlag, Berlin, 1961) p. 124. It should be noted that part of the discrepancy between K and K_{uv} could be due to the fact that CCl_4 is used as the inert solvent in the uv measurements, while n-hexane is used in our case. The estimated errors in our determination of K and $(\Delta\omega_v)_o$ are around 5 %.

32. With an 85% confidence level, the uncertainties in the values of

α_1, α_2, and β_2 can be as large as 200%, but the uncertainties in the values of β_1 are less than 30%.

33. H. A. Szymanski, Raman Spectroscopy (Plenum Press, New York, 1967) p. 217.

M. V. Klein and S. P. S. Porto, Phys. Rev. Letters 22, 782 (1969).

R. C. C. Leite, J. P. Scott, and T. C. Damen, Phys. Rev. Letters 22, 780 (1969).

34. J. Walkley, D. N. Glew, and J. H. Hildebrand, J. Chem. Phys. 33, 621 (1960).

Table I. Mean frequencies of the I_2 fundamental vibration in various solvents.

Solvents	Frequency (cm^{-1})
vapor	213.3
n-hexane	210.1 ± 0.1
n-heptane	210.0 ± 0.1
carbontetrachloride	209.7 ± 0.3
chloroform	209.6 ± 0.4
cyclohexane	208.9 ± 0.4
nitrobenzene	208.1 ± 0.4
chlorobenzene	207.1 ± 0.4
bromobenzene	205.9 ± 0.4
benzene	204.6 ± 0.1
toluene	203.6 ± 0.2
m-xylene	202.1 ± 0.15
mesitylene	200.0 ± 0.3

Table II. Values of $(\Delta\omega_v)_o$ and K in Eq. (5) derived from the best fit of the experimental data to Eq. (5) as shown in Fig. 3. The equilibrium constants K_{uv} deduced from the uv absorption measurements are obtained from (a) R. M. Keefer and L. J. Andrews, Ref. 30 and (b) L. J. Andrews and R. M. Keefer, Ref. 5.

	$(\Delta\omega_v)_o$	K (liters/mole)	K_{uv} (liters/mole)	
Benzene	8.6 cm^{-1}	0.17	0.157	(a)
Toluene	10.3 cm^{-1}	0.21	0.16	(b)
m-xylene	10.5 cm^{-1}	0.40	0.31	(b)
Mesitylene	12.8 cm^{-1}	0.62	.534	(a)

Table III. Values of α_1, α_2, β_1, and β_2 in Eq. (10) derived from the best fit of the experimental data to Eq. (10) as shown in Fig. 3.

	α_1	α_2	β_1	β_2
Benzene	2.64	4.53	13.20	31.71
Toluene	3.24	1.05	22.0	14.26
m-xylene	3.0	3.6	30.6	29.37
Mesitylene	3.68	0.724	53.11	2.72

FIGURE CAPTIONS

Fig. 1. A typical Raman spectrum (the central line) of the I_2 fundamental vibration in pure benzene at 55°C. The dots correspond to the number of counts in the channels of the multichannel analyzer. The two side lines are Ne calibration lines at 6402.25 Å and 6421.71 Å. The instrumental linewidth is 4 cm^{-1}. Note that only one spectral line of I_2 shows up, while the model of a 1-1 complex would predict two.

Fig. 2. Mean frequency shift of the I_2 fundamental vibration from its value in vapor in various solvents vs $n^2 - 1$, where n is the refractive index of solvent.

1 - n-hexane; 2 - n-heptane; 3 - carbon tetrachloride;

4 - chloroform; 5 - cyclohexane; 6 - nitrobenzene;

7 - chlorobenzene; 8 - bromobenzene; 9 - benzene;

10 - toluene; 11 - m-xylene; 12 - mesitylene.

Fig. 3. Comparison of the theoretical curve of Eq. (10) and the Benesi-Hildebrand curve of Eq. (5) with the experimental data. The inverse mean vibrational frequency shifts $1/\langle \Delta\omega_v \rangle$ of I_2 in solutions of benzene or methylated benzene and n-hexane, with respect to the frequency in pure n-hexane, are plotted as a function of inverse normalized concentration of benzene or methylated benzene ρ_{Bo}/ρ_B, where ρ_{Bo} is the density of pure benzene or methylated benzene and ρ_B is the density of benzene or methylated benzene in the mixtures.

Fig. 4. Apparent Raman linewidth of the I_2 fundamental vs the normalized benzene concentration. The instrumental linewidth is 4 cm^{-1}. The true width of the I_2 line in n-hexane obtained by deconvolution of the line with the slit function is 5.1 cm^{-1}.

Fig. 5. Mean frequency shift of the I_2 fundamental as a function of normalized benzene concentration at two temperatures 25°C and 55°C.

Fig. 6. Variation of the Raman scattering cross-section of the I_2 fundamental (normalized against the Raman scattering cross-section of the 217 cm^{-1} line of CCl_4) as a function of the normalized benzene concentration.

Fig. 7. Mean frequency of the I_2 first overtone vs the normalized benzene concentration.

Fig. 8. Variation of $2\omega_f - \omega_o$ as a function of the normalized benzene concentration, where ω_f and ω_o are the mean frequencies of the fundamental and the first overtone of the I_2 vibration respectively.

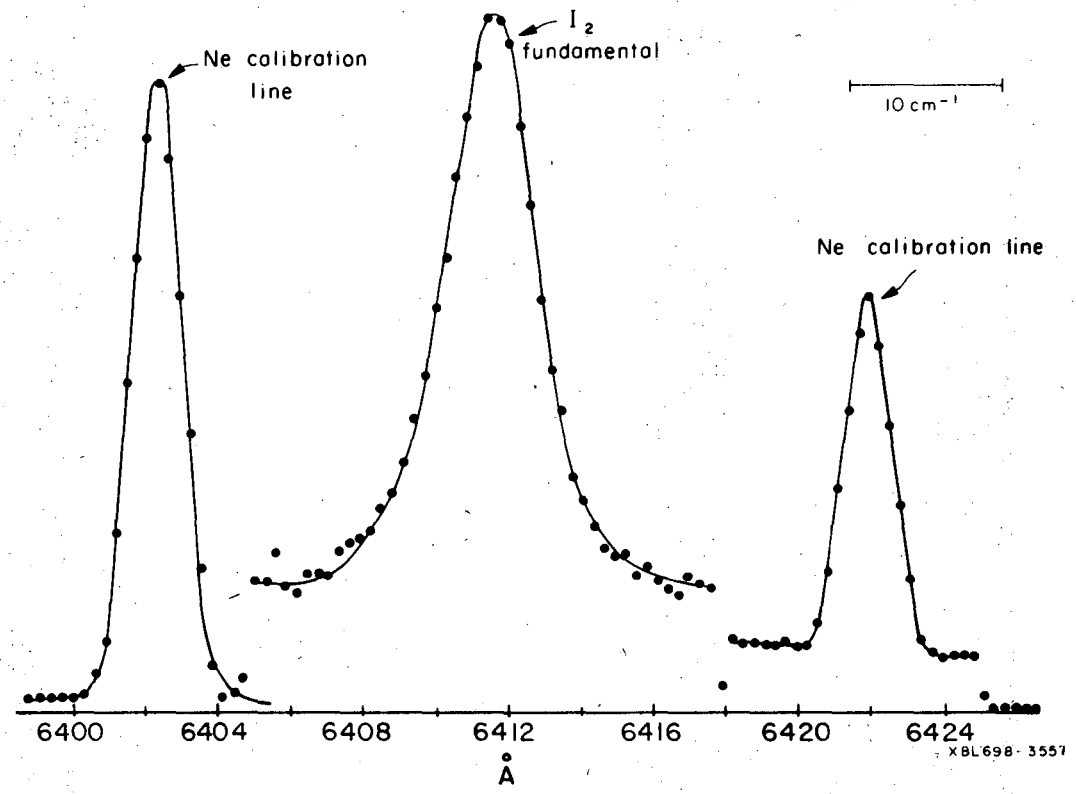

Fig. 1

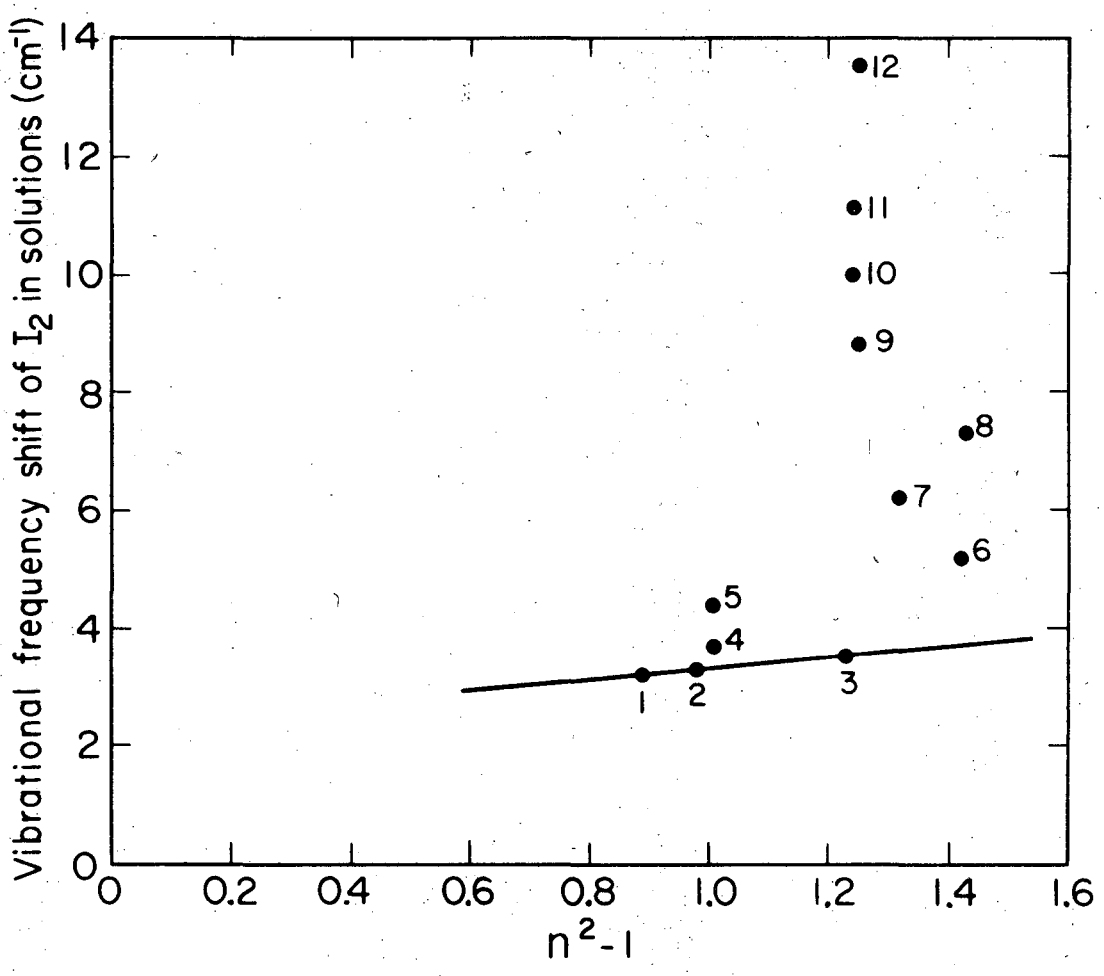
Vibrational frequency shift of I_2 in solutions (cm^{-1})
n^2-1
0
2
4
6
8
10
12
14
0
0.2
0.4
0.6
0.8
1.0
1.2
1.4
1.6
1
2
3
4
5
6
7
8
9
10
11
12
XBL697-3334

Fig. 2

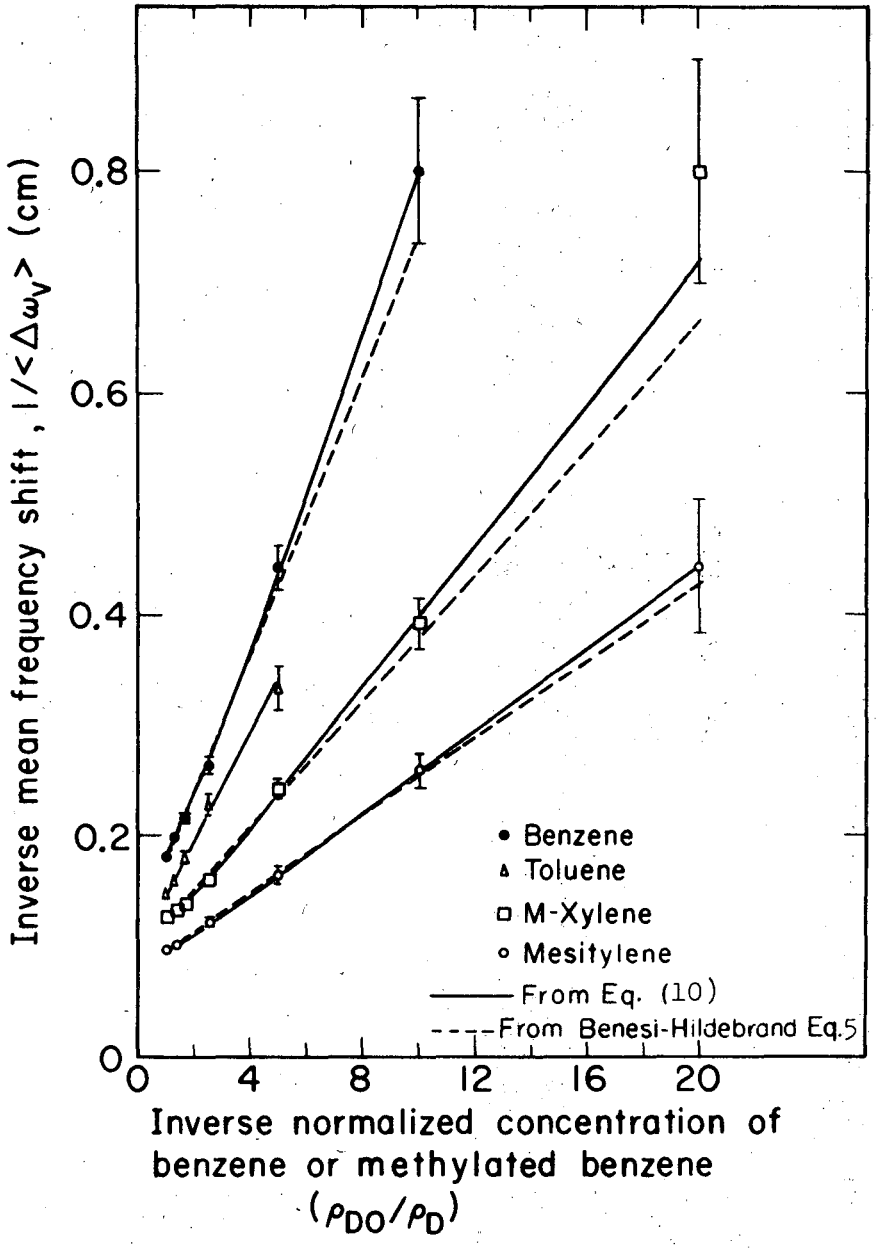

XBL697-3278

Fig. 3

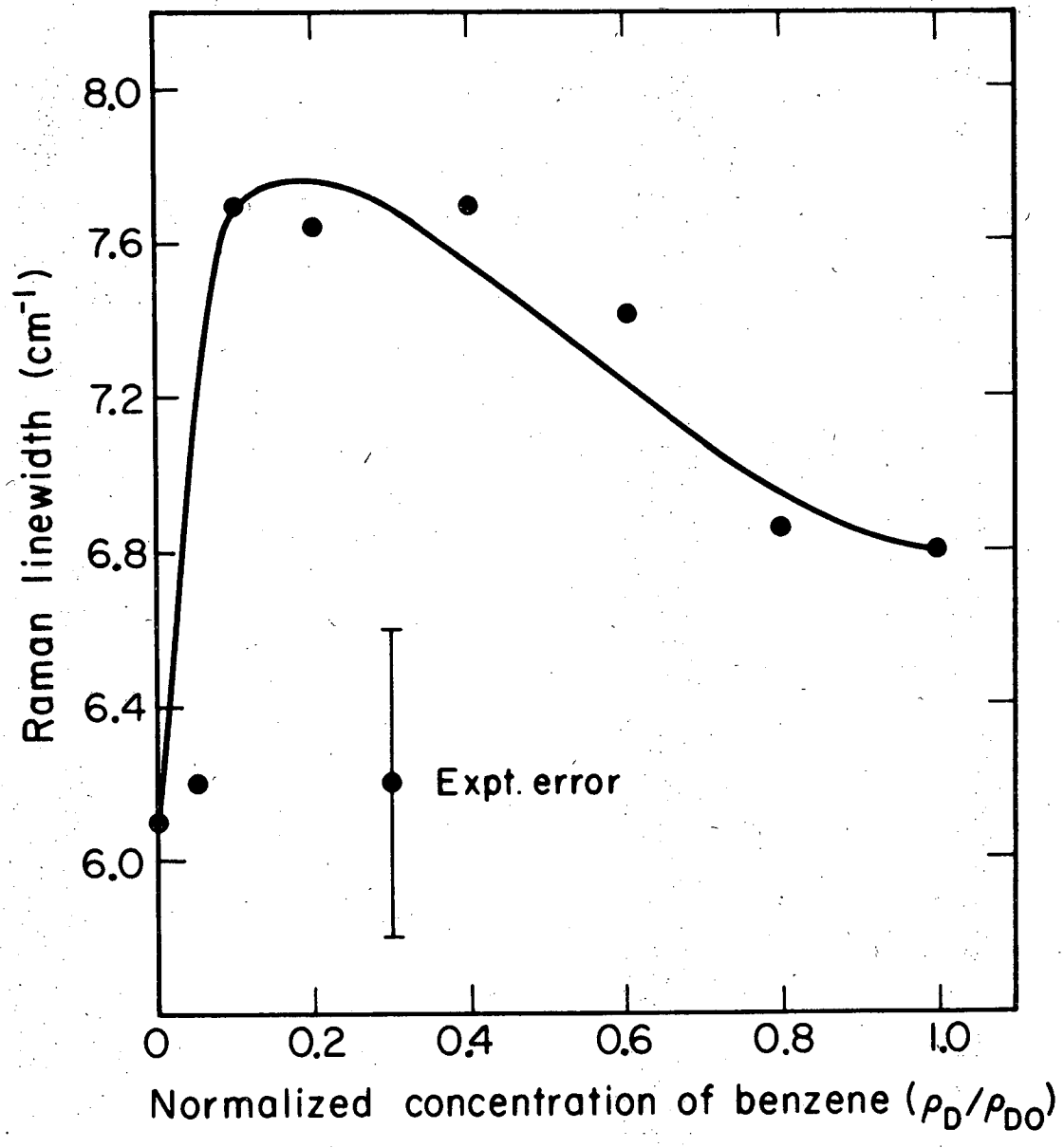

XBL697-3336

Fig. 4

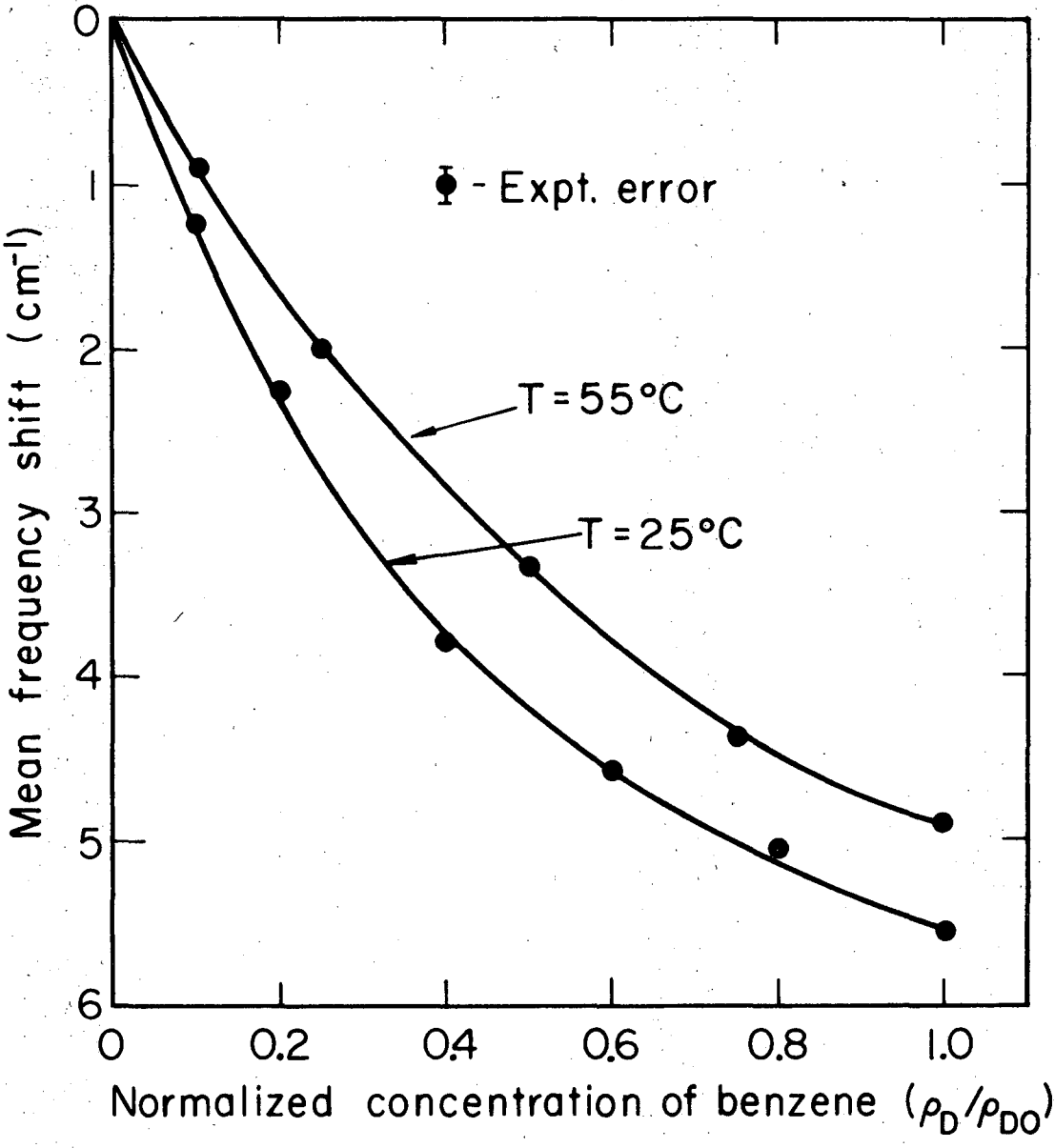

XBL697-3332

Fig. 5

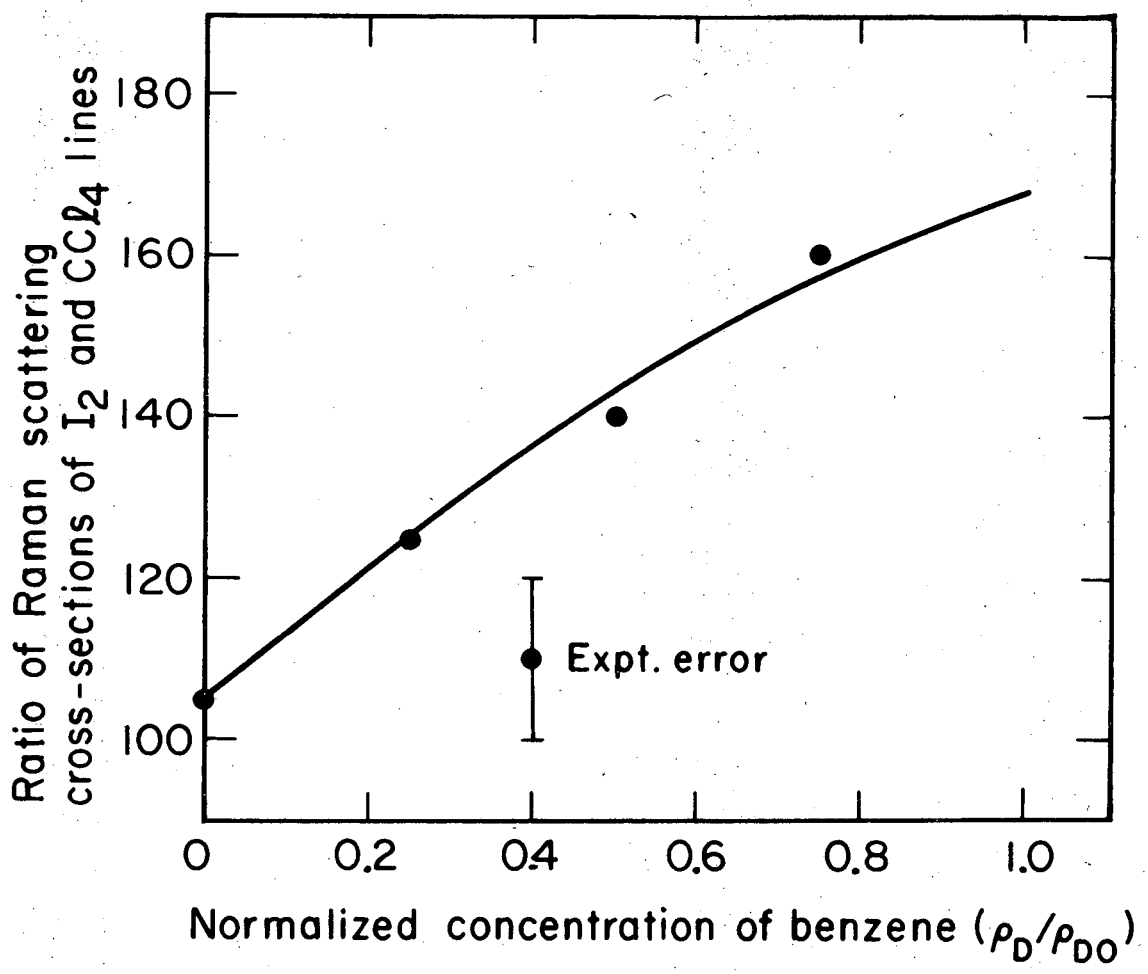

XBL697-3337

Fig. 6

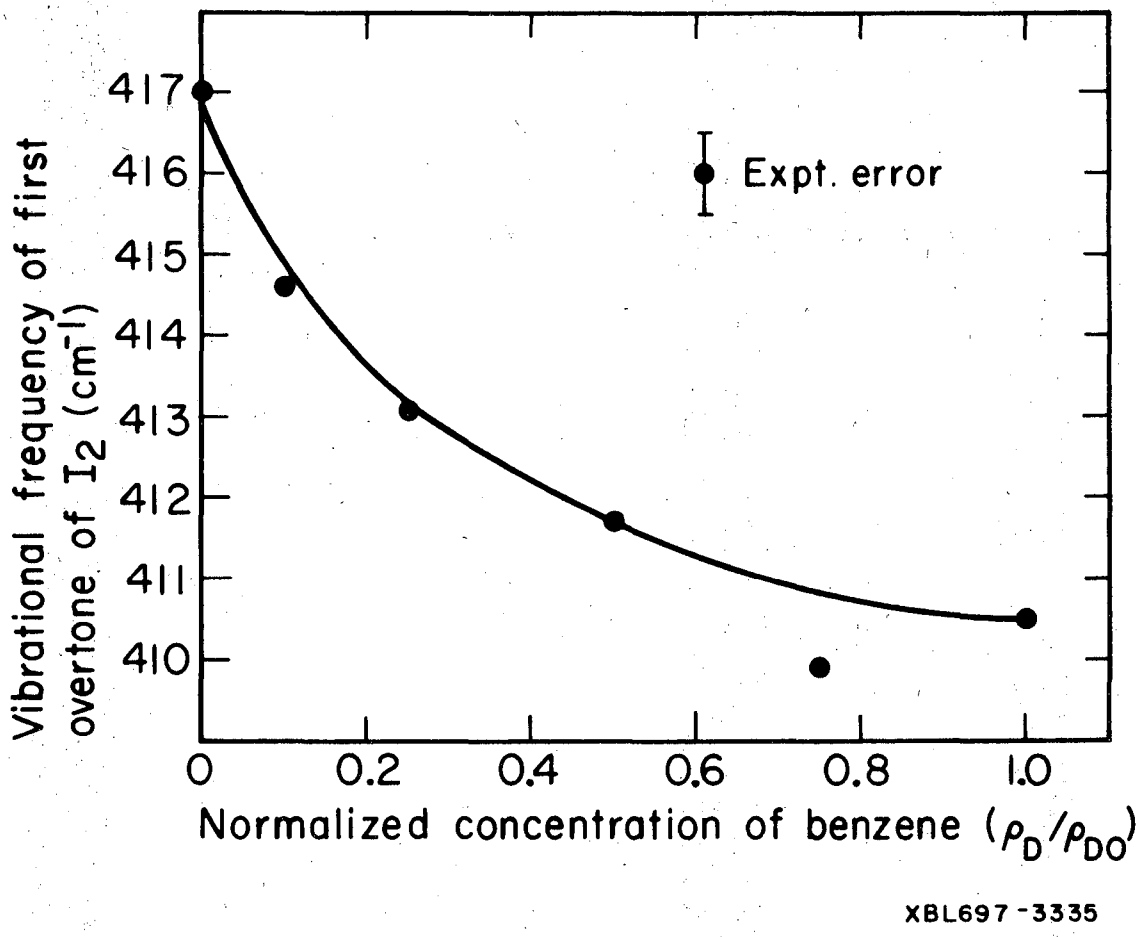

Fig. 7

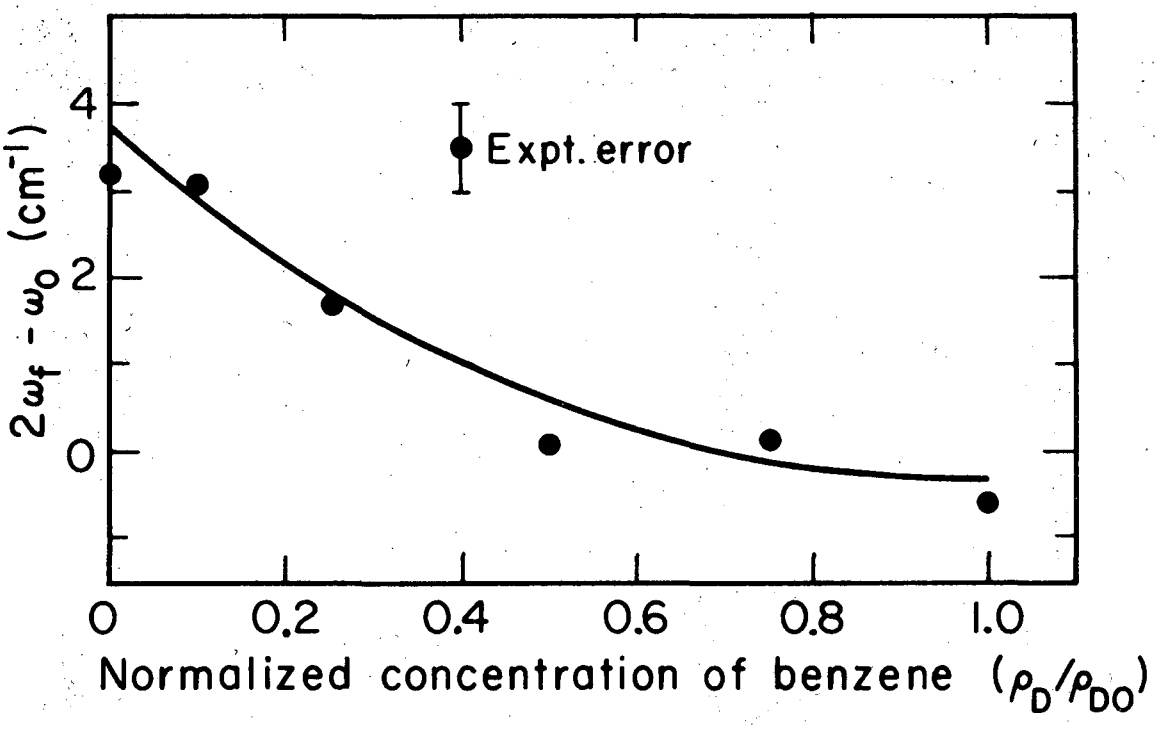

XBL697-3333

Fig. 8

SECTION III
RAMAN STUDY OF PARA-AZOXYDIANISOLE AT THE PHASE TRANSITIONS*

Using Raman scattering technique, we have investigated the phase transitions of the nematic liquid-crystalline substance p-azoxydianisole (PAA). Although Raman spectra of this substance have previously been obtained,[1,2] no systematic investigation of the temperature dependence of the Raman modes has been reported. Furthermore, to our knowledge, no investigation of the low-frequency Raman modes has ever been made. In this note, we would like to report the results of our measurements of the temperature dependence of the Raman modes in two spectral regions: 30-100 and 1225-1300 cm^{-1}. The intensities of these modes change significantly during the phase transitions. Our results indicate that the Raman spectrum of PAA is affected mainly by short-range interaction between neighboring molecules, and that Raman scattering, in general, can be used to probe the change of short-range ordering during the phase transitions.

The experimental setup was the same as that described by Landon and Porto,[3] with a 40 mW He-Ne laser as the exciting source. The PAA sample was recrystallized three times for purity. For better temperature control, the sample cell was inserted in a copper block and then immersed in an oil bath. The sample temperature was monitored constantly, and temperature fluctuations were less than 0.035°C.

A spectral range of ±1900 cm^{-1} about the laser line was investigated. There are around 30 strong Raman lines (of the same order as the 992 cm^{-1} line of pure benzene) in that range. As the substance changes phases from solid to nematic and into isotropic liquid, some of the lines disappear, but most of them decrease in intensity and become broader. Three

*Published in Phys. Rev. Letters 24, 718 (1970).

of the lines, however, show little change (<10%) in their integrated intensities. In particular, the line at 1095 cm^{-1} also shows essentially no change in its linewidth. It was, therefore, chosen as the internal calibration line in our intensity measurements. Generally speaking, the spectra of the nematic phase resemble those of the isotropic liquid more than those of the solid. None of the observed Raman lines show any detectable frequency shift in the phase transformation. For the high-frequency Raman modes, our spectra have general resemblance to those obtained by others[1,2] but the detailed structure is quite different, especially for nematic and liquid phases. The difference may be attributed to the better quality of our spectra.[4]

Two spectral regions show more significant changes under phase transformation (see Fig. 1). The first region from 1225 to 1300 cm^{-1} was first investigated by Freymann and Servant.[1] They reported observing two lines at 1247 and 1276 cm^{-1} in the solid and nematic phases and that the line at 1247 cm^{-1} disappeared in the liquid phase. Our spectrum for solid PAA in Fig. 1a, however, indicates that the composite spectrum of this region can be decomposed into four symmetric lines at 1246 (±2), 1252, 1261, and 1276 cm^{-1}, with the respective intensity ratio of 3.7:1:4.2:6.3. The strongest line is roughly 1/2 as strong as the 992 cm^{-1} line of benzene. As the temperature increases through the solid-nematic transition, the three lines at lower frequencies decrease sharply in intensity and merge into a single broad peak. However, assuming that the lines are always symmetric, we can still decompose the spectrum into four lines at approximately the same frequencies as before. In figure 2a, we

plotted the normalized integrated intensity of the 1246 cm^{-1} (calibrated against the intensity of the 1095 cm^{-1} line) as a function of temperature.[5] It is seen that the curve has the characteristic quasidiscontinuity at the solid-nematic phase transition. However, no such discontinuity occurs at the nematic-isotropic transition. The integrated intensity of the 1276 cm^{-1} line remains unchanged through the phase transitions, but the linewidth changes as shown in Fig. 2b. Again, the variation of the linewidth with temperature has a quasidiscontinuity at the solid-nematic transition.

The low-frequency region from 30 to 100 cm^{-1} is also of interest. The spectrum of solid PAA shows three Raman modes at 40 (±2), 52, and 72 cm^{-1} located on the tail of the central scattering component, as shown in Fig. 1. The intensity ratio is 1:1.4:2.4, respectively, the 72 cm^{-1} mode being 1/4 as intense as the 1276 cm^{-1} mode. In transition from solid to the nematic phase, the 72 cm^{-1} mode vanished completely, and the intensities of the modes at 40 and 52 cm^{-1} drop sharply with their intensity ratio becoming 4:1. The latter two modes also disappear suddenly at the nematic-to-liquid transition. While the intensities vary, the frequencies and the linewidths of the three modes remain unchanged. Figure 3 shows the variation of the normalized integrated intensities of the three modes with temperature. Here again, the curves exhibit the characteristic discontinuities at the phase transitions.

To explain our results qualitatively, we can use the simple model suggested for PAA.[6,7] In the solid phase, the molecules CH_3O-(C_6H_4)-N_2-(C_6H_4)-CH_3O are all aligned and fixed in regular positions. Two neighboring molecules are half overlapped, with the benzene rings facing

each other and the CH_3O groups in close contact with the N_2O groups.[6] In the nematic phase, the long axes of the molecules are still essentially aligned, but the molecules are no longer rigidly fixed in position and they can rotate more or less freely about their own long axes.[7] The rotation of the benzene-ring groups is presumably less hindered because no permanent dipole moment is attached to the benzene ring. Finally, in the liquid phase, disordering in the molecular alignment sets in.

As suggested by Freymann and Servant,[1] the Raman lines around 1260 cm^{-1} should arise from the vibrational modes of the CH_3O-(C_6H_4)-N_2O group. These modes are likely to be strongly affected by intermolecular interaction when neighboring molecules are overlapping in a manner described above for the solid phase. In the nematic phase, since the molecules can move and can rotate about their long axes, the probability of finding two neighboring molecules with this particular relative position and orientation is smaller than that of the solid phase. Consequently, the intensities of these modes drop sharply. That the mode frequencies remain unchanged suggests that here only the optical excited states are modified by the intermolecular interaction. The sudden increase in the linewidth of the Raman modes at the phase transition indicates the onset of roataional freedom the molecules acquire in going to the nematic phase.

The same model can be used to explain the observation of the low-frequency modes. Unlike the soft lattice modes in ferroelectrics,[8] these modes do not change in frequency during the phase transition. They are most likely the intermolecular modes arising from interaction between the CH_3O-(C_6H_4)-N_2O groups of two neighboring molecules and

should be affected primarily by short-range ordering. The 72 cm^{-1} mode may depend strongly, and the other two less strongly, on the relative position and orientation of the neighboring molecules. As a result, the 40 and 52 cm^{-1} modes persist in the nematic phase although their intensities decrease. It is interesting to note from Fig. 3 and the modes with higher frequencies show more drastic changes at the solid-nematic transition. This seems to suggest that the modes with higher frequencies have deeper but narrower intermolecular potential wells. These intermolecular modes do not have sidebands due to rotation or libration of individual molecules. Consequently, little change in their linewidths should be expected at the phase transition.

In an attempt to study the influence of magnetic field on ordering in PAA, we applied a field of 4.0 kOe on the sample and varied the temperature. The field is strong enough to induce macroscopic alignment and, hence, saturation of the dielectric constant in PAA.[9] We have, however, seen no effect of the field on the phase-transition temperatures of PAA. The Raman spectrum, after calibration against the 1095 cm^{-1} line, also showed no field dependence at any temperature. The field is apparently not strong enough to modify the short-range interaction between molecules. This is in agreement with the conclusion drawn by others that in nematic substances a magnetic field has effect only on a macroscopic scale but not on local individual molecules.[10]

We also observed in our experiment abrupt broadening of the central Rayleigh-wing component at both solid-to-nematic and nematic-to-liquid phase transitions. This is clearly due to the onset of rotation and libration of the molecules at the phase transitions. However, systematic investigation on this Rayleigh-wing scattering is yet to be performed.

We have shown here that Raman scattering can be used to probe phase transitions and short-range ordering in liquid crystalline materials. Combination of Raman studies with other methods of investigation, such as NMR, etc. may yield a better picture of intermolecular interaction in these materials. We are extending our study to the other members of the homologous series of the 4, 4'-bis (alkoxy) azoxybenzenes. Preliminary results indicate that, in general, the temperature dependence of both the low-frequency and the high-frequency Raman modes conform with the results obtained from PAA. A full report of the investigation will be published elsewhere.

REFERENCES

1. R. Freymann and R. Servant, Ann. Phys. 20, 131 (1945).

2. A. S. Zhdanova, L. F. Morozova, G. V. Peregudov. and M. M. Sushchinskii, Opt. i Spektroskopiya 26, 209 (1969) [Opt. Spectry. (USSR) 26, 112 (1969)].

3. D. Landon and S. P. S. Porto, Appl. Opt. 4, 762 (1965).

4. Zhdanova et al. reported in Ref. 2 the disappearance of several high-frequency Raman modes in the nematic and isotropic-liquid phases. However, we were unable to confirm their observation. Our complete Raman spectra of PAA in the three phases will be published elsewhere.

5. Because of inaccuracy caused by decomposition of the spectrum, the quantitative results of intensity variation of the other two lines are not presented here.

6. J. D. Bernal and D. Crowfoot, Trans. Faraday Soc. 29, 1032 (1933).

7. For example, see G. Meier and A. Saupe, Mol. Cryst. 1, 515 (1966).

8. W. Cochran, Advan. Phys. 9, 387 (1960), and 10, 401 (1961).

9. W. Maier and G. Meier, Z. Naturforsch. 16a, 470 (1961).

10. L. S. Ornstein, Z. Krist. 79, 90 (1931); L. S. Ornstein and W. Kast, Trans. Faraday Soc. 29, 931 (1933); A. Saupe, Z. Naturforsch. 15a 815 (1960).

FIGURE CAPTIONS

Fig. 1 Raman spectra of PAA from 30 to 100 cm^{-1} and from 1225 to 1300 cm^{-1} in the three phases a) solid phase at T = 113.9°C; b) nematic phase at T = 116.8°C; c) liquid phase at T = 134.8°C. The slit width is 2 cm^{-1}.

Fig. 2 a) Normalized integrated intensity of the 1246 cm^{-1} line as a function of temperature. b) Variation of the linewidth of the 1276 cm^{-1} Raman mode with temperature.

Fig. 3 Normalized integrated intensity of the low-frequency Raman modes as a function of temperature.

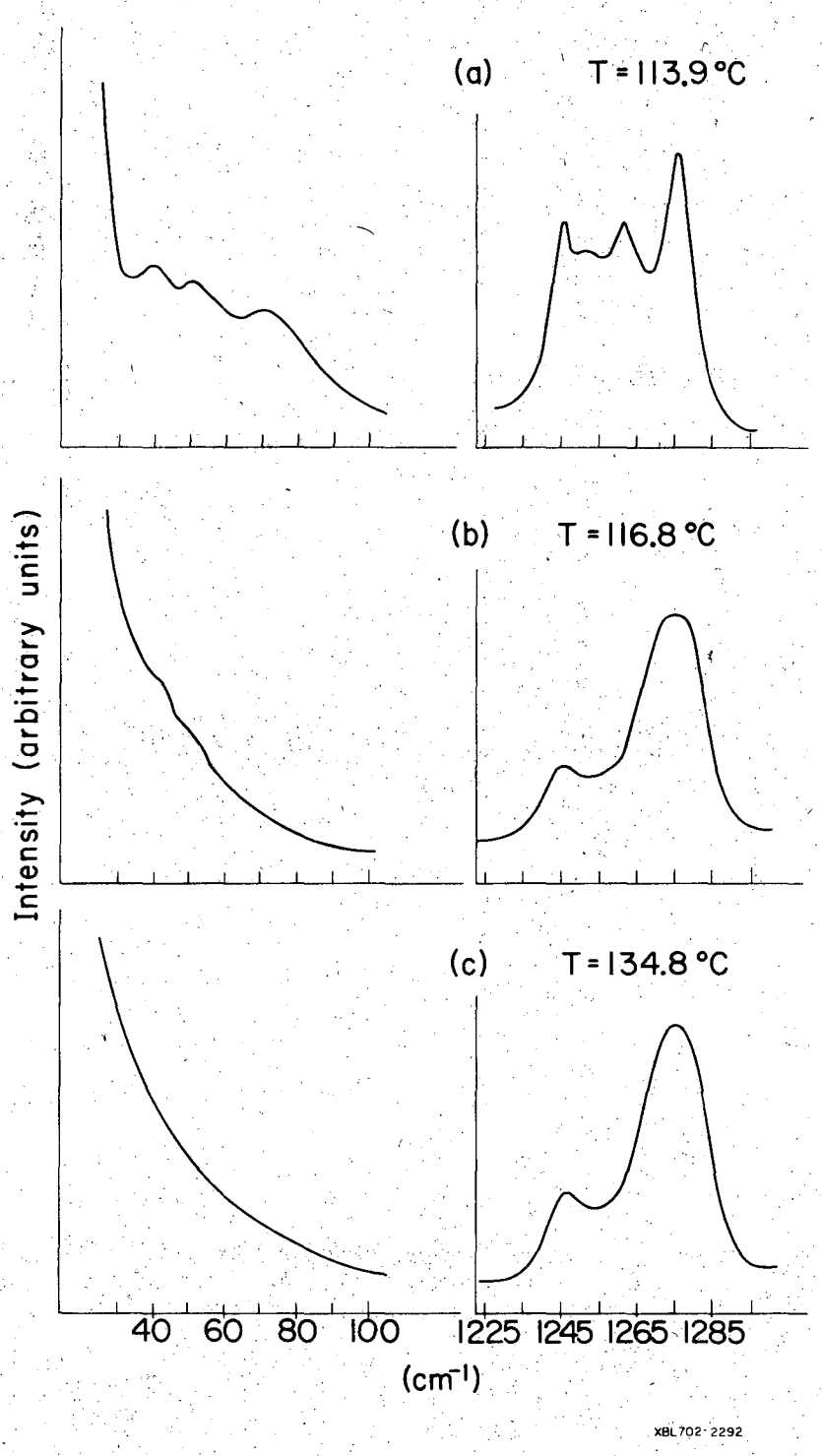

Fig. 1

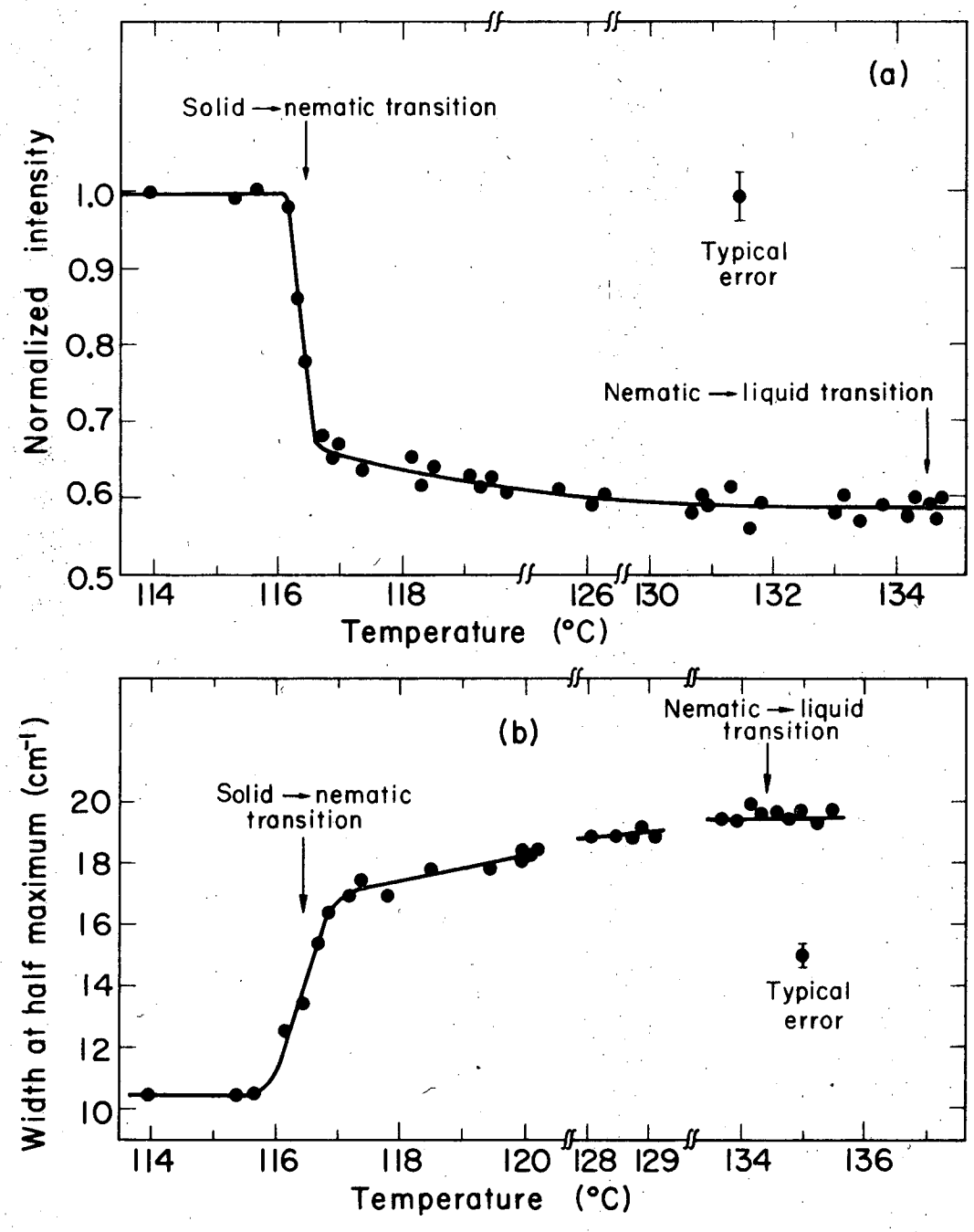

XBL702-2297

Fig. 2

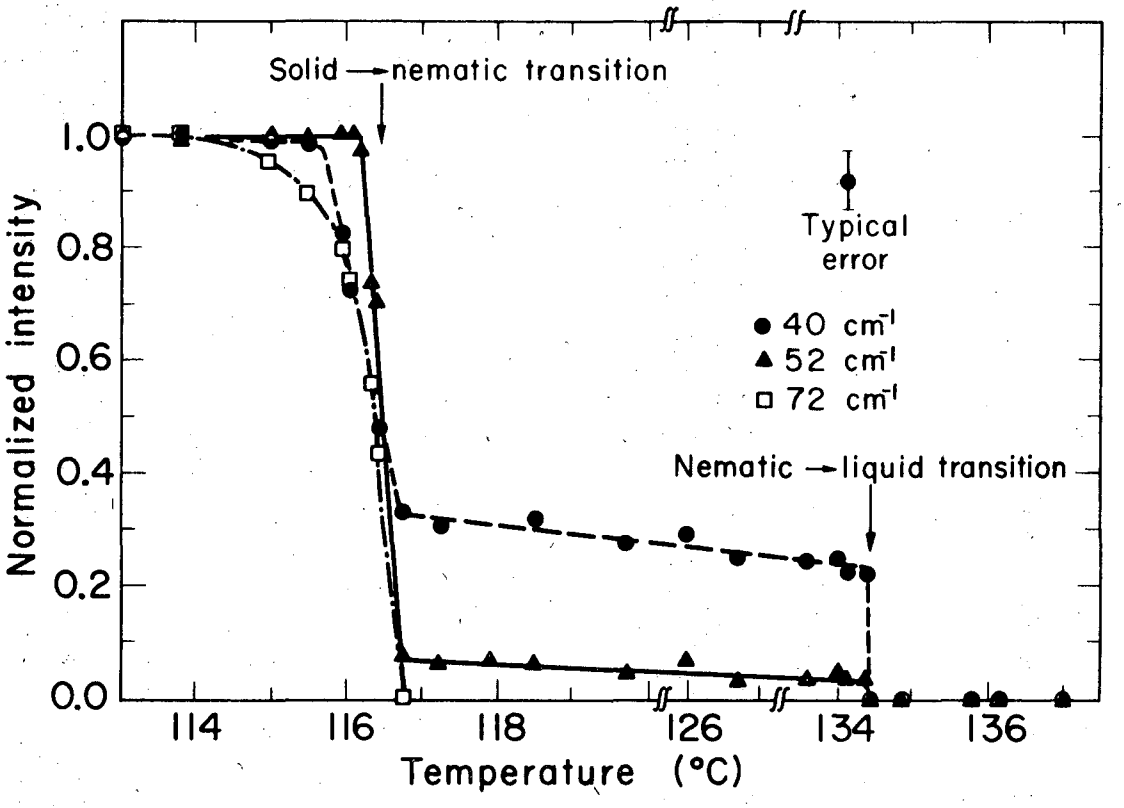

XBL702-2298

Fig. 3

SECTION IV

BRILLOUIN SCATTERING FROM A CHOLESTERIC MEDIUM AT ITS LIQUID-TO-LIQUID CRYSTAL TRANSITION

I. INTRODUCTION

There have been many investigations of the acoustic properties of substances in the phase transition region. Such diverse transitions as the liquid-vapor, order-disorder, superconducting, ferroelectric and ferromagnetic have been studied rather thoroughly over a wide range of frequencies.[1] These studies have yielded a great deal of information about the dynamical properties of these systems in the transition region. One would hope that similar investigations of the liquid crystal-liquid transition could be just as fruitful. However, so far, there have been only a few reports in existence on the subject.[2-6]

Hoyer and Nolle[2], using the standard ultrasonic technique have investigated the liquid crystal-liquid transition of p-azoxyanisole (P.A.A.) and cholesteryl benzoate in a frequency range of .5 to 6 MHz. They observed almost a two order of magnitude increase in the attenuation and a 10% dip in the velocity of the sound waves at the transition. Hoyer and Nolle attributed these effects to structural relaxation[7] and were able to quantitatively interpret their results. Zvereva and Kapustin obtained similar results in the same frequency range for p,p'-nonoxybenzaltoluidine,[3] cholesteryl caprate[4] and cholesteryl caprinate.[5]

Durand and Rao[6] have extended the investigation of the liquid crystal-liquid transition to hypersonic frequencies (10 GHz) using the Brillouin scattering technique. Their investigation of cholesteryl 2-(2 ethoxy ethoxy) ethyl carbonate (CEC) showed that the sound wave became highly damped (large broadening of the Brillouin line) in the transition region, and that its velocity changed by approximately

5%. These effects appear similar to those observed at lower frequencies. However, since in this case, the liquid crystal had domain sizes comparable to the wavelength of the acoustic excitation, we suspect that these effects could be due to an increase of scattering loss induced by the small domains at the transition rather than structural relaxation.

In order to minimize the scattering loss, we should therefore choose a sample with sufficiently large domains. In this paper, we would like to report on our Brillouin scattering measurements at the liquid crystal-liquid phase transition of a thin film sample which has domain sizes approximately one hundred times greater than the wavelength of the hypersonic waves. Contrary to the results obtained by Durand and Rao,[6] we have found no anomalous behavior in the attenuation or in the velocity of the hypersonic wave at the transition.

II. EXPERIMENTAL METHODS

Figure 1 shows our experimental set-up which is similar to that of Durand and Pine's.[8] A coherent Radiation Model 52 argon laser with a 100 mW single-mode output at 5145 Å was used as the light source. The laser beam was focused on the sample by a condensing lens L_1 via a small reflecting mirror (4 × 3 mm). The sample was surrounded by a copper block which acted like a thermal reservoir and was temperature controlled to ± .01°C. The back-scattered radiation from the sample was spectrally analyzed by a combined set of a Fabry-Perot and a double monochromator. It was collected by the lens L_2, and focused on a 500 μ pinhole after passing through an I_2 absorption cell.[9] The pinhole was located at the focus of the third lens L_3. Then, the parallel rays from L_3 were incident on a piezeoelectrically scanned Fabry-Perot interferometer whose plates were λ/100 flat and had a 97.8% reflectivity. The output from the Fabry-Perot was focused by the lens L_4 on the slit of a Spex double monochromator with a bandpass of 20 cm^{-1} centered at 5145Å. Detection was accomplished using the photon counting method in conjunction with a multichannel analyzer. In this experiment the Fabry-Perot was used in a multiscanning mode to improve the signal-to-noise ratio. A sawtooth voltage applied to the piezeoelectric disks periodically scanned the mirrors, in synchronization with the scan of the multichannel analyzer. A typical spectrum was taken in about 2 minutes and consisted of 20 scans. The integration time per channel was 0.4 seconds which yielded a signal to noise ratio of 20:1. The Fabry-Perot was alligned before each run and typically had a finesse of 70 over its 1.85 cm aperture. After 20 scans the effective finesse was degraded to approximately 60 which corresponded to a

resolution of 0.016 cm^{-1} for the free spectral range of 0.960 cm^{-1} used in our experiments.

The major difficulty often encountered in Brillouin scattering experiments is in the discrimination against elastic scattering from the sample. For clean liquids and homogeneous crystals, the elastic scattering is about 100 times stronger than inelastic scattering and hence the typical discrimination factor of 1000 of a Fabry-Perot interferometer is sufficient. However, in our case the elastic scattering from the liquid crystal was about seven orders of magnitude stronger than the inelastic scattering and detection of the Brillouin signal would have been impossible without much higher discrimination. Recently, Devlin et al.[9] found that the argon laser frequency at 5145 Å can be tuned to coincide with a strong, but narrow (0.05 cm^{-1}) absorption line of I_2 vapor. One can therefore use an I_2 cell as a very effective filter for the elastically scattered light. Using such a cell at a temperature of 67°C we were able to attenuate the elastic scattering from our sample by five orders of magnitude. Unfortunately I_2 has other absorption lines nearby which may distort the Brillouin lines and make the spectral analysis more difficult. We shall discuss in detail how the observed Brillouin spectra were analyzed in the next section.

The liquid crystal sample used in our experiments was a mixture of 34% cholesteryl nonanoate, 34% cholesteryl oleyl carbonate and 32% cholesteryl chloride (by weight). This mixture was in the cholesteric phase from 20°C to 56°C with corresponding pitch in the infrared varying from 1.4u to 2.8 u. With this mixture it was relatively easy to

make thin film samples 250 u thick which appeared homogeneous and transparent to the naked eye. Under a polarizing microscope, we could however see domains of about 30 u in size. The samples were prepared by pressing a few drops of the mixture between two glass slides. Initially, the sample was hazy, but it became transparent after a few days. The chemicals were obtained from Eastman Kodak and were used without further purification.

III. RESULTS AND DATA ANALYSIS

In a liquid medium, the spectrum of Brillouin scattering has two components[10] shifted on either side of the exciting frequency ω_o by the frequency of the hypersonic excitation[11]

$$\Omega = (2\omega_o nv/c) \sin(\theta/2) \qquad (1)$$

where v is the acoustic velocity, n is the refractive index, c is the light velocity in vacuum, and θ is the angle between the directions of incident and scattered radiation. In obtaining Eq. (1), we have assumed that each wave propagating in the medium is characterized by a single wave vector. This is not quite true in cholesteric liquid crystals. There, even for waves propagating along the helical axis, each eigenmode is a linear combination of waves with wave vectors k and $k + 4\pi/p$ where p is the helical pitch of the liquid crystal.[12] However, if the wavelengths involved are far from the periodicity p/2, then the component with the wave vector $k + 4\pi/p$ in each eigenmode has a negligibly small amplitude.[12] In that limit, Eq. (1) is a very good approximation. This is the case for our experiments.

We chose to investigate Brillouin scattering in the backward direction ($\theta = \pi$), corresponding to an acoustic excitation with a frequency of approximately 10 GHz. By varying θ, we can also study the characteristics of the acoustic excitations at lower frequencies. We have not yet carried out such an experiment completely.

In Fig. 2 we show a typical Brillouin spectrum of the liquid crystal taken at room temperature. The Stokes component is distorted by the I_2 absorptions, but the anti-Stokes component, on the other hand, is in a flat region of the absorption spectrum and is undistorted.

As the temperature increases, the distortion of the Stokes component becomes greater while distortion of the anti-Stokes component remains small. We therefore chose to analyze only the anti-Stokes component and were able to determine its frequency to ± 1% and its linewidth to ± 10%.

We have measured the temperature dependence of the Brillouin shift, Ω, and the Brillouin linewidth, Γ, in the cholesteric liquid crystalline phase and through the liquid crystal-liquid phase transition. Typical values for Ω and Γ are .375 cm^{-1} and .06 cm^{-1}. The corresponding value for the acoustic velocity v deduced from Eq. (1) is 1.9×10^5 cm/sec. As the temperature of the liquid crystal increased from 20°C and through the phase transition in steps of 0.1°C. Ω gradually decreased (see Fig. 3) and Γ remained constant within the experimental error. Contrary to the results of the ultrasonic measurements[2-5] and those of Durand and Rao,[6] no anomalous change in either v or Γ was observed in the transition region (see Figs. 3 and 4).

In order to determine the frequency shift and the linewidth of the Brillouin mode accurately, it was necessary to take into account the effects of the I_2 absorption cell which we used to eliminate the elastic scattering. Let $G(\omega)$ be the true Brillouin spectrum and $T(\omega)$ is the transmissivity of the I_2 cell. Then, the observed Brillouin spectrum $S_B(\omega)$ is given by

$$S_B(\omega) = \int_{-\infty}^{\infty} I_B(\omega - \omega_o)\, T(\omega_o)\, G(\omega_o)\, d\omega_o \qquad (2)$$

where $I_B(\omega)$ is the instrumental function of the Fabry-Perot spectrometer set-up, and was obtained in our experiment by using a single-mode laser beam as the incoming source.

We are interested in knowing $G(\omega)$. To find $G(\omega)$, we must first obtain the transmissivity $T(\omega)$ of the I_2 cell. This was done by measuring the transmission of the I_2 cell with broadband radiation shining on the Fabry-Perot-spectrometer setup. The spectrometer limited the radiation to a band narrower than the free spectral range of the Fabry-Perot. If $I_T(\omega)$ is the instrumental linewidth in this measurement, the measured transmissivity $S_T(\omega)$ is related to the true transmissivity $T(\omega)$ by the equation

$$S_T(\omega) = \int_{-\infty}^{\infty} I_T(\omega - \omega_o)\, T(\omega_o)\, d\omega_o. \qquad (3)$$

Then, through deconvolution of Eqs. (2) and (3), we can find $T(\omega)$ and $G(\omega)$.

The standard technique of deconvolution is to substitute a known functional form for the spectral function and vary the parameters in the function until the integral gives a spectrum which fits well with the measured spectrum. In our case, this would be quite difficult since $T(\omega)$ does not have a known functional form. Here, we used the Fourier transform technique to deconvolve our spectra. It is well known that the Fourier transform of a convolution integral $\int_{-\infty}^{\infty} A(X - X_o)\, B(X_o)\, dX_o$ is the product of the Fourier transforms of $A(X)$ and $B(X)$.[13] Therefore, by Fourier-transforming Eqs. (2) and (3), we can find the Fourier transforms of $G(\omega)T(\omega)$ and $T(\omega)$, if the

Fourier transforms of the instrumental functions are known. Then, the inverse Fourier transforms enable us to determine the spectral functions $G(\omega)$ and $T(\omega)$ separately.

In our analysis, the instrumental functions were approximated by Airy functions. The fast Fourier transform technique was used to carry out the Fourier transformations on a 6600 Control Data computer. (See Appendix III for details.) In order to reduce random fluctuations in the spectra, an observed spectrum was first approximated by the best polynomial fit (typically a 20th-order polynomial) and then used in the analysis. Since the sharp structure of the I_2 absorption spectrum coincides with the Brillouin-Stokes frequency, the accuracy of our analysis for the Stokes component was much worse than that for the anti-Stokes component. We therefore chose to analyze only the anti-Stokes component. We were able to determine its peak position to ± 1% and its linewidth to ± 10%.

IV. DISCUSSION

Except for the gradual decrease in Ω or v with increasing temperature which is presumably due to thermal expansion, our results are quite different from those obtained in the Brillouin measurements of Durand and Rao[6] or the ultrasonic studies of Hoyer and Nolle,[2] and Zverera and Kapustin.[3-5] All these workers observed intense acoustic attenuation as well as changes in the velocity of the sound wave in the transition region.

We believe that the difference between our results and those of Durand and Rao[6] can be explained by the difference in the domain sizes of the samples in the two cases. We realize that scattering of acoustic waves by domain walls increases the damping constant of the acoustic waves. If the domain size is much larger than the mean free path or the attenuation length ℓ_α of the acoustic waves, then most of the acoustic waves excited in a domain decay away before hitting the domain walls, and hence the effect of the domain walls can be neglected. If the domain size is comparable with ℓ_α, then the effective damping constant increases as the domain size decreases. We have observed that at the liquid-crystal-to-liquid transition, the domain size of liquid crystals changes rapidly. It decreases by a factor larger than 2 in a pre-transitional region of about 3°C and then within 0.1°C of the transition, suddenly disappears. This behavior is similar to that of the order parameter.[14] In our case, the domain size in the liquid crystal phase was about 30 μm, and the attenuation length obtained from $\ell_\alpha = v/\Gamma$ was about 0.2 μm. Therefore, it is clear that we should not expect to observe any change in the acoustic damping constant due to scattering by domain walls in the pre-transition region. Since in our

experiment, the temperature was raised in steps of 0.1°C, we were also unable to resolve any change which happened within 0.1°C of the transition. In the case of Durand and Rao,[6] the domain size of their sample was about 0.2 μm, which was comparable to ℓ_α. Then, in the pre-transition region, the acoustic damping constant should increase as the domain size decreased. Finally, after the transition, the domains disappeared in the liquid phase, and the acoustic damping returned to its normal value. This explains why Durand and Rao[6] observed the anomalous increase of acoustic damping and the corresponding dispersion of acoustic velocity at the transition.

The difference between our results and those of the ultrasonic studies[2-5] can be explained by the difference in the acoustic frequencies in the two cases. The ultrasonic studies have been carried out in the frequency range of 0.5 to 15 MHZ. They typically show almost a two order-of-magnitude increase in the ultrasonic attenuation in the transition region. Away from the transition the results of Hoyer and Nolle fit the classical absorption coefficient[15] which has an ω^2 frequency dependence. However, in the transition region the acoustic attenuation appears to have a frequency dependence of $\omega^2/(1+\omega^2\tau^2)$ [16] which is characteristic of a relaxational process with τ being the relaxation time. Hoyer and Nolle suggested that this attenuation was due to structural relaxation[7] and using Frenkel's hetrophase fluctuation theory,[17] were able to explain their results fairly well.

The model of structural relaxation is based on the supposition that an increase of pressure can convert a fluid to a more compact local molecular arrangement (larger order parameter) which has a smaller specific

volume. This induced change is more pronounced at the phase transition since the pressure affects the equilibrium between the two phases. However, the response of this structural change to the pressure cannot be instantaneous, but has a finite relaxation time τ. Therefore, as a sound wave propagates in the medium, the induced change in the order parameter or in the volume lags in phase behind the pressure wave, and consequently, causes attenuation of the sound wave. The acoustic attenuation constant ξ ($= \Gamma/v$) due to structural relaxation can be written as[7,2]

$$\xi/\omega^2 = \frac{1}{2} \frac{v_\infty^2 - v_o^2}{v_o^2 v_\infty^2} \frac{\tau v(\omega)}{1 + \omega^2\tau^2} \tag{4a}$$

$$v^2(\omega) = \frac{1 + \omega^2\tau^2}{(\frac{1}{v_o})^2 + (\frac{\omega\tau}{v_\infty})^2} \tag{4b}$$

Here v_∞ is the sound velocity at very high frequencies and has no contribution from structural relaxation since the structure or volume change can not respond to a high-frequency pressure wave. v_o is the sound velocity at very low frequencies and its value depends on how the structure responds to the pressure wave. Since v_o is not very different from v_∞, the frequency dependence of $v(\omega)$ is weak and hence ξ/ω^2 is proportional to $\tau/(1+\omega^2\tau^2)$ approximately. As the medium approaches the liquid crystal-to-liquid transition, the decrease of v_o with temperature due to structural relaxation becomes large. This leads to the large acoustic attenuation and the corresponding dip in the velocity $v(\omega)$ at the transition as Hoyer and Nolle have observed.[18] From their results, they found $\tau = 3.5\times10^{-8}$ sec at the transition.

In our case, the hypersonic wave probed by the Brillouin scattering was at about 10 GHz. At such a high frequency, ξ/ω^2 should nearly vanish since we do not expect the structural relaxation time to vary much with frequency. Then, the classical acoustic attenuation, which is proportional to ω^2, should dominate. This was indeed the case. Using Eq. (4) with values of v_o, v_∞, and τ given by Hoyer and Nolle,[2] we found that in our case the linewidth of the Brillouin mode due to structural relaxation should be about 3×10^{-5} cm^{-1}, and the change of acoustic velocity at the transition is less than one part in 10^5. These effects are of course too small to be observed in the Brillouin scattering measurements.

CONCLUSIONS

We have used Brillouin scattering to study the hypersonic properties of a cholesteric mixture in the liquid crystal-liquid phase transition region. Contrary to the results of similar measurements by Durand and Rao[6] and the results of the ultrasonic studies,[2-5] we have found no anomalous change in either the velocity or the attenuation of the hypersonic waves at the transition. We realize that in the case of Durand and Rao, the anomalous change is due to acoustic scattering by the small domains in their sample, and in the case of the ultrasonic studies, it is due to structural relaxation. Neither of these mechanisms has any appreciable effect in our case.

References

1. C. W. Garland in Physical Acoustics, edited by W. P. Mason and R. N. Thurston (Academic Press, New York and London, 1970) Vol. VII, p. 51.
2. W. A. Hoyer and A. W. Nolle, J. Chem. Phys. 24, 803 (1956).
3. A. P. Kapustin and G. E. Zvereva, Soviet Physics (Crystallography) 10, 603 (1966).
4. G. E. Zvereva and A. P. Kapustin, Soviet Physics (Acoustics) 10, 97 (1964).
5. G. E. Zvereva, Soviet Physics (Acoustics) 11, 212 (1965).
6. G. Durand and D. V. G. L. Narasimha Rao, Physics Letters 27A, 455 (1968).
7. J. J. Markham, R. T. Beyer and R. B. Lindsay, Revs. Modern Phys. 23, 353 (1951); K. F. Herzfeld and T. A. Litovitz, Absorption and Dispersion of Ultrasonic Waves (Academic Press, New York and London, 1958); L. Hall, Phys. Rev. 73, 775 (1948).
8. G. E. Durand and A. S. Pine, IEEE J. Quantum Electron. 4, 523 (1968).
9. G. E. Devlin, J. L. Davis, L. Chase and S. Geschwind, Applied Phys. Letters 19, 138 (1971).
10. Actually one would expect to see four modes since viscous fluids are known to have transverse as well as longitudinal acoustic waves. (See G. I. A. Stegeman and B. P. Stoicheff, Phys. Rev. Letters 21, 202 (1968). However, the transverse modes are much weaker than the longitudinal modes and were not observed in this experiment.
11. See for example, L. D. Landau and E. M. Lifshitz, Electrodynamics of Continuous Media (Pergamon Press, Oxford, London, New York, Paris, 1960) p. 390.

12. J. W. Shelton and Y. R. Shen, Phys. Rev. Lett. 26, 538 (1971).

13. See for example, I.S. Sokolnikoff and R. M. Redheffer, Mathematics of Physics and Modern Engineering (McGraw-Hill Book Co. Inc., New York-Toronto-London, 1958), p. 488.

14. N. V. Madhusudana, R. Shashidhar and S. Chandrasekhar, Molecular Crystals and Liquid Crystals 13, 61 (1971).

15. See for example, K. F. Herzfeld and T. A. Litovitz, Absorption and Dispersion of Ultrasonic Waves (Academic Press, New York and London, 1959) p. 44.

16. It is clear that this frequency dependence can not be explained by acoustic scattering which should have an ω^4 dependence since the domains in the sample are much smaller than the ultrasonic wavelength.

17. J. Frenkel, Kinetic Theory of Liquids (Oxford University Press, New York, 1946) p. 382.

18. The relaxation time τ increases by a factor of about two at the transition. In the frequency range of interest, $\omega\tau \lesssim 1$.

FIGURE CAPTIONS

Fig. 1. Schematic of experimental setup. S-sample; L_1, L_2, L_3, L_4 - lenses with respective focal lengths of 8, 8, 31, and 15 cm; M - small mirror; I_2 - iodine absorption cell; P - 500u pinhole; FP - Fabry-Perot interferometer; SPEC- SPEX Double monochrometer; PM - EMI 9558 photomultiplier, PCE - Standard photon counting electrons; MCA - multichannel analyzer; SCAN - sawtooth generator for scanning the Fabry-Perot.

Fig. 2. A typical Brillouin spectrum of the cholesteric mixture of 34% cholesteryl nonanoate, 34% cholesteryl oleyl carbonate and 32% cholesteryl chloride taken at 20°C. The Stokes component is somewhat distorted by the I_2 absorptions but the anti-Stokes component is almost undistorted. The structure in the background is due to I_2 absorption lines.

Fig. 3. Brillouin frequency shift of the cholesteric mixture of 34% cholesteryl nonanoate, 34% cholesteryl oleyl carbonate and 32% cholesteryl chloride as a function of temperature in the liquid crystal phase and through the liquid crystal-to-liquid phase transition. The insert shows the Brillouin frequency shift in the transition region.

Fig. 4. Brillouin linewidth of the cholesteric mixture of 34% cholesteryl nonanoate, 34% cholesteryl oleyl carbonate and 32% cholesteryl chloride as a function of temperature in the liquid crystal-to-liquid transition region.

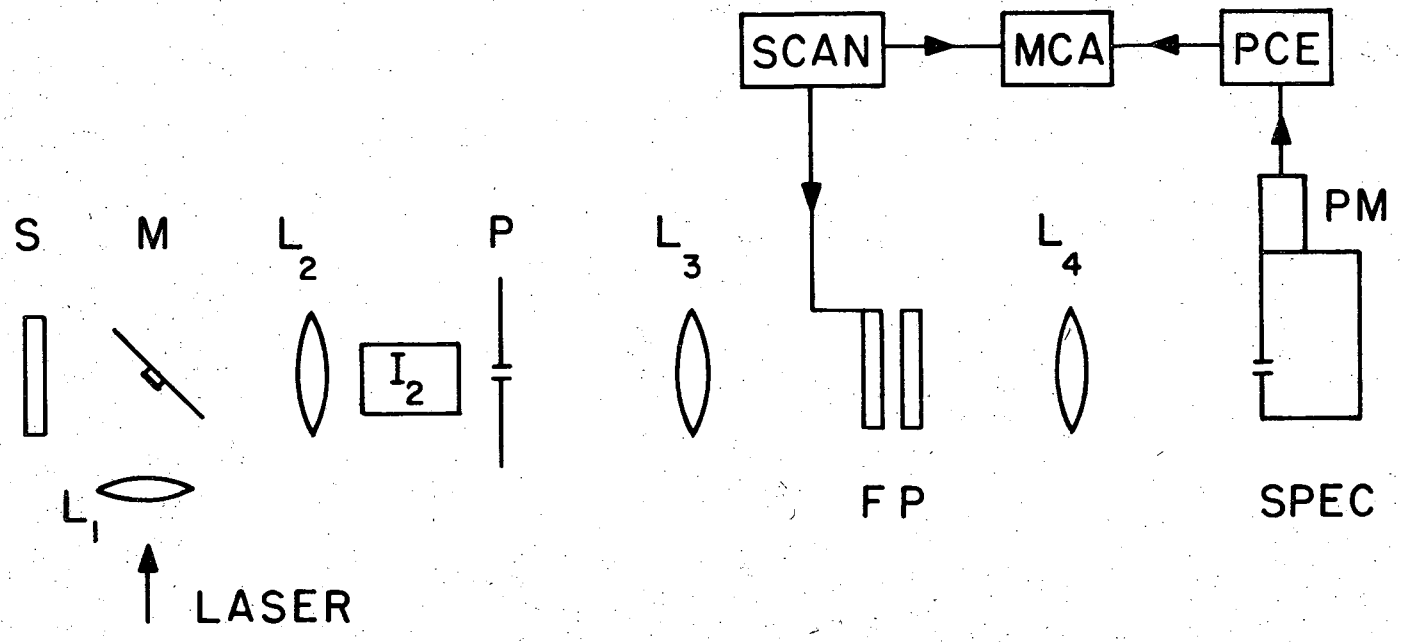

XBL 7111-1651

Fig. 1

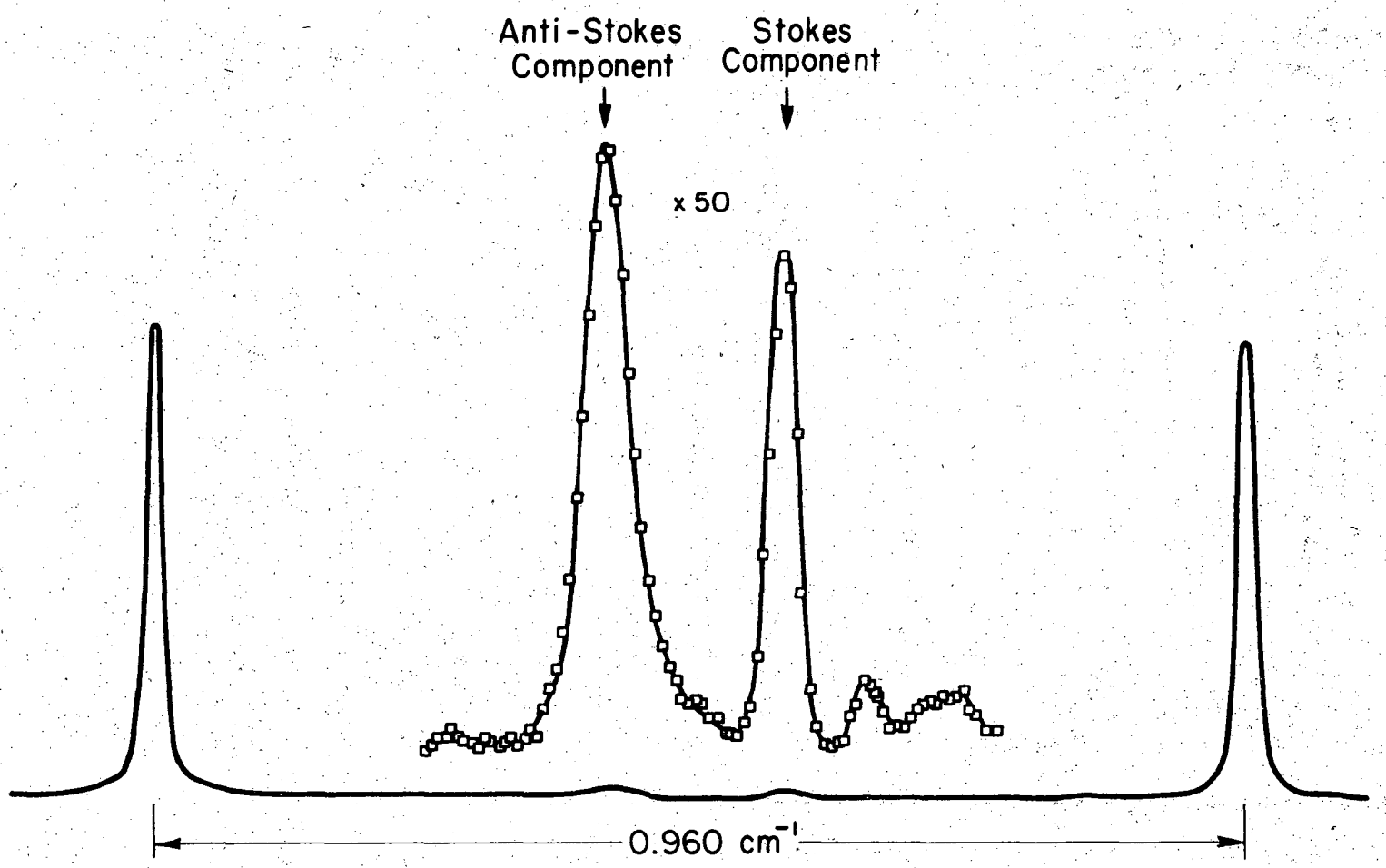
Anti-Stokes Component
Stokes Component
x 50
0.960 cm⁻¹
XBL 7111-1650

Fig. 2

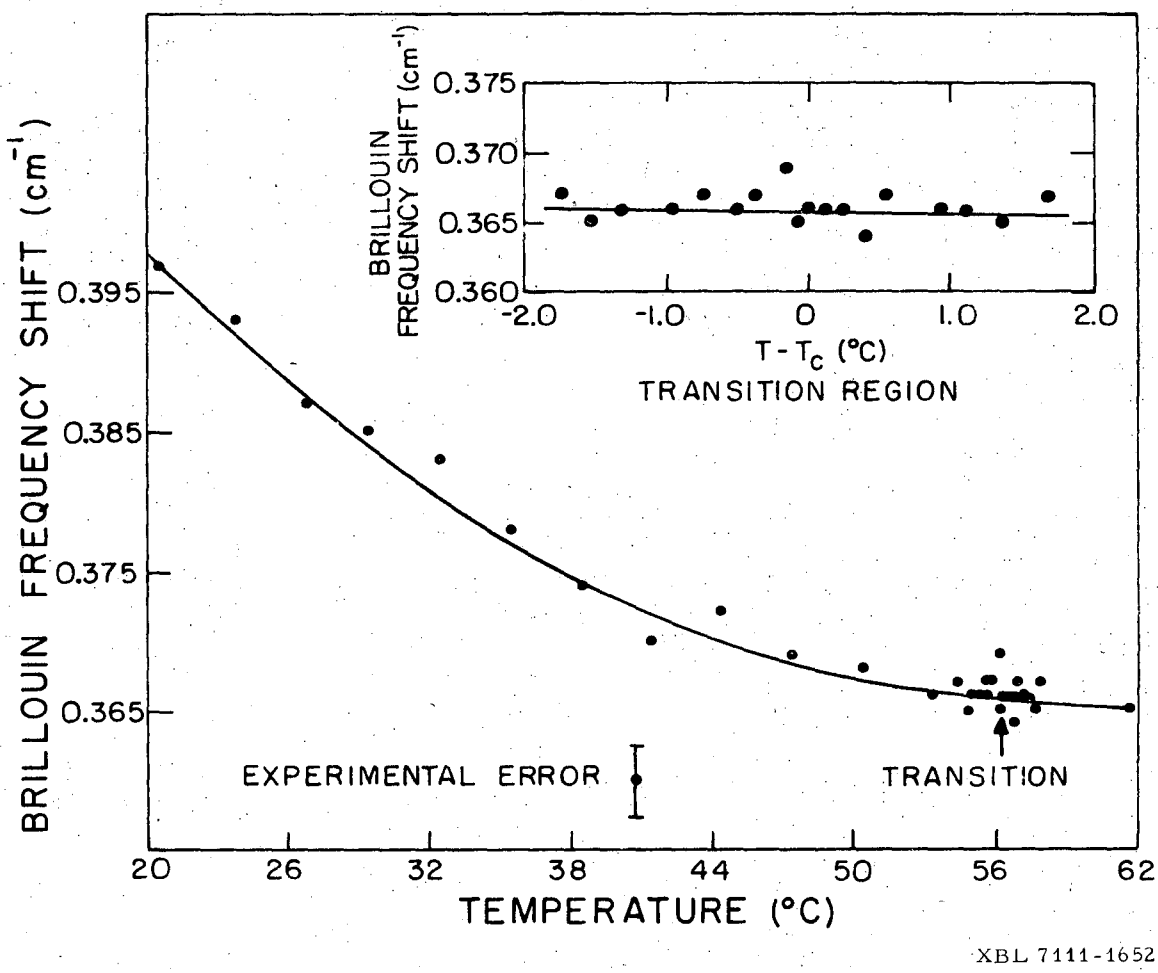

Fig. 3

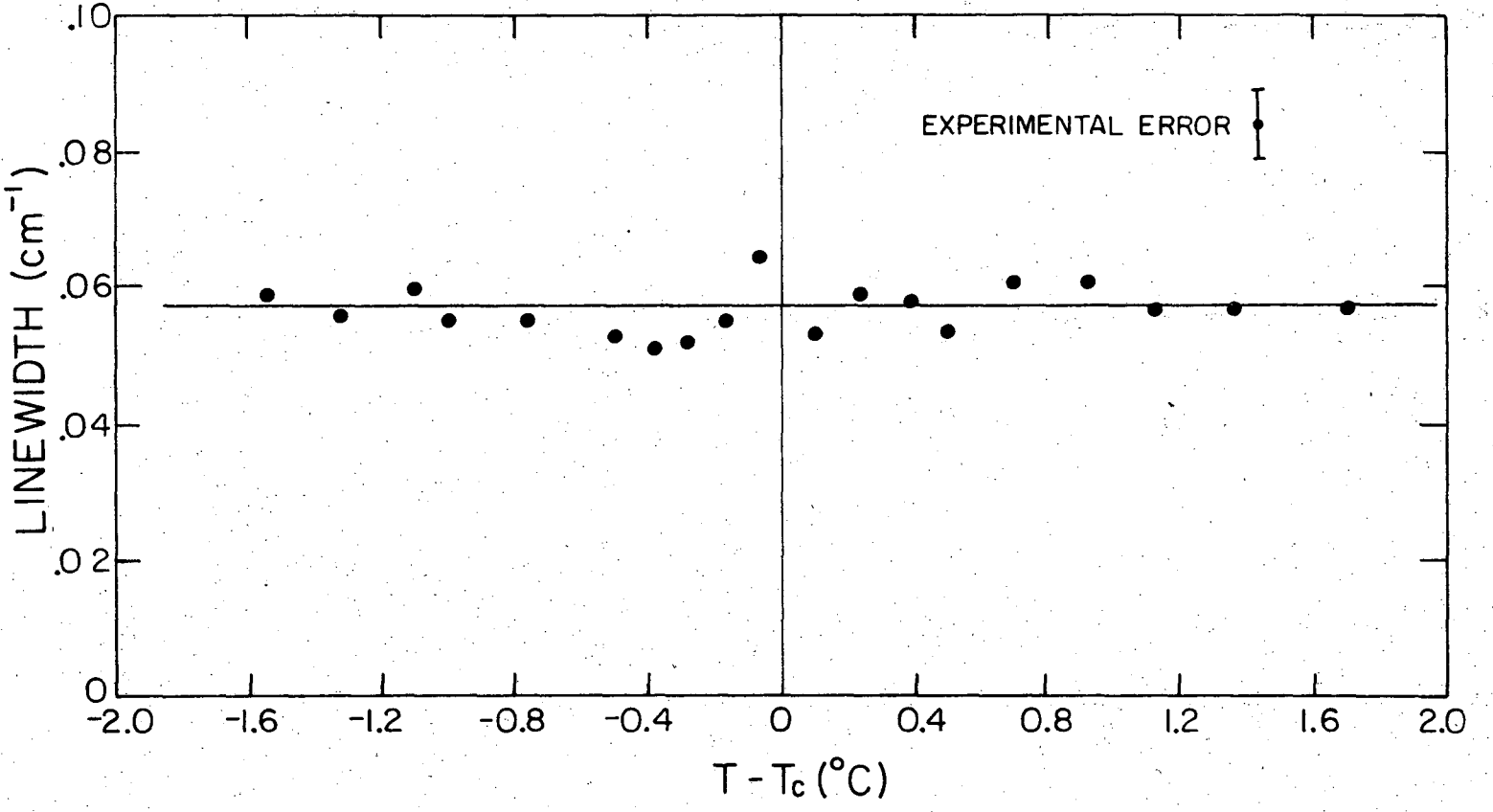

XBL 7111-1649

Fig. 4

APPENDIX I

Statistical Theory Complexes in Solution

ABSTRACT

A statistical theory of complexes in solution is presented. It takes into account the statistical distribution of all attainable complex configurations and the effect of inert solvent molecules in a solution. The formalism should be generally applicable to problems involving physical and chemical reaction in solution.

I. INTRODUCTION

When different molecular species are brought in contact with each other, molecular complexes may appear as a result of intermolecular interaction. This often happens in the process of physical or chemical reaction of the species. The subject of molecular complexes in solution has always been of great interest to many research workers. In particular, charge-transfer complexes in solution have been the subject of active research in recent years.[1]

While experimental reports on the subject of complexes in solution have been numerous, no satisfactory theory has yet been developed. The usual approach is to assume reaction equilibrium for complex formation, and then use the mass-action law to find the concentrations of complex and uncomplexed molecules. There are two obvious shortcomings of this approach. First, one usually assumes that only a few definite complex configurations exist in a solution. For each complex configuration, there is a corresponding reaction rate equation. However, it is conceivable that in a general case, many attainable complex configurations could appear with comparable probabilities. This happens particularly with weak complexes. Only in special cases, where the interaction energy is much stronger for a few complex configurations than for the others, can we consider it as a good approximation to assume the existence of only these few complex configurations. Second, one usually assumes that the equilibrium constant in the mass-action law is a constant independent of the molecular concentrations, but this is true only in the case of ideal gases.[2] Furthermore, one usually neglects, in the above approach, the effect of inert molecules present in the solution in order to simplify

the calculations.

From what we have discussed here, it is clear that the usual equilibrium approach is certainly unsatisfactory for describing weak complexes in solution, although it might be sufficient for describing strong complexes in some cases. A correct theory must take into account the statistical distribution of all attainable complex configurations[3] and the effect of inert molecules if present. It is the purpose of this paper to construct such a statistical theory, and to show that in the ideal limiting case our results agree with those obtained from the equilibrium approach. We present the general formalism in Sec. II. We then apply the formalism to the special cases of 1:1 complexes in solution and 1:1 and 1:2 complexes in solution respectively in Secs. III and IV. The theory is used to interpret the experimental results of Raman scattering from iodine complexes in solutions in the following paper.

II. GENERAL FORMALISM

Consider a solution composed of a small amount of "A" molecules dissolved in a solvent mixture of molecular species "B" and "C". In general, all the three molecular species can interact with one another, and our formalism developed in the following can account for this. However, in order to restrict our discussion to molecular complexes, we assume that only"A" molecules interact with "B" molecules to form complexes, with "C" molecules present as inert molecules interacting only weakly with both "B" and "C" molecules. For charge-transfer complexes in solution, we may have "A" molecules acting as acceptors, "B" as donors, and "C" as inert solvent molecules.

Thus, in a solution, each "A" molecule may interact with zero, one,

or more "B" molecules depending on the relative positions and orientations of the "A" molecule with the surrounding "B" molecules.[4] The strength of interaction between an "A" molecule and a "B" molecule should also be a function of the relative position and orientation of the two molecules. The inert "C" molecules, although ineffective in interacting with other molecules, may still affect the interaction of "A" and "B" molecules by shielding one from the other. This is particularly true for solutions of weak complexes, where around an "A" molecule, no specific configuration of "B" and "C" molecules dominates. Our formalism must therefore take into account all possible configurations around an "A" molecule with proper statistical average.

Let us imagine that at any instant the region around an "A" molecule can be divided into cells of equal volumes. Each cell is normally filled with zero or one molecule. The probability of a cell being occupied by more than one molecule can be neglected. Let V_o be some volume which covers the entire effective interaction volume around the "A" molecule and contains an integer number of cells of volume V_c. Then, the n "B" molecules within V_o at $\underset{\sim}{r}_1$, ---, $\underset{\sim}{r}_n$ with respect to the "A" molecule could interact with the "A" molecule and the m "C" molecules at $\underset{\sim}{R}_1$ ---$\underset{\sim}{R}_m$ within V_o could affect the interaction between the "A" molecule and the "B" molecules. (Here, the notations $\underset{\sim}{r}$ and $\underset{\sim}{R}$ are generalized to indicate not only the positions but also the relative orientations fo "B" and "C" molecules with respect to the "A" molecule.) If X represents a certain physical property of the "A" molecule, e.g., the oscillator strength of a certain uv absorption band, then since the "A" molecule is under the influence of both the "B" and "C" molecules, the

quantity X should be a function of the positions and orientations of "B" and "C" molecules in V_o,

$$X = X^{(n,m)}(\underset{\sim}{r}_1 \text{ --- } \underset{\sim}{r}_n ; \underset{\sim}{R}_1, \text{ ---} R_m). \tag{1}$$

The corresponding observed quantity should, however, be given by the statistical average over all possible configurations of "B" and "C" molecules in V_o,

$$\langle X \rangle = \sum_{n,m} \int_{V_o} X^{(n,m)}(\underset{\sim}{r}_1 \text{ --- } \underset{\sim}{r}_n ; \underset{\sim}{R}_1 \text{ ---} \underset{\sim}{R}_m) \times$$

$$\times \rho^{(n,m)} (\underset{\sim}{r}_1 \text{ ---} \underset{\sim}{r}_n ; \underset{\sim}{R}_1 \text{ ---} \underset{\sim}{R}_m) \, d\underset{\sim}{r}_1 \text{ ---} dR_m \tag{2}$$

where $\rho^{(n,m)}(\underset{\sim}{r}_1 \text{ ---} r_n ; \underset{\sim}{R}_1 \text{ ---} \underset{\sim}{R}_m)$ is the probability distribution function for the n "B" molecules at $\underset{\sim}{r}_1 \text{ ---} \underset{\sim}{r}_n$, and m "C" molecules at $\underset{\sim}{R}_1$, --- $\underset{\sim}{R}_m$, and we have the normalization condition

$$\sum_{n,m} \int_{V_o} \rho^{(n,m)} \, d\underset{\sim}{r}_1 \text{ ---} d\underset{\sim}{r}_n d\underset{\sim}{R}_1 \text{ ---} dR_m = 1.$$

From statistical mechanics, the probability distribution function $\rho^{(N,M)}(\underset{\sim}{r}_1 \text{ ---} r_N ; \underset{\sim}{R}_1 \text{ ---} \underset{\sim}{R}_M)$ for N "B" molecules and M "C" molecules in the entire solution is given by [5]

$$\rho^{(N,M)}(\underset{\sim}{r}_1 \text{ ---} r_N ; \underset{\sim}{R}_1 \text{ ---} R_M)$$

$$= [1/N!M! \; Q_{N,M}] \exp[-\beta \Phi^{(N,M)}(\underset{\sim}{r}_1 \text{ --- } \underset{\sim}{r}_N ; \underset{\sim}{R}_1 \text{ --- } \underset{\sim}{R}_M)] \tag{3}$$

where $$\beta = 1/kT$$

$$Q_{N,M} = \left(1/N!M!\right) \int_V \exp[-\beta \Phi^{(N,M)}] \, d\underset{\sim}{r}_1 \text{ ---} d\underset{\sim}{r}_N d\underset{\sim}{R}_1 \text{ --- } d\underset{\sim}{R}_M$$

and $\Phi^{(N,M)}(\underset{\sim}{r}_1 \text{ --- } \underset{\sim}{r}_N;\ \underset{\sim}{R}_1 \text{ ---} \underset{\sim}{R}_M)$ is the potential function for the particular distribution of "B" molecules at $\underset{\sim}{r}_1$ --- $\underset{\sim}{r}_N$ and M "C" molecules at $\underset{\sim}{R}_1$ --- $\underset{\sim}{R}_M$. The normalization condition for $\rho^{(N,M)}$ in a solution of volume V is

$$\int_V \rho^{(N,M)} d\underset{\sim}{r}_1 \text{ --- } d\underset{\sim}{r}_N d\underset{\sim}{R}_1 \text{ --- } d\underset{\sim}{R}_M = 1. \tag{4}$$

Then, the function $\rho^{(n,m)}$ can be derived from $\rho^{(N,M)}$ as[5]

$$\rho^{(n,m)}(\underset{\sim}{r}_1 \text{---} \underset{\sim}{r}_n;\ \underset{\sim}{R}_1 \text{---} \underset{\sim}{R}_m) = [1/(N-n)!\ (M-m)!\ n!\ m!] \times \int_{V-V_o} \rho^{(N,M)} d\underset{\sim}{r}_{n+1} \text{---} d\underset{\sim}{r}_N d\underset{\sim}{R}_{m+1} \text{---} d\underset{\sim}{R}_M. \tag{5}$$

As a simplifying assumption, we neglect the correlation between the system of molecules inside V_o and the system of molecules outside V_o. Then, the potential $\Phi^{(N,M)}$ can be written as

$$\Phi^{(N,M)} = U^{(n,m)}(\underset{\sim}{r}_1 \text{---} \underset{\sim}{r}_n;\ \underset{\sim}{R}_1 \text{---} \underset{\sim}{R}_m) + \Phi'^{(n,m)}(\underset{\sim}{r}_{n+1} \text{---} \underset{\sim}{r}_N;\ \underset{\sim}{R}_{m+1} \text{---} \underset{\sim}{R}_M) \tag{6}$$

where $U^{(n,m)}(\underset{\sim}{r}_1 \text{---} \underset{\sim}{r}_n;\ \underset{\sim}{R}_1 \text{---} \underset{\sim}{R}_m)$ is the interaction potential for the particular distribution of n "B" molecules at $\underset{\sim}{r}_1, \text{---}, \underset{\sim}{r}_n$ and m "C" molecules at $\underset{\sim}{R}_1, \text{---}, \underset{\sim}{R}_m$ in V_o, and $\Phi'^{(n,m)}$ is the remaining part of $\Phi^{(N,M)}$ depending only on coordinates of molecules outside the volume V_o. We then have, from Eq. (5),

$$\rho^{(n,m)} = \left[1/(N-n)!\ (M-m)!\ n!\ m!\right] \left(1/N!M!Q_{NM}\right) \exp[-\beta U^{(n,m)}] \times \int_{V-V_o} \exp[-\beta \Phi'^{(n,m)}] d\underset{\sim}{r}_{n+1} \text{---} d\underset{\sim}{r}_N d\underset{\sim}{R}_{m+1} \text{---} d\underset{\sim}{R}_M \tag{7}$$

where Q_{NM} can also be written in the form

$$Q_{NM} = \left(1/N!M!\right) \sum_{n,m} \left[1/(N-n)!\ (M-m)!\ n!\ m!\right]$$
$$\times \int_{V_o} \exp[-\beta U^{(n,m)}] d\underset{\sim}{r}_1 \cdots d\underset{\sim}{r}_n d\underset{\sim}{R}_1 \cdots d\underset{\sim}{R}_m$$
$$\times \int_{V-V_o} \exp[-\beta \Phi'^{(n,m)}] d\underset{\sim}{r}_{n+1} \cdots d\underset{\sim}{r}_N d\underset{\sim}{R}_{m+1} \cdots d\underset{\sim}{R}_M . \qquad (8)$$

With Eqs. (7) and (8), we can now obtain from Eq. (2) an expression for the observed quantity $\langle X \rangle$ in terms of $X^{(n,m)}$ and interaction potentials. For a specified V_o, the maximum value of (n+m) is given by (V_o/V_c). The expression for $\langle X \rangle$ can be greatly simplified if $(n+m)_{max}$ is a small number. In liquid solutions which are nearly incompressible, we can assume that each cell is occupied by one and only one molecule; the probability of being otherwise should be negligible. Then, for a specific V_o, the number (n+m) is always equal to (V_o/V_c). In the following sections, we consider the special cases of $(n+m)_{max}$ being 1 and 2. They appear as good approximation to many physical cases one encounters in practice.

III. ONE-TO-ONE COMPLEXES IN SOLUTION

Let us first consider the special case where the volume V_o is of one cell volume V_c (or $(n+m)_{max}=1$). Each "A" molecule can interact with at most one "B" molecule. This is the case for 1:1 complexes in solution. Note, however, that our picture is quite different from the usual picture of 1:1 complexes often assumed in the literature. Here, the 1:1 complexes have no definite configuration in general. The relative position and orientation of the two molecules in a complex may vary. Only in the limiting case, would a particular complex configuration dominate.

From Eq. (7), we find

$$\rho^{(1,0)}(\underset{\sim}{r}) = (N/Z)\exp[-\beta U^{(1,0)}(\underset{\sim}{r})]$$
$$\rho^{(0,1)}(\underset{\sim}{R}) = (MC_2/Z)\exp[-\beta U^{(0,1)}(\underset{\sim}{R})] \tag{9}$$

where

$$Z = C_1 + N\int_{V_o}\exp[-\beta U^{(1,0)}]\,d\underset{\sim}{r} + C_2 M\int_{V_o}\exp[-\beta U^{(0,1)}]d\underset{\sim}{R}$$

$$C_1 = \int_{V-V_o}\exp[-\beta\Phi'^{(0,0)}]d\underset{\sim}{r}_1\cdots d\underset{\sim}{R}_M/\int_{V-V_o}\exp[-\beta\Phi'^{(1,0)}]d\underset{\sim}{r}_2\cdots d\underset{\sim}{R}_M$$

$$C_2 = \int_{V-V_o}\exp[-\beta\Phi'^{(0,1)}]d\underset{\sim}{r}_1\cdots d\underset{\sim}{r}_N d\underset{\sim}{R}_2\cdots d\underset{\sim}{R}_M/\int_{V-V_o}\exp[-\beta\Phi'^{(1,0)}]d\underset{\sim}{r}_2\cdots d\underset{\sim}{R}_M.$$

To find C_1 and C_2, we notice that in the absence of the "A" molecule, we would expect $U^{(1,0)}(\underset{\sim}{r}) \approx U^{(0,1)}(\underset{\sim}{R}) = \Delta\Phi$ and we should have $(1/V_o)\int_{V_o}\rho^{(1,0)}d\underset{\sim}{r}$ $= \rho_B = N/V$ and $(1/V_o)\int_{V_o}\rho^{(0,1)}d\underset{\sim}{R} = \rho_C = M/V$. Using Eq. (9) together with these conditions, we find readily

$$C_1 = V(1-\rho_B V_o - \rho_C V_o)\exp[-\beta\langle\Delta\Phi\rangle]$$
$$C_2 = 1 \tag{10}$$

where

$$\exp[-\beta\langle\Delta\Phi\rangle] \equiv (1/V_o)\int_{V_o}\exp(-\beta\Delta\Phi)d\underset{\sim}{r}.$$

We therefore obtain, from Eqs. (2) and (9)

$$\langle X\rangle = \left\{\rho_B\int_{V_o} X^{(1,0)}\exp[-\beta(U^{(1,0)} - \langle\Delta\Phi\rangle)]d\underset{\sim}{r} +\right.$$

$$+ \rho_C \int_{V_o} X^{(0,1)} \exp[-\beta(U^{(0,1)} - \langle \Delta\Phi \rangle)] d\underset{\sim}{R} \Big\}$$

$$\times \; 1/\Big\{(1 - \rho_B V_o - \rho_C V_o) +$$

$$+ \rho_B \int_{V_o} \exp[-\beta(U^{(1,0)} - \langle \Delta\Phi \rangle)] d\underset{\sim}{r} + \rho_C \int_{V_o} \exp[-\beta(U^{(0,1)} - \langle \Delta\Phi \rangle)] d\underset{\sim}{R} \Big\} \tag{11}$$

In the case of liquid solution of constant volume V, there exists the relation $(\rho_B/\rho_{Bo}) + (\rho_C/\rho_{Co}) = 1$, with ρ_{Bo} and ρ_{Co} being the densities of pure donor and pure inert solvents respectively. If we recall that the liquid is nearly incompressible, then we expect that in the cell model every cell in the liquid should be occupied, and hence $1 - (\rho_B + \rho_C)V_o \approx 0$ in Eq. (11). Physically, we are often interested in the variation of the quantity

$$\langle \Delta X \rangle = \langle X \rangle - \langle X_C \rangle \tag{12}$$

as a function of ρ_B, where $\langle X_C \rangle$ is the value of $\langle X \rangle$ in the case of pure inert solvent ($\rho_B = 0$). In the present case, we have

$$\langle X_C \rangle = \langle X^{(0,1)} \rangle = \int_{V_o} X^{(0,1)} \exp[-\beta U^{(0,1)}] d\underset{\sim}{R} / \int_{V_o} \exp[-\beta U^{(0,1)}] d\underset{\sim}{R} \tag{13}$$

and hence from Eq. (11), we can write

$$\langle \Delta X \rangle = \frac{\rho_B \int_{V_o} [X^{(1,0)} - \langle X_C \rangle] \exp[-\beta U^{(1,0)}] d\underset{\sim}{r}}{\rho_B \int_{V_o} \exp[-\beta U^{(1,0)}] d\underset{\sim}{r} + [1 - \rho_B/\rho_{Bo}] \rho_{Co} \int_{V_o} \exp[-\beta U^{(0,1)}] d\underset{\sim}{R}} . \tag{14}$$

becomes equal to K_{eq}.

The usual equilibrium constant, K_{eq}, is obtained from the mass-action

Inversion of the above equation leads to the form

$$1/\langle \Delta X \rangle = (1/\Delta X_o) + (1/K\Delta X_o\, \rho_{Bo})(\rho_{Bo}/\rho_B) \qquad (15)$$

where

$$\Delta X_o = \int_{V_o} [X^{(1,0)} - \langle X_C \rangle] \exp[-\beta U^{(1,0)}] d\underset{\sim}{r}$$
$$\times 1/\int_{V_o} \{\exp[-\beta U^{(1,0)}] - (\rho_{Co}/\rho_{Bo}) \exp[-\beta U^{(0,1)}]\} d\underset{\sim}{r}$$

$$K = \int_{V_o} \{\exp[-\beta U^{(1,0)}] - (\rho_{Co}/\rho_{Bo}) \exp[-\beta U^{(0,1)}]\} d\underset{\sim}{r}$$
$$\times 1/\rho_{Co} \int_{V_o} \exp[-\beta U^{(0,1)}] d\underset{\sim}{r}.$$

Equation (15) is in the form of the Benesi-Hildebrand equation.[6] The quantities $\langle \Delta X \rangle$, ΔX_o, and K in Eq. (15) corresponds respectively to the observed uv extinction coefficient $\langle \varepsilon \rangle$, the uv extinction coefficient for complexes ε_C, and the equilibrium constant K_{eq} in their equation. However, the physical meanings of ΔX_o and K in our case are rather different from those of ε_C and K_{eq}. The Benesi-Hildebrand equation was originally derived using the mass-action law for 1:1 stable complexes and neglecting the effect of inert molecules. Here, from our more general model, ΔX_o corresponds to some kind of average uv extinction coefficient for complexes over the interaction volume, with the effect of inert molecules taken into account. The quantity K also depends on the presence of inert molecules, and is clearly different from K_{eq}. We can, however, show that in the ideal limiting case, K becomes equal to K_{eq}.

The usual equilibrium constant, K_{eq}, is obtained from the mass-action

law, assuming absence of inert molecules ($\rho_C = 0$),

$$K_{eq} = \rho_K/(\rho_A - \rho_K)\rho_B \tag{16}$$

for the case where the density of "B" molecules, ρ_B, is much larger than the density of "A" molecules, ρ_A. The density of complex molecules is ρ_K. From our picture, a 1:1 complex is defined as an "A" molecule with its interaction volume V_I filled by a "B" molecule. Then the complex concentration can be written as

$$\rho_K = \rho_A \int_{V_I} \rho^{(1,0)} d\underset{\sim}{r}. \tag{17}$$

With the help of Eqs. (9) and (10) (with $\rho_C = 0$), we can now find from Eqs. (17) and (16)

$$\rho_K = \frac{\rho_A\rho_B \int_{V_I} \exp[-\beta(U^{(1,0)} - \langle \Delta\Phi \rangle)]d\underset{\sim}{r}}{(1 - \rho_B V_o) + \int_{V_o} \exp[-\beta(U^{(1,0)} - \langle \Delta\Phi \rangle)]d\underset{\sim}{r}}$$

$$K_{eq} = \int_{V_I} \exp[-\beta(U^{(1,0)} - \langle \Delta\Phi \rangle)]d\underset{\sim}{r}/(1 - \rho_B V_I). \tag{18}$$

On the other hand, if we let $\rho_C = 0$ in Eq. (11), we still have Eq. (15), but with

$$\Delta X_o = \frac{\int_{V_o} \Delta X^{(1,0)} \exp[-\beta(U^{(1,0)} - \langle \Delta\Phi \rangle)]d\underset{\sim}{r}}{\int_{V_o} \{\exp[-\beta(U^{(1,0)} - \langle \Delta\Phi \rangle)] - 1\}d\underset{\sim}{r}}$$

$$K = \int_{V_o} \{\exp[-\beta(U^{(1,0)} - \langle \Delta\Phi \rangle)] - 1\}d\underset{\sim}{r}. \tag{19}$$

From Eqs. (18) and (19), we find

$$K_{eq} = (K + V_I)/(1 - \rho_B V_I) \tag{20}$$

we then recognize that in the limit $V_I \to 0$, the equilibrium constant K_{eq} reduces to K. This is just the limit of ideal gases. For non-ideal gases, $V_I \neq 0$, the mass action law leads to an equilibrium constant which depends on ρ_B as shown in Eq. (20).

In gas mixtures, we can also have ρ_C = constant, but vary ρ_B. For this case, Eq. (15) still holds if we define $\langle X_C \rangle = \langle X \rangle_{\rho_{B=0}}$. The expression for ΔX_o and K would, of course, change accordingly.

IV. ONE-TO-ONE AND ONE-TO-TWO COMPLEXES IN SOLUTION

We now apply our formalism to the case where each "A" molecule can interact with two molecules. We consider here only complexes in liquid solution. With n+m=2 in Eq. (7) and (8). An "A" molecule can interact with zero (n=0), one (n=1), or two (n=2) "B" molecules. The n=1 and n=2 cases correspond to 1:1 and 1:2 complexes respectively, but again the complexes here do not have definite configurations in general.

With two molecules in V_o, Eqs. (7) and (8) yield

$$\rho^{(2,0)}=[N(N-1)/2Z_2]\exp[-\beta U^{(2,0)}]\int_{V-V_o}\exp[-\beta\Phi'^{(2,0)}]d\underset{\sim}{r}_3\cdots d\underset{\sim}{r}_N d\underset{\sim}{R}_1\cdots d\underset{\sim}{R}_M.$$

$$\rho^{(1,1)}=[NM/Z_2]\exp[-\beta U^{(1,1)}]\int_{V-V_o}\exp[-\beta\Phi'^{(1,1)}]d\underset{\sim}{r}_2\cdots d\underset{\sim}{r}_N d\underset{\sim}{R}_2\cdots d\underset{\sim}{R}_M.$$

$$\rho^{(0,2)}=[M(M-1)/2Z_2]\exp[-\beta U^{(0,2)}]\int_{V-V_o}\exp[-\beta\Phi'^{(0,2)}]d\underset{\sim}{r}_1\cdots d\underset{\sim}{r}_N d\underset{\sim}{R}_3\cdots d\underset{\sim}{R}_M. \tag{21}$$

where

$$Z_2 = (N!M!)^2 Q_{NM}\big|_{n+m=2}.$$

Again, we are often interested in the quantity

$$\langle \Delta X \rangle = \langle X \rangle - \langle X_C \rangle$$

$$= \sum_{\substack{n,m \\ n+m=2}} \int_{V_o} [X^{(n,m)} - \langle X_C \rangle] \rho^{(n,m)} d\underset{\sim}{r}_1 \cdots d\underset{\sim}{r}_n d\underset{\sim}{R}_1 \cdots d\underset{\sim}{R}_m \qquad (22)$$

with

$$\langle X_C \rangle = \langle X^{(0,2)} \rangle = \int_{V_o} X^{(0,2)} \exp[-\beta U^{(0,2)}] d\underset{\sim}{R} d\underset{\sim}{R}'$$

$$\times 1 \Big/ \int_{V_o} \exp[-\beta U^{(0,2)}] d\underset{\sim}{R} d\underset{\sim}{R}'$$

we can obtain from Eq. (2), after some straightforward manipulation,

$$1/\langle \Delta X \rangle = [1 + a\,(\rho_B/\rho_{Bo}) + b(\rho_B/\rho_{Bo})^2]/[c(\rho_B/\rho_{Bo}) + d\,(\rho_B/\rho_{Bo})^2] \qquad (23)$$

where

$$a = 2\int_{V_o} \left\{ (\rho_{Bo}/\rho_{Co}) \exp[-\beta(U^{(1,1)} - \langle U^{(0,2)} \rangle)] - 1 \right\} d\underset{\sim}{r} d\underset{\sim}{r}'$$

$$b = \int_{V_o} \left\{ (\rho_{Bo}/\rho_{Co})^2 \exp[-\beta(U^{(2,0)} - \langle U^{(0,2)} \rangle)] \right.$$

$$\left. -2(\rho_{Bo}/\rho_{Co}) \exp[-\beta(U^{(1,1)} - \langle U^{(0,2)} \rangle)] + 1 \right\} d\underset{\sim}{r} d\underset{\sim}{r}'$$

$$c = 2\int_{V_o} \left\{ (\rho_{Bo}/\rho_{Co}[X^{(1,1)} - \langle X_C \rangle] \exp[-\beta(U^{(1,1)} - \langle U^{(0,2)} \rangle)] \right\} d\underset{\sim}{r} d\underset{\sim}{r}'$$

$$d = \int_{V_o} \left\{ (\rho_{Bo}/\rho_{Co})^2 [X^{(2,0)} - \langle X_C \rangle] \exp[-\beta(U^{(2,0)} - \langle U^{(0,2)} \rangle)] \right.$$

$$\left. -2(\rho_{Bo}/\rho_{Co})[X^{(1,1)} - \langle X_C \rangle] \exp[-\beta(U^{(1,1)} - \langle U^{(0,2)} \rangle)] \right\} d\underset{\sim}{r} d\underset{\sim}{r}' \qquad (24)$$

with $\langle U^{(0,2)} \rangle$ defined by the relation

$$\exp[-\beta\langle U^{(0,2)} \rangle] \equiv (1/V_o)^2 \int_{V_o} \exp[-\beta U^{(0,2)}] d\underset{\sim}{r} d\underset{\sim}{r}'.$$

We recall that in the present case, V_o contains two cells. It may happen that the "B" molecule in the second cell is shielded from interaction with the "A" molecule by either "B" or "C" molecule in the first cell. One would expect that if the shielding is strong, then the "B" molecule in the second cell cannot interact effectively with the "A" molecule, and our Eq. (23) should approach the Benesi-Hildebrand form of Eq. (15). In the limit where the shielding is perfect, Eq. (23) should reduce to Eq. (15). This can be seen by letting $U^{(2,0)} \to U^{(1,0)}$, $U^{(0,2)} \to U^{(0,1)}$, $X^{(2,0)} \to X^{(1,0)}$ in Eq. (24), and $U^{(1,1)} \to U^{(1,0)}$, $X^{(1,1)} \to X^{(1,0)}$ if the "B" molecule is in the first cell.

In the other limit, we assume no shielding, so that $X^{(2,0)} = 2X^{(1,1)}$ and $U^{(2,0)} = 2U^{(1,1)}$.[7] We also assume that the interaction potential between "A" and "B" is much larger than "A" and "C" ($U^{(2,0)} >> U^{(1,1)} >> U^{(0,2)}$). This is equivalent to neglecting the effect of inert molecules. By keeping only the leading terms in the expressions in Eq. (24), we can again show that Eq. (23) reduces to the Benesi-Hildebrand form of Eq. (15). Physically, these assumptions mean that the two molecules in the two cells are uncorrelated.

If we plot $1/\langle \Delta X \rangle$ vs ρ_{Bo}/ρ_B, then Eq. (15) yields a straight line, but Eq. (23) gives a curve with definite curvature. However, in practice, experimental errors of $1/\langle \Delta X \rangle$ at small ρ_B are often large, so that with the least-square fit, the discrimination between Eq. (15) and Eq. (23) is difficult, unless the curvature of Eq. (23)

is large. This happens, for example, when a and c in Eq. (23) are sufficiently small.

Recently, Deranleau[8] has derived an equation similar to our Eq. (23) for charge-transfer complexes in solution using the usual equilibrium approach. He assumes that an acceptor can interact with one or two different sites. He then sets up three rate equations for the formation of the three possible complex configurations. This enables him to calculate the average uv extinction coefficient as a function of donor concentration. His approach, however, has not taken into account the statistical distribution of complex configurations and the effect of inert solvent molecules.

V. DISCUSSION AND CONCLUSION

The main assumption in our derivation is that the molecules within the volume V_o around an "A" molecule are uncorrelated with molecules outside the volume. We believe that this is a reasonable approximation in most cases. The approximation would, of course, be better if the volume V_o contains more molecules.

We have derived from our general formalism the results of two special cases where an "A" molecule can interact with at most one and two "B" molecules respectively. We can, of course, extend the calculations to the more general case where an "A" molecule can interact with at most p "B" molecules. The general expression for $^1/\langle \Delta X \rangle$ with p molecules in V_o should be a quotient with p^{th}-order polynomials of (ρ_B/ρ_{Bo}) in both the numerator and the denominator.

What we should emphasize in our statistical theory is that we have taken into account both the statistical distribution of complex

configurations and the effect of inert solvent molecules. While our equations for $^{1}/\langle \Delta X \rangle$ vs $^{\rho}B_{o}/\rho_{B}$ appear to be the same as, or close to those of others, the physical pictures are quite different. Thus, for example, if the spectrum for a complex depends on the complex configuration, then by assuming only one complex configuration, we should find for complexes in solution two spectra, one for unassociated molecules and one for complexes. However, if there is a distribution of complex configurations, then we should find a group of spectra, one for each complex configuration, superimposed on one another according to the statistical distribution of complex configurations. A practical example is given in Sec. I, where we apply our theory to Raman scattering from iodine complexes in solutions.

REFERENCES

1. See, for example, the review articles by R. S. Mulliken and W. B. Person, Ann. Rev. Phys. Chem. 13, 107 (1962); G. Briegleb, Electronen-Donor-Acceptor-Komplexes (Springer-Verlag, Berlin, 1961); L. J. Andrews and R. M. Keefer, Molecular Complexes in Organic Chemistry (Holden-Day, Inc., San Francisco, 1964).

2. T. L. Hill, Introduction to Statistical Mechanics (Addison-Wesley Publishing, Inc., Reading, Mass. 1960), p. 276.

3. L. E. Orgel and R. S. Mulliken, J. Amer. Chem. Soc. 79, 4939 (1957).

4. Since we assume low concentration of "A" molecules, we can neglect the probability that a "B" molecule can interact simultaneously with more than one "A" molecule.

5. See, for example, J. O. Hirschfelder, C. F. Curtis, and B. B. Bird, Molecular Theory of Gases and Liquids (John Wiley and Sons, Inc., New York, 1954).

6. H. A. Benesi and J. H. Hildebrand, J. Amer. Chem. Soc. 71, 2703 (1949).

7. We let the potentials be infinite when two molecules appear in the same cell.

8. D. A. Deranleau, J. Am. Chem. Soc. 91, 4044; 91, 4050 (1969).

APPENDIX II

Photon Counting Electronics

In this appendix I will give a detailed description of the photon counting electronics[1] used in my experiments. The current pulses produced by the photon pulses from an EMI 9558A photomultiplier[2,3] cooled to dry ice temperatures were sent to amplifier which had an input impedance of 50 Ω. The negative voltage pulse developed across this impedance ranged between -1 mv to -30 mv and was approximately 25 nanasec wide. The positive output of this amplifier ranged in voltage from 100 mV to 3V and had the same width as the imput pulse. This output pulse was passed through an inverter (transformer) and then into a constant delay discriminator. The discriminator produced a constant negative output pulse which was -0.5 V high and 25 NS wide whenever the imput pulse was above a preset threshold. The threshold was chosen to optimize signal to noise (i.e. the dark current and amplifier noise had a different pulse height distribution than the signal). Typically the threshold was chosen to be 200 mv which corresponds to a setting of 600 on the discriminator dial. With this setting approximately 30% of the signal counts are lost. The output of the discriminator goes to an inverter and then to another amplifier. The positive 10 V, 50 ns output of the amplifier then goes to a Delay Gate. The width of the -4V output pulse of the Delay Gate can be adjusted from 1 μs to 1 s. For weak signals 100 counts/sec or less the delay gate can be used to improve signal to noise. For a cooled photomultiplier the dark current pulses tend to come in groups which are less than 0.1 ms long. By choosing the output pulse of the delay gate to be 1 ms or greater one can count this

group of pulses as a single pulse and therefore improve signal to noise. For example, if one choses a 1 ms setting rather than a 1 μsec setting the dark current goes down approximately by a factor of three and is typically 6 counts/sec. For normal operation, however, the 1 us setting should be used so that one can measure count rates over a large dynamic range. The output of the delay gate goes to an amplifier whose -12 V output goes into the data input of the multichannel analyzer.

References

1. For a description of photon counting technique see G. A. Morton, Applied Optics 7, 1 (1968); J. K. Nakamura and S. E. Schwarz, Applied Optics 7, 1073 (1968); R. G. Tull, Applied Optics 7, 2033 (1968).

2. For a comparison of photomultipliers for use in photon counting technique see R. Foord, R. Jones, C. J. Oliver and E. R. Pike, Applied Optics 8, 1975 (1969).

3. For Merits of photomultiplier cooling see Y. D. Harker, Jon D. Masso and David F. Edwards, Applied Physics 8, 2563 (1969).

APPENDIX III

Computer Programs for Deconvolving Spectra

In this appendix the computer programs used in my analysis of the Brillouin scattering measurements will be presented and described. In order to use the Fourier transform technique to deconvolve a spectrum it is first necessary to smooth the data. This was done using Program CRSFIT. For a given order Legendre polynomial (1-40) Program CRSFIT finds the polynomial coefficients which minimize Chi-Square for this order of fit. Chi-Square is defined as

$$\sum_{I=1}^{I = IMAX} (FIT(I)-ARG(I))^2/(DARG(I))^2$$

where ARG(I) is the value of the I^{th} data point, FIT(I) is the value of the polynomial fit for the I^{th} data point, DARG(I) is the error in the I^{th} data point and IMAX is the number of data points. In practice one simply reads in ARG(I), DARG(I), IMAX, MAXP which the maximum order of the polynomial to be fit and NCAS the number of spectra to be fit and the program will print out the polynomial coefficients which minimize Chi-Square for each order of fit up to MAXP. For the best fit at each order it will also print out Chi-Square and FIT(I). One can then either use Chi-Square tables or one's own judgment to determine which order of fit should be used.

Once the spectrum is fit to a polynomial one can use Program BRILL to deconvolve it. For Program BRILL one reads in the polynomial coefficinets, C(I), the order of the polynomial fit which is called MAXP in this program, the free spectral range of the Fabry-Perot, TCHA, and

the full width at 1/2 max of the Fabry-Perot instrumental function, WA. The output of this program will be a Cal Comp plot of the deconvolution of the polynomial fit.

Program BRILL works in the following way. The Real Fast Fourier Transform subroutine is used to find the real and imaginary parts of the Fourier transform of the polynomial fit and of an Airy Function with a finesse given by TCHA/WA. Using the fact that the Fourier transform of a convolution integral is the product of the Fourier transform of the integrands we can now determine the real and imaginary parts of the Fourier transform of the deconvolution of the polynomial fit. They are given respectively by:

$$G_1(\tau) = (S_1(\tau)I_1(\tau) + S_2(\tau)I_2(\tau))/(I_1^2(\tau) + I_2^2(\tau))$$

$$G_2(\tau) = (S_2(\tau)I_1(\tau) - S_1(\tau)I_2(\tau))/(I_1^2(\tau) + I_2^2(\tau))$$

where $S_1(\tau)$, $S_2(\tau)$ are the real and imaginary parts of the Fourier transform of the polynomial fit and $I_1(\tau)$, $I_2(\tau)$ are the real and imaginary parts of the Fourier transform of the instrumental function. We can now use the inverse Real Fast Fourier Transform Subroutine to determine the deconvolved spectrum.

PROGRAM CRSFIT

```
                PROGRAM CRSFIT (INPUT,OUTPUT,PUNCH,TAPE 2=INPUT,TAPE 3=OUTPUT,
               1TAPE 4=PUNCH)
000002          DIMENSION CHISQ(40),FIT(80),CRSEC(80),DCRSEC(80)
000002          COMMON/FIT/ARG(80),DARG(80),X(80),C(40),C2Z(40)
          C     READ NO. OF CASES TO BE FIT
000002          READ 20,NCAS
000010       20 FORMAT(I2)
          C     READ MAX ORDER OF KNOWN COEFF, MAX NO. OF PTS. TO FIT AND MAX
          C          ORDER OF POLYFIT
000010      100 READ1,NMAX,IMAX,MAXP,IFIX
000024        1 FORMAT(4I2)
000024          READ 2, (ARG(I), I=1,IMAX)
000033        2 FORMAT(16F5.1)
000033          DO 99 I=1,IMAX
000041       99  DARG(I)=1.00
000042          DO 4 I=1,IMAX
000053          X(I)=-1.0+2.0*(I-1)/(IMAX-1)
000060        4 CONTINUE
000061          JJ=1
000061          KK=1
000062          KM=IMAX
          C     FIND CHI SQUARE AND PRINT RESULTS
000064          DO 40 J=1,MAXP
000066          IF(20-J)40,11,40
000070       11 CALL POLYFIT(KK,J,IMAX)
          C     CALC. CHI SQUARE FOR THIS ORDER FIT
000073          CHISQ(J)=0.0
000075       13 DO14 I=1,KM
000077          FIT(I)=0.0
000100          DO18 N=1,J
          C     FIT(I) IS THE VALUE OF THE LTH ORDER FITTED FN AT PT X(I)
000102          AP=POLYNOM(J),N,X(I))
000105          FIT(I)=FIT(I)+C(N)*AP
000111       18 CONTINUE
000114          CHISQ(J)=CHISQ(J)+((FIT(I)-ARG(I))**2)/(DARG(I)**2)
000121       14 CONTINUE
000123          PRINT 25,PIMOM
000131       25 FORMAT(/14H LAB MOMENTUM=,F10.4)
000131          PRINT15,J
000137       15 FORMAT(19H ORDER OF THIS FIT=,I2)
000137          IDF=IMAX-J
000141          PRINT16,CHISQ(J),IDF,KM,NFICT,FUJFACT
000157       16 FORMAT(//12H CHI SQUARE=,F10.4,5X,8H D.O.F.=,I2,5X,1CH REAL PTS=,
             *  I2,5X,7H NFICT=,I2,5X,9H FUJFACT=,F10.5)
000157          DO62 L=1,J
000161          AB=C2Z(L)
000162          C2Z(L)=SQRT(AB)
000166       62 CONTINUE
000171          PRINT17,(L,C(L),C2Z(L),L=1,J)
000206       17 FORMAT(/3H L=,I2,4X,6H C(L)=,F10.4,10X,8H ZC2(L)=,F10.4)
000206          PUNCH 103,(C(L),L=1,MAXP)
000215      103 FORMAT(8F9.5)
000215          DO 10 L=1,IMAX
000217          XSEC=0.0
000220          DO 61 K=1,J
000221          Z=-1.0+2.0*(L-1)/(IMAX-1)
000230          XSEC=XSEC+C(K)*POLYNOM(KK,K,Z)
000236       61 CONTINUE
```

```
000241          PRINT 60, X(L),XSEC,ARG(L)
000252       60 FORMAT(/*X=*F10.4,10X,*XSEC=*F10.4,10X,*ARG=*F10.4)
000252       10 CONTINUE
000255       40 CONTINUE
000260          NCAS=NCAS-1
000261          IF(NCAS)102,102,100
000262      102 CONTINUE
000262          STOP
000264          END



          SUBROUTINE POLYFIT(ITYPE,IORDER,NMEAS  )
        C       S.R. POLYFIT FITS A SET OF MEASUREMENTS TO A SERIES EXPANSION
        C        OF ORDER ( IORDER) USING (LEGENDRE,ASSOC. LEGENDRE) POLYNOMIALS
        C        IF ITYPE=(1,2).
        C         THERE ARE NMEAS MEASUREMENTS-- QMEAS+/-ZQMEAS  AT ABCISSA X
        C         THE FITTED COEF. ARE C(N)+/- ZC(N)...ZC2(N) ARE ERROR SQUARE
        C          ARRAYS A,B,D ARE USED IN THE SOLUTION--SEE NOTES
        C          F(N,I) IS THE VALUE OF THE N-TH POLYNOMIAL AT X=X(I)

000005          COMMON/FIT/QMEAS(80),ZQMEAS(80),X(80),C(40),ZC2(40)
000005          DIMENSION D(40),B(40,40),SCRATCH(5080),A(40,80),F(40,80)
000005          IF(IORDER.GT.40)IORDER=40
000010          DO3 I=1,NMEAS
000012          DO3 N=1,IORDER
000013          GO TO (1,2),ITYPE
000020        1 F(N,I)=POLYNOM(ITYPE,N,X(I))
000027          GO TO 3
000032        2 F(N,I)=POLYNOM(ITYPE,N+1,X(I))
000045        3 CONTINUE
        C        FORM DRIVING TERMS AND MATRIX TO BE INVERTED
000052          DO 10 N=1,IORDER
000053          DO 11 K=1,IORDER
000061       11 B(N,K)=0.
000065       10 D(N)  =0.
000070          DO 20 I=1,NMEAS
000072          DO 15 N=1,IORDER
000073          DO 14 K=1,IORDER
000111       14 B(N,K)=B(N,K)+(F(N,I)*F(K,I))/(ZQMEAS(I)**2)
000116       15 D(N)=D(N)+(F(N,I)*QMEAS(I))/(ZQMEAS(I)**2)
000131       20 CONTINUE
000133          L=40
000133          M=1
        C        INVERT MATRIX EQN B*C=D  TO GET EXPANSION COEFFICIENTS C
000135          CALL LINIT(B,D,C,IORDER,M,DET,IEX,CNR,SINGUL,L,SCRATCH)
000150          IF(SINGUL) GO TO 30
000153          GO TO 31
000154       30 WRITE(3,1030) IORDER,ITYPE
000164     1030 FORMAT(25H FOUND SINGULAR MATRIX IN, I3,15H TH FIT OF TYPE,I2)
000166          DO 29 N=1,40
000173          C(N)=C.
000174       29 ZC2(N)=0.
000175          RETURN
        C        CALCULATE ERRORS ON COEFFICIENTS C
        C           INVERT MATRIX EQN  B(N,L)*A(L,I)=F(N,I)
000176       31 L=40
000177          CALL LINIT(B,F,A,IORDER,NMEAS,DET,IEX,CNR,SINGUL,L,SCRATCH)
000213          IF(SINGUL) GO TO 30
        C        FORM ERROR SQUARED ZC2
000216          DO 45 N=1,IORDER
000220          ZC2(N)=0.
000221          DO 40 I=1,NMEAS
000232       40 ZC2(N)=ZC2(N)+A(N,I)**2 /ZQMEAS(I)**2
000240       45 CONTINUE
000242          RETURN
000242          END
```

```
                FUNCTION POLYNOM(ITYPE,NORDER,X)
000005          DIMENSION POLY(2)
          C      NORDER=1 FOR L=0  ETC
000005          GO TO (1,2),ITYPE
          C       LEGENDRE FUNCTION
000012        1 POLY(1)=1.
000013          M=0
000014          POLY(2)=X
000015          GO TO 25
000016        2 POLY(1)=0.
000017          M=1
000020          POLY(2)=SQRT(1.-X**2)
000027       25 DO 26 J=1,2
000031          IF(NORDER.EQ.J) GO TO 27
000032          GO TO 26
000033       27 POLYNOM=POLY(J)
000035          RETURN
000036       26 CONTINUE
000040          DO 30 L=3,NORDER
000047          P=((2*L-3)*X*POLY(2)-(L+M-2)*POLY(1) )/(L-M-1)
000062          POLY(1)=POLY(2)
000063       30 POLY(2)=P
000064          POLYNOM=P
000066          RETURN
000066          END
```

```
                SUBROUTINE LINIT(A,B,X,N,M,DET,EX,CNR,SINGUL,L,SCR)                0001
000015          DIMENSION A(L,1),B(L,1),X(L,1),SCR(L,1)                            0002
          C     MOVE A AND B TO SCRATCH AREA                                       0003
000015          N=MINO(N,L)                                                        0004
000020          IF (N .LT. 1) GO TO 4                                              0005
000022          DO 3 I=1,N                                                         0006
000023          DO 1 J=1,N                                                         0007
000033          SCR(I,J)=A(I,J)                                                    0008
000034        1 CONTINUE                                                           0009
000036          IF (M .LT. 1) GO TO 3                                              0010
000043          DO 2 J=1,M                                                         0011
000057          K=2*N+4+J                                                          0012
000060          SCR(I,K)=B(I,J)                                                    0013
000066        2 CONTINUE                                                           0014
000075        3 CONTINUE                                                           0015
000100        4 CONTINUE                                                           0016
000100          CALL LINEAR(SCR(1,1),SCR(1,2*N+5),X,N,M,DET,EX,CNR,SINGUL,L      0017
                X,SCR(1,N+1),SCR(1,2*N+1),SCR(1,2*N+2),SCR(1,2*N+3),SCR(1,2*N+4))  0018
                                                                                   0019
000162          RETURN                                                             0020
000162          END
```

```
                SUBROUTINE LINEAR(A,B,X,N,M,DET,EX,CNR,SINGUL,L                  0021
               X,LU,PIVOT,Y,RES,MULT)                                            0022
      C PROCEDURE #LINEAR SYSTEM#                                                0023
      C      6600    6600    6600    6600    6600    6600    6600                0024
      C      N=ORDER, B=RH SIDES, M=NO OF RH SIDES, X=ANSWERS,                   0025
      C      (DET*10**EX)=DETERMINANT, CNR=CONDITION, SINGUL=.FALSE. IF OK.      0026
000021        INTEGER EX,PIVOT                                                   0027
000021        REAL LU ,MULT                                                      0028
000021        LOGICAL SINGUL                                                     0029
000021        DIMENSION A(L,1),B(L,1),X(L,1),LU(L,1)                             0030
             X,PIVOT(1),Y(1),RES(1),MULT(1)                                      0031
      C.....LINEAR IS BASED ON ALGORITHM 135, CACM NOVEMBER 1962 PAGE 553,       0032
      C      AS CORRECTED CACM JULY 1964 PAGE 421.                               0033
      C      IT USES CROUT#S METHOD WITH ROW EQUILIBRATION, ROW INTERCHANGES,    0034
      C      AND ITERATIVE IMPROVEMENT FOR SOLVING THE MATRIX EQUATION AX=B,     0035
      C      WHERE A IS N BY N, X AND B ARE N BY M.  IN CASE M .LE. 0, ONLY THE  0036
      C      DETERMINANT OF A IS EVALUATED.  FOR M=1, THE SUBROUTINE SOLVES A    0037
      C      SYSTEM OF LINEAR EQUATIONS IN N UNKNOWNS.  FOR M=N AND B=(THE       0038
      C      IDENTITY MATRIX), X IS SET TO THE INVERSE OF A.                     0039
      C      IF A IS NEARLY SINGULAR, #SINGUL# IS SET TO .TRUE.                  0040
      C                                                                          0041
000021        DATA EPS / O 1640777777777777777 /                                 0042
000021        SINGUL=.FALSE.                                                     0044
000021        CNR=1.0                                                            0045
000023        DET=0.0                                                            0046
000024        EXP=0                                                              0047
000025        IF ((N .GE. 1) .AND. (N .LE. L)) GO TO 1000                        0048
000036        SINGUL=.TRUE.                                                      0049
000037        RETURN                                                             0050
000037     1000 CONTINUE                                                         0051
      C                                                                          0052
      C      REMOVE APPROPRIATE FACTORS FROM THE ROWS OF A.                      0053
      C      CALL #EQUILIBRATE#                                                  0054
000037        CALL EQUILI(A,N,MULT,SINGUL,L)                                     0055
000043        IF(SINGUL) RETURN                                                  0056
      C      SAVE THE RESULT FOR COMPUTATION OF RESIDUALS DURING ITERATION.      0057
000051        DO 1002 I=1,N                                                      0058
000053        DO 1001 J=1,N                                                      0059
000063        LU(I,J)=A(I,J)                                                     0060
000064     1001 CONTINUE                                                         0061
000071     1002 CONTINUE                                                         0062
      C      DECOMPOSE THE MATRIX INTO TRIANGULAR FACTORS.                       0063
      C      CALL #CROUT#                                                        0064
000074        CALL CROUT(LU,N,PIVOT,DET,SINGUL,L)                                0065
000100        IF (SINGUL) RETURN                                                 0066
      C      EVALUATE THE DETERMINANT IN THE FORM (DET*10.0**EX)                 0067
000106        DO 1003 I=1,N                                                      0068
000117        Y(I)=LU(I,I)*MULT(I)                                               0069
000121     1003 CONTINUE                                                         0070
      C      #PRODUCT#                                                           0071
000123        DET=DET*PRODUC(Y,1,N,EX)                                           0072
      C      NOW BEGIN TO PROCESS RIGHT HAND SIDES.                              0073
000137        IF (M .LT. 1) RETURN                                               0074
000141        DO 1004 K=1,M                                                      0075
000143        RK=FLOAT(K)                                                        0076
      C      SCALE THE RIGHT HAND SIDES                                          0077
000144        DO 1005 I1=1,N                                                     0078
000154        RES(I1)=B(I1,K)/MULT(I1)                                           0079
```

```
000156          B(I1,K)=RES(I1)                                         0080
000157    1005  CONTINUE                                                0081
          C     STORE THE FIRST APPROXIMATION AND ITS NORM.             0082
000160          YNORM=0.0                                               0083
          C     CALL *SOLVE*                                            0084
000161          CALL SOLVE(LU,N,RES,PIVOT,Y,L)                          0085
000171          DO 1006 I1=1,N                                          0086
000205          YNORM=YNORM+ABS(Y(I1))                                  0087
000210          X(I1,K)=Y(I1)                                           0088
000210    1006  CONTINUE                                                0089
          C     BEGIN THE ITERATION LOOP.  THE NUMBER OF ITERATIONS IS DETERMINED  0090
          C     DURING THE FIRST ITERATION.                             0091
000211          KOUNT=1                                                 0092
000216    1012  CONTINUE                                                0093
          C     COMPUTE THE RESIDUALS OF THE SOLUTION Y.                0094
          C     CALL *RESIDUALS*                                        0095
000216          CALL RESIDU(A,N,B,K,X,RES,L)                            0096
          C     FIND NEXT INCREMENT TO THE SOLUTION                     0097
          C     CALL *SOLVE*                                            0098
000225          CALL SOLVE(LU,N,RES,PIVOT,Y,L)                          0099
          C     SET UP TERMINATION CONDITIONS                           0100
000236          IF (KOUNT .NE. 1) GO TO 1007                            0101
000244          DYNORM=0.0                                              0102
000245          DO 1008 I2=1,N                                          0103
000251          DYNORM=DYNORM+ABS(Y(I2))                                0104
000254    1008  CONTINUE                                                0105
000255          IF (DYNORM .EQ. 0.0) GO TO 1009                         0106
000261          T=YNORM/DYNORM                                          0107
          C     CNR IS AN APPROXIMATION TO THE SPECTRAL NORM OF A, WHICH IS THE  0108
          C     PRODUCT OF THE NORM OF A AND THE NORM OF A-INVERSE.  SEE  0109
          C     WILKINSON, JACM JULY 1961 PAGE 281.                     0110
000262          CNR=((RK-1.0)*CNR + 1.0/(EPS*T))/RK                     0111
000270          IF (T .GE. 2.0) GO TO 1010                              0112
000273          SINGUL = .TRUE.                                         0113
000274          RETURN                                                  0114
000274    1010  CONTINUE                                                0115
000274          LIMIT=IFIX(ALOG(EPS)/ALOG(1.0/T))                       0116
000310    1007  CONTINUE                                                0117
          C     STORE THE NEW APPROXIMATION                             0118
000310          DO 1011 I2=1,N                                          0119
000320          X(I2,K)=X(I2,K)+Y(I2)                                   0120
000322    1011  CONTINUE                                                0121
000323          KOUNT=KOUNT+1                                           0122
000325          IF (KOUNT .LE. LIMIT) GO TO 1012                        0123
000333    1009  CONTINUE                                                0124
000333    1004  CONTINUE                                                0125
000336          RETURN                                                  0126
000336          END                                                     0127
```

```
                      SUBROUTINE EQUILI(A,N,MULT,SINGUL,L)                      0128
                C PROCEDURE #EQUILIBRATE#                                       0129
                C     N=ORDER,MULT=MULTIPLIERS                                  0130
000007                REAL MULT,MX,MASK                                         0131
000007                LOGICAL SINGUL                                            0132
000007                DIMENSION A(L,1)                                          0133
                     X,MULT(1)                                                  0134
                C.....SCALING THE ROWS OF THE MATRIX (A) TO ROUGHLY THE SAME MAXIMUM  0135
                C     MAGNITUDE ALLOWS THE PROCEDURE (CROUT) TO SELECT EFFECTIVE 0136
                C     PIVOTAL ELEMENTS FOR GAUSSIAN DECOMPOSITION OF THE MATRIX.  A  0137
                C     POWER OF 2 IS USED INSTEAD OF THE ACTUAL LARGEST ELEMENT TO  0138
                C     REDUCE ROUNDING ERROR IN THE DIVISION.                    0139
                C     SEE WILKINSON, JACM JULY 1961 PAGE 284.                   0140
000007                DATA MASK / O 777740000000000000 /                        0141
000007                DO 2001 I=1,N                                             0142
000010                MX=0.0                                                    0143
                C     FIND THE LARGEST ELEMENT                                  0144
000011                DO 2002 J=1,N                                             0145
000012                IF (ABS(A(I,J)) .GT. MX) MX=ABS(A(I,J))                   0146
000020           2002 CONTINUE                                                  0147
000025                IF (MX .GT. 0.0) GO TO 2003                               0148
000033                SINGUL=.TRUE.                                             0149
000033                RETURN                                                    0150
000034           2003 CONTINUE                                                  0151
                C     NOW STORE THE MULTIPLIER AND SCALE THE ROW.                0152
000034                MULT(I)=AND(MX,MASK)                                      0153
000040                IF (MULT(I) .EQ. 1.0) GO TO 2004                          0154
000042                DO 2005 J=1,N                                             0155
000056                A(I,J)=A(I,J)/MULT(I)                                     0156
000057           2005 CONTINUE                                                  0157
000063           2004 CONTINUE                                                  0158
000063           2001 CONTINUE                                                  0159
000066                RETURN                                                    0160
000066                END                                                       0161



                      SUBROUTINE SOLVE(A,N,V,PIVOT,Y,L)                         0284
                C PROCEDURE #SOLVE#                                             0285
                C     N=ORDER, V=RH VECTOR, PIVOT=PERMUTATION VECTOR, Y=ANSWER.  0286
000010                INTEGER PIVOT,P                                           0287
000010                DIMENSION A(L,1)                                          0288
                     X,PIVOT(1),V(1),Y(1)                                       0289
                C.....PROCESSES A RH VECTOR AND THEN BACK-SOLVES FOR Y USING THE L*U  0290
                C     DECOMPOSITION PROVIDED BY (CROUT).                        0291
000010                DO 6001 K=1,N                                             0292
000011                J=PIVOT(K)                                                0293
000013                T=V(J)                                                    0294
000014                V(J)=V(K)                                                 0295
000016                KM1=K-1                                                   0296
000020                IF (KM1 .LT. 1) GO TO 6102                                0297
000022                DO 6002 P=1,KM1                                           0298
000032                T=T-A(K,P)*V(P)                                           0299
000034           6002 CONTINUE                                                  0300
000041           6102 CONTINUE                                                  0301
000041                V(K)=T                                                    0302
                C     HAVING MODIFIED V BY L-INVERSE...                         0303
000043           6001 CONTINUE                                                  0304
                C     NOW THE BACK SOLUTION FOR Y.                              0305
000045                DO 6003 NK=1,N                                            0306
000047                K=N+1-NK                                                  0307
000051                T=V(K)                                                    0308
000053                KP1=K+1                                                   0309
000054                IF (KP1 .GT. N) GO TO 6005                                0310
000057                DO 6004 P=KP1,N                                           0311
000067                T=T-A(K,P)*Y(P)                                           0312
000071           6004 CONTINUE                                                  0313
000076           6005 CONTINUE                                                  0314
000076                Y(K)=T/A(K,K)                                             0315
000103           6003 CONTINUE                                                  0316
000106                RETURN                                                    0317
000106                END                                                       0318
```

```
                      SUBROUTINE CROUT(A,N,PIVOT,SG,SINGUL,L)                    0162
                C PROCEDURE *CROUT*                                              0163
                C     N=ORDER, PIVOT=PIVOTS, SG=INTERCHANGES.                    0164
      0C0010          INTEGER PIVOT,P                                            0165
      0C0010          DOUBLE PRECISION D                                         0166
      0C0010          LOGICAL SINGUL                                             0167
      0C0010          DIMENSION A(L,1)                                           0168
                     X,PIVOT(1)                                                  0169
                C.....CROUT*S METHOD WITH ROW INTERCHANGES FOR A=L*U WITH L(K,K)=1.0.  0170
                C     (PIVOT) STORES THE PERMUTATION MATRIX.                     0171
      0C0010          SG=1.0                                                     0172
                C     K IS THE STAGE OF THE ELIMINATION.                         0173
      000011          DO 3001 K=1,N                                              0174
      000012          T=0.0                                                      0175
      000013          DO 3002 I=K,N                                              0176
                C     COMPUTE L.                                                 0177
      000015          KM1=K-1                                                    0178
      000016          D=DBLE(A(I,K))                                             0179
      000031          IF (KM1 .LT. 1) GO TO 3003                                 0180
      000033          DO 3004 P=1,KM1                                            0181
      000035          D=D-DBLE(A(I,P))*DBLE(A(P,K))                              0182
      000074   3004 CONTINUE                                                     0183
      000076   3003 CONTINUE                                                     0184
      000076          A(I,K)=SNGL(D)                                             0185
      000111          IF (ABS(A(I,K)) .LE. T) GO TO 3005                         0186
      000120          T=ABS(A(I,K))                                              0187
      000121          IMAX=I                                                     0188
      000122   3005 CONTINUE                                                     0189
      000122   3002 CONTINUE                                                     0190
      000125          IF (T .GT. 0.0) GO TO 3105                                 0191
      000127          SINGUL=.TRUE.                                              0192
      000127          RETURN                                                     0193
      000130   3105 CONTINUE                                                     0194
                C     A(IMAX,K) IS LARGEST ELEMENT IN REMAINDER OF COLUMN K.     0195
                C     INTERCHANGE ROWS IF NECESSARY.                             0196
      000130          PIVOT(K)=IMAX                                              0197
      000131          IF (IMAX .EQ. K) GO TO 3006                                0198
      000133          SG=-SG                                                     0199
      000134          DO 3007 J=1,N                                              0200
      000146          T=A(K,J)                                                   0201
      000147          A(K,J)=A(IMAX,J)                                           0202
      000150          A(IMAX,J)=T                                                0203
      000151   3007 CONTINUE                                                     0204
      000156   3006 CONTINUE                                                     0205
                C     COMPUTE A COLUMN OF MULTIPLIERS.                           0206
      000162          QUOT=1.0/A(K,K)                                            0207
      000163          KP1=K+1                                                    0208
      000164          IF (KP1 .GT. N) GO TO 3109                                 0209
      000170          DO 3008 I=KP1,N                                            0210
      000177          A(I,K)=A(I,K)*QUOT                                         0211
      000200   3008 CONTINUE                                                     0212
                C     AND COMPUTE A ROW OF U                                     0213
      000201          DO 3009 J=KP1,N                                            0214
      000207          D=DBLE(A(K,J))                                             0215
      000221          IF (KM1 .LT. 1) GO TO 3010                                 0216
      000223          DO 3011 P=1,KM1                                            0217
      000225          D=D-DBLE(A(K,P))*DBLE(A(P,J))                              0218
      000264   3011 CONTINUE                                                     0219
```

```
000266     3010 CONTINUE                                                    0220
000266          A(K,J)=SNGL(D)                                              0221
000301     3009 CONTINUE                                                    0222
000303     3109 CONTINUE                                                    0223
000303     3001 CONTINUE                                                    0224
000306          RETURN                                                      0225
000306          END                                                         0226


                REAL FUNCTION PRODUC(FACTOR,S,F,EX)                         0227
           C PROCEDURE #PRODUCT#                                            0228
           C     S=START, F=FINISH, EX=EXPONENT                             0229
000006          INTEGER S,F,EX                                              0230
000006          DIMENSION FACTOR(1)                                         0231
           C.....MULTIPLIES FACTOR(S) THROUGH FACTOR(F), CORRECTING TO PREVENT 0232
           C     OVERFLOW.  THE ABSOULTE VALUE OF THE RESULT IS BETWEEN 0.1 AND 1.0 0233
           C     AND THE EXPONENT APPEARS IN (EX).                          0234
000006          EX=0.0                                                      0235
000006          P=1.0                                                       0236
000007          IF (S .GT. F) GO TO 4008                                    0237
000013          DO 4001 I=S,F                                               0238
000014          P1=FACTOR(I)                                                0239
000015          IF (ABS(P1) .GE. 0.1) GO TO 4002                            0240
000021          P1=10.0*P1                                                  0241
000022          EX=EX-1                                                     0242
000023     4002 CONTINUE                                                    0243
000023          P=P*P1                                                      0244
000025          IF (P .NE. 0.0) GO TO 4003                                  0245
000026          EX=0                                                        0246
000026          GO TO 4008                                                  0247
000027     4003 CONTINUE                                                    0248
000027     4004 IF (ABS(P) .GE. 0.1) GO TO 4005                             0249
000033          P=P*10.0                                                    0250
000034          EX=EX-1                                                     0251
000035          GO TO 4004                                                  0252
000036     4005 CONTINUE                                                    0253
000036     4006 IF (ABS(P) .LT. 1.0) GO TO 4007                             0254
000042          P=P/10.0                                                    0255
000043          EX=EX+1                                                     0256
000044          GO TO 4006                                                  0257
000045     4007 CONTINUE                                                    0258
000045     4001 CONTINUE                                                    0259
000050     4008 CONTINUE                                                    0260
000050          PRODUC=P                                                    0261
000052          RETURN                                                      0262
000052          END                                                         0263


                SUBROUTINE RESIDU(A,N,B,K,X,RES,L)                          0264
           C PROCEDURE #RESIDUALS#                                          0265
           C     N=ORDER, B=RH SIDES, K=COLUMN OF B, X=APPROXIMATE SOLUTION, 0266
           C     RES=RESIDUALS                                              0267
000011          DIMENSION A(L,1),B(L,1),X(L,1)                              0268
                 X,RES(1)                                                   0269
000011          INTEGER P                                                   0270
000011          DOUBLE PRECISION D                                          0271
           C.....COMPUTES B(.,K)-A*X(.,K)                                   0272
000011          DO 5001 I=1,N                                               0273
000012          D=DBLE(B(I,K))                                              0274
000025          IF (N .LT. 1) GO TO 5003                                    0275
000027          DO 5002 P=1,N                                               0276
000030          D=D-DBLE(A(I,P))*DBLE(X(P,K))                               0277
000070     5002 CONTINUE                                                    0278
000072     5003 CONTINUE                                                    0279
000072          RES(I)=SNGL(D)                                              0280
000101     5001 CONTINUE                                                    0281
000103          RETURN                                                      0282
000103          END                                                         0283
```

PROGRAM BRILL

```
                      PROGRAM BRILL(INPUT,OUTPUT,PUNCH,TAPE 98,PLOT,TAPE99=PLOT)
000002   000113       DIMENSION C(43),A(100),FPA(1026),XA(1026),AM(1026),AT(1026),
                     1Z(1026),Y(100),AK(1026),ATP(120),INV(300),SA(300)
000002   000113       COMMON/CCPOOL/XMIN,XMAX,YMIN,YMAX,CCXMIN,CCXMAX,CCYMIN,CCYMAX
000002   000113       COMMON/CCFACT/FACTOR
000002   000113    10 CONTINUE
000002   000113       READ 1,KPUR,IMAX,MAXP
000014   000125     1 FORMAT(3I2)
000014   000125       IF(IMAX.LE.0.0)GO TO 18
000016   000127       READ 3,(A(I),I=1,IMAX)
000024   000135     3 FORMAT(16F5.1)
000024   000135       READ 2,(C(I),I=1,MAXP)
000033   000144     2 FORMAT(8F9.5)
000033   000144       READ 4, TCHA,WA
000043   000154     4 FORMAT(2F10.2)
000043   000154       KK=1
000044   000155       DO 75 I=1,1024
000046   000157       AM(I)=0.0
000047   000160       DO 76 L=1,MAXP
000051   000162       Z(I)=-1.0+2.0*(I-1)/1023
000057   000170    76 AM(I)=AM(I)+C(L)*POLYNOM(KK,L,Z(I))
000070   000201    75 CONTINUE
000072   000203       DO 13 I=1,512
000074   000205       AI=I
000074   000205       XA(I)=3.1416*(AI-1.0)*(IMAX-1)/(1023.0*TCHA)
000104   000215       FPA(I)=1.0/(1.0+0.40528*(TCHA*SIN(XA(I))/WA)*(TCHA*SIN(XA(I))/WA))
000115   000226    13 FPA(1025-I)=FPA(I)
000121   000232       DO 100 I=1,1026
000126   000237   100 AK(I)=I
000130   000241       CALL RFFT(9,FPA   ,INV,SA,1,IE)
000134   000245       CALL RFFT (9,AM   ,INV,SA,1,IE)
000140   000251       DO 99 I=1,1026
000146   000257       AMIN=0.01*AM(1)
000147   000260    99 IF(ABS(AM(I)).LE.AMIN)AM(I)=0.0
000154   000265       DO 16 I=1,250
000164   000275       AT(2*I-1)=(AM(2*I-1)*FPA(2*I-1)+AM(2*I)*FPA(2*I))/(FPA(2*I-1)
                     1*FPA(2*I-1)+FPA(2*I)*FPA(2*I))
000171   000302    16 AT(2*I)=(AM(2*I)*FPA(2*I-1)-AM(2*I-1)*FPA(2*I))/(FPA(2*I-1)
                     1*FPA(2*I-1)+FPA(2*I)*FPA(2*I))
000202   000313       DO 73 I=501,1026
000207   000320    73 AT(I)=0.0
000211   000322       CALL RFFT(9,AT   ,INV,SA,-1,IE)
000215   000326       CALL GRAPH(AK,AT   ,1024,15HTRUE ABSOR SPEC,6HX-AXIS,6HY-AXIS)
000221   000332       CALL RFFT (9,AM,INV,SA,-1,IE)
000225   000336       DO 77 I=1,IMAX
000236   000347    77 Y(I)=-1.0+2.0*(I-1)/(IMAX-1)
000244   000355       XMIN=-1.0
000245   000356       XMAX=1.0
000246   000357       YMIN=-10.0
000250   000361       YMAX=+60.0
000252   000363       CALL CCPLOT(Z,AM,1024,4HJOIN)
000255   000366       CALL CCPLOT(Y,A,IMAX,6HNOJOIN,80,1)
000261   000372       CALL CCNEXT
000262   000373       DO 80 I=1,103
000272   000403       K=10*I-9
000274   000405    80 ATP(I)=AT(K)
000277   000410       PUNCH 78,(ATP(I),I=1,103)
000304   000415    78 FORMAT(13F6.1)
000304   000415       GO TO 10
000305   000416    18 CALL CCEND
000306   000417       STOP
000310   000421       END
```

```
                      FUNCTION POLYNOM(ITYPE,NORDER,X)
000005    030746      DIMENSION POLY(2)
                C      NORDER=1 FOR L=0  ETC
000005    030746      GO TO (1,2),ITYPE
                C        LEGENDRE FUNCTION
000012    030753    1 POLY(1)=1.



000013    030754      M=0
000014    030755      POLY(2)=X
000015    030756      GO TO 25
000016    030757    2 POLY(1)=0.
000017    030760      M=1
000020    030761      POLY(2)=SQRT(1.-X**2)
000027    030770   25 DO 26 J=1,2
000031    030772      IF(NORDER.EQ.J) GO TO 27
000032    030773      GO TO 26
000033    030774   27 POLYNOM=POLY(J)
000035    030776      RETURN
000036    030777   26 CONTINUE
000040    031001      DO 30 L=3,NORDER
000047    031010      P=((2*L-3)*X*POLY(2)-(L+M-2)*POLY(1) )/(L-M-1)
000062    031023      POLY(1)=POLY(2)
000063    031024   30 POLY(2)=P
000064    031025      POLYNOM=P
000066    031027      RETURN
000066    031027      END



                      SUBROUTINE RFFT(M,A,INV,S,IFSET,IFERR)
000010    032743      DIMENSION A(1),L(3),INV(1),S(1)
000010    032743      DATA PI/1721 6220 7732 5042 0550 B/
000010    032743      IFERR=1
000010    032743      IF(M.GT.15.OR.M.LT.3) RETURN
000020    032753      L(1)=M
000021    032754      L(2)=0
000022    032755      L(3)=0
000022    032755      N=2**M
000026    032761      NT=2*N
000030    032763      NTM=N-2
000031    032764      P=PI/FLOAT(NT)
000033    032766      IF(IFSET.LT.0) GO TO 20
000035    032770      CALL CFFT(L,A,INV,S,IFSET,IFERR)
000037    032772      IF(IFSET.EQ.0) RETURN
000044    032777      DO  10 I=2,NTM,2
000046    033001      J=I+1
000047    033002      K=NT-I+1
000050    033003      JJ=J+1
000052    033005      KK=K+1
000053    033006      A1R=.5*(A(J)+A(K))
000056    033011      A1I=.5*(A(JJ)-A(KK))
000063    033016      A2R=.5*(A(JJ)+A(KK))
000064    033017      A2I=.5*(A(K)-A(J))
000070    033023      ARG=FLOAT(I)*P
000073    033026      C=COS(ARG)
000075    033030      D=SIN(ARG)
000103    033036      TA=A2R*C+A2I*D
000106    033041      TB=A2I*C-A2R*D
000110    033043      A(J)=A1R+TA
000112    033045      A(JJ)=-(A1I+TB)
000115    033050      A(K)=A1R-TA
000117    033052      A(KK)=A1I-TB
000122    033055   10 CONTINUE
000127    033062      TA=A(1)+A(2)
000130    033063      TB=A(1)+A(2)
```

```
000131   033064          A(1)=TA
000132   033065          A(2)=0.
000133   033066          A(NT+1)=TB
000135   033070          A(NT+2)=0.
000137   033072          RETURN
000137   033072    20    DO 30 I=2,NTM,2
000141   033074          J=I+1
000142   033075          JJ=J+1
000143   033076          K=NT-I+1
000144   033077          KK=K+1
000145   033100          A(J)=.5*A(J)
000150   033103          A(JJ)=-.5*A(JJ)
000153   033106          A(K)=.5*A(K)
000155   033110          A(KK)=-.5*A(KK)
000157   033112          A1R=A(J)+A(K)
000162   033115          A1I=A(JJ)-A(KK)
000166   033121          ARG=FLOAT(I)*P
000171   033124          C=COS(ARG)
000172   033125          D=SIN(ARG)
000210   033143          TA=A(J)-A(K)
000212   033145          TB=A(JJ)+A(KK)
000214   033147          A2R=TA*C-TB*D
000220   033153          A2I=TA*D+TB*C
000221   033154          A(J)=A1R-A2I
000223   033156          A(JJ)=A1I+A2R
000225   033160          A(K)=A1R+A2I
000226   033161          A(KK)=A2R-A1I
000230   033163    30    CONTINUE
000237   033172          A(1)=.5*A(1)
000240   033173          A(NT+1)=.5*A(NT+1)
000242   033175          A(2)=A(1)-A(NT+1)
000243   033176          A(1)=A(1)+A(NT+1)
000244   033177          CALL CFFT(L,A,INV,S,IFSET,IFERR)
000246   033201          RETURN
000247   033202          END
```

```
000010   033277          SUBROUTINE CFFT(M,A,INV,S,IFSET,IFERR)
000010   033277          DIMENSION A(1),INV(1),S(1),N(3),M(3),NP(3),W(2),W2(2),W3(2)
000010   033277          EQUIVALENCE (N1,N(1)),(N2,N(2)),(N3,N(3))
000010   033277          DATA PI/1721 6220 7732 5042 0550 8/
000010   033277       10 IF( IABS(IFSET) - 1) 900,900,12
000013   033302       12 MTT=MAX0(M(1),M(2),M(3)) -2
000022   033311          IF(MTT-1) 13,11,11
000024   033313    11    MSUM=M(1)+M(2)+M(3)
000027   033316          IF(MSUM-15) 15,15,13
000031   033320    15    ROOT2 = SQRT(2.)
000033   033322          IF (MTT-MT ) 14,14,13
000042   033331       13 IFERR=1
000043   033332          RETURN
000044   033333       14 IFERR=0
000045   033334          M1=M(1)
000046   033335          M2=M(2)
000047   033336          M3=M(3)
000051   033340          N1=2**M1
000055   033344          N2=2**M2
000061   033350          N3=2**M3
000065   033354    16    IF(IFSET) 20,18,18
000067   033356       18 NX= N1*N2*N3
000072   033361          FN = NX
000074   033363          DO 19 I = 1,NX
000107   033376          A(2*I-1) = A(2*I-1)/FN
000110   033377       19 A(2*I) = -A(2*I)/FN
000116   033405       20 NP(1)=N1*2
000120   033407          NP(2)= NP(1)*N2
000122   033411          NP(3)=NP(2)*N3
000124   033413          DO 250 ID=1,3
000126   033415          IL = NP(3)-NP(ID)
000130   033417          IL1 = IL+1
000132   033421          MI = M(ID)
000133   033422          IF (MI)250,250,30
000136   033425       30 IDIF=NP(ID)
000136   033425          KBIT=NP(ID)
000137   033426          MEV = 2*(MI/2)
000141   033430          IF (MI - MEV )60,60,40
000143   033432       40 KBIT=KBIT/2
000144   033433          KL=KBIT-2
000146   033435          DO 50 I=1,IL1,IDIF
000147   033436          KLAST=KL+I
000150   033437          DO 50 K=I,KLAST,2
000160   033447          KD=K+KBIT
000161   033450          T=A(KD)
000162   033451          A(KD)=A(K)-T
000163   033452          A(K)=A(K)+T
000165   033454          T=A(KD+1)
000166   033455          A(KD+1)=A(K+1)-T
000170   033457       50 A(K+1)=A(K+1)+T
000202   033471          IF (MI - 1)250,250,52
000204   033473       52 LFIRST =3
000205   033474          JLAST=1
000206   033475          GO TO 70
000207   033476       60 LFIRST = 2
000210   033477          JLAST=0
```

```
000211   033500        70 DO 240 L=LFIRST,MI,2
000213   033502           JJDIF=KBIT
000214   033503           KBIT=KBIT/4
000215   033504           KL=KBIT-2
000216   033505           DO 80 I=1,IL1,IDIF
000220   033507           KLAST=I+KL
000221   033510           DO 80 K=I,KLAST,2
000232   033521           K1=K+KBIT
000233   033522           K2=K1+KBIT
000234   033523           K3=K2+KBIT
000235   033524           T=A(K2)
000236   033525           A(K2)=A(K)-T
000237   033526           A(K)=A(K)+T
000240   033527           T=A(K2+1)
000241   033530           A(K2+1)=A(K+1)-T
000244   033533           A(K+1)=A(K+1)+T
000246   033535           T=A(K3)
000247   033536           A(K3)=A(K1)-T
000251   033540           A(K1)=A(K1)+T
000252   033541           T=A(K3+1)
000253   033542           A(K3+1)=A(K1+1)-T
000256   033545           A(K1+1)=A(K1+1)+T
000261   033550           T=A(K1)
000262   033551           A(K1)=A(K)-T
000263   033552           A(K)=A(K)+T
000264   033553           T=A(K1+1)
000265   033554           A(K1+1)=A(K+1)-T
000270   033557           A(K+1)=A(K+1)+T
000272   033561           R=-A(K3+1)
000273   033562           T = A(K3)
000275   033564           A(K3)=A(K2)-R
000277   033566           A(K2)=A(K2)+R
000300   033567           A(K3+1)=A(K2+1)-T
000303   033572        80 A(K2+1)=A(K2+1)+T
000320   033607           IF (JLAST) 235,235,82
000321   033610        82 JJ=JJDIF   +1
000323   033612           ILAST= IL +JJ
000325   033614           DO 85 I = JJ,ILAST,IDIF
000326   033615           KLAST = KL+I
000327   033616           DO 85 K=I,KLAST,2
000340   033627           K1 = K+KBIT
000341   033630           K2 = K1+KBIT
000342   033631           K3 = K2+KBIT
000343   033632           R =-A(K2+1)
000344   033633           T = A(K2)
000346   033635           A(K2) = A(K)-R
000350   033637           A(K) = A(K)+R
000351   033640           A(K2+1)=A(K+1)-T
000353   033642           A(K+1)=A(K+1)+T
000355   033644           AWR=A(K1)-A(K1+1)
000357   033646           AWI = A(K1+1)+A(K1)
000361   033650           R=-A(K3)-A(K3+1)
000364   033653           T=A(K3)-A(K3+1)
000366   033655           A(K3)=(AWR-R)/ROOT2
000371   033660           A(K3+1)=(AWI-T)/ROOT2
000373   033662           A(K1)=(AWR+R)/ROOT2
000376   033665           A(K1+1)=(AWI+T)/ROOT2
000401   033670           T= A(K1)
000402   033671           A(K1)=A(K)-T
000403   033672           A(K)=A(K)+T
000404   033673           T=A(K1+1)
000405   033674           A(K1+1)=A(K+1)-T
```

```
000410   033677          A(K+1)=A(K+1)+T
000412   033701          R=-A(K3+1)
000413   033702          T=A(K3)
000415   033704          A(K3)=A(K2)-R
000417   033706          A(K2)=A(K2)+R
000420   033707          A(K3+1)=A(K2+1)-T
000423   033712       85 A(K2+1)=A(K2+1)+T
000440   033727          IF(JLAST-1) 235,235,90
000442   033731       90 JJ= JJ + JJDIF
000444   033733          DO 230 J=2,JLAST
000445   033734       96 I=INV(J+1)
000447   033736       98 IC=NT-I
000451   033740          W(1)=S(IC)
000452   033741          W(2)=S(I)
000454   033743          I2=2*I
000455   033744          I2C=NT-I2
000455   033744          IF(I2C)120,110,100
000457   033746      100 W2(1)=S(I2C)
000461   033750          W2(2)=S(I2)
000463   033752          GO TO 130
000464   033753      110 W2(1)=0.
000465   033754          W2(2)=1.
000467   033756          GO TO 130
000467   033756      120 I2CC = I2C+NT
000471   033760          I2C=-I2C
000471   033760          W2(1)=-S(I2C)
000473   033762          W2(2)=S(I2CC)
000475   033764      130 I3=I+I2
000477   033766          I3C=NT-I3
000500   033767          IF(I3C)160,150,140
000502   033771      140 W3(1)=S(I3C)
000504   033773          W3(2)=S(I3)
000506   033775          GO TO 200
000507   033776      150 W3(1)=0.
000510   033777          W3(2)=1.
000512   034001          GO TO 200
000512   034001      160 I3CC=I3C+NT
000514   034003          IF(I3CC)190,180,170
000515   034004      170 I3C=-I3C
000516   034005          W3(1)=-S(I3C)
000520   034007          W3(2)=S(I3CC)
000522   034011          GO TO 200
000523   034012      180 W3(1)=-1.
000524   034013          W3(2)=0.
000525   034014          GO TO 200
000526   034015      190 I3CCC=NT+I3CC
000530   034017          I3CC = -I3CC
000530   034017          W3(1)=-S(I3CCC)
000532   034021          W3(2)=-S(I3CC)
000535   034024      200 ILAST=IL+JJ
000537   034026          DO 220 I=JJ,ILAST,IDIF
000540   034027          KLAST=KL+I
000541   034030          DO 220 K=I,KLAST,2
000552   034041          K1=K+KBIT
000553   034042          K2=K1+KBIT
000554   034043          K3=K2+KBIT
000555   034044          R=A(K2)*W2(1)-A(K2+1)*W2(2)
000560   034047          T=A(K2)*W2(2)+A(K2+1)*W2(1)
000564   034053          A(K2)=A(K)-R
000566   034055          A(K)=A(K)+R
000567   034056          A(K2+1)=A(K+1)-T
000571   034060          A(K+1)=A(K+1)+T
```

```
000573   034062          R=A(K3)*W3(1)-A(K3+1)*W3(2)
000576   034065          T=A(K3)*W3(2)+A(K3+1)*W3(1)
000602   034071          AWR=A(K1)*W(1)-A(K1+1)*W(2)
000605   034074          AWI=A(K1)*W(2)+A(K1+1)*W(1)
000611   034100          A(K3)=AWR-R
000613   034102          A(K3+1)=AWI-T
000615   034104          A(K1)=AWR+R
000617   034106          A(K1+1)=AWI+T
000621   034110          T=A(K1)
000622   034111          A(K1)=A(K)-T
000623   034112          A(K)=A(K)+T
000624   034113          T=A(K1+1)
000625   034114          A(K1+1)=A(K+1)-T
000630   034117          A(K+1)=A(K+1)+T
000632   034121          R=-A(K3+1)
000633   034122          T=A(K3)
000635   034124          A(K3)=A(K2)-R
000637   034126          A(K2)=A(K2)+R
000640   034127          A(K3+1)=A(K2+1)-T
000643   034132      220 A(K2+1)=A(K2+1)+T
000660   034147      230 JJ=JJDIF+JJ
000664   034153      235 JLAST=4*JLAST+3
000666   034155      240 CONTINUE
000671   034160      250 CONTINUE
000673   034162          NTSQ=NT*NT
000675   034164          M3MT=M3-MT
000677   034166      350 IF(M3MT) 370,360,360
000701   034170      360 IG03=1
000702   034171          N3VNT=N3/NT
000705   034174          MINN3=NT
000706   034175          GO TO 380
000707   034176      370 IG03=2
000710   034177          N3VNT=1
000711   034200          NTVN3=NT/N3
000714   034203          MINN3=N3
000715   034204      380 JJD3 = NTSQ/N3
000720   034207          M2MT=M2-MT
000722   034211      450 IF (M2MT)470,460,460
000724   034213      460 IG02=1
000725   034214          N2VNT=N2/NT
000730   034217          MINN2=NT
000731   034220          GO TO 480
000732   034221      470 IG02 = 2
000733   034222          N2VNT=1
000734   034223          NTVN2=NT/N2
000737   034226          MINN2=N2
000740   034227      480 JJD2=NTSQ/N2
000743   034232          M1MT=M1-MT
000745   034234      550 IF(M1MT)570,560,560
000747   034236      560 IG01=1
000750   034237          N1VNT=N1/NT
000753   034242          MINN1=NT
000754   034243          GO TO 580
000755   034244      570 IG01=2
000756   034245          N1VNT=1
000757   034246          NTVN1=NT/N1
000762   034251          MINN1=N1
000763   034252      580 JJD1=NTSQ/N1
000766   034255      600 JJ3=1
000767   034256          J=1
000770   034257          DO 880 JPP3=1,N3VNT
000771   034260          IPP3=INV(JJ3)
```

```
000773   034262          DO 870 JP3=1,MINN3
000774   034263          GO TO (610,620),IGO3
001002   034271      610 IP3=INV(JP3)*N3VNT
001006   034275          GO TO 630
001006   034275      620 IP3=INV(JP3)/NTVN3
001012   034301      630 I3=(IPP3+IP3)*N2
001016   034305      700 JJ2=1
001017   034306          DO 870 JPP2=1,N2VNT
001021   034310          IPP2=INV(JJ2)+I3
001023   034312          DO 860 JP2=1,MINN2
001025   034314          GO TO (710,720),IGO2
001033   034322      710 IP2=INV(JP2)*N2VNT
001037   034326          GO TO 730
001037   034326      720 IP2=INV(JP2)/NTVN2
001043   034332      730 I2=(IPP2+IP2)*N1
001047   034336      800 JJ1=1
001050   034337          DO 860 JPP1=1,N1VNT
001052   034341          IPP1=INV(JJ1)+I2
001054   034343          DO 850 JP1=1,MINN1
001056   034345          GO TO (810,820),IGO1
001064   034353      810 IP1=INV(JP1)*N1VNT
001070   034357          GO TO 830
001070   034357      820 IP1=INV(JP1)/NTVN1
001074   034363      830 I=2*(IPP1+IP1)+1
001077   034366          IF (J-I) 840,845,845
001113   034402      840 T=A(I)
001114   034403          A(I)=A(J)
001115   034404          A(J)=T
001117   034406          T=A(I+1)
001120   034407          A(I+1)=A(J+1)
001121   034410          A(J+1)=T
001122   034411      845 CONTINUE
001122   034411      850 J=J+2
001126   034415      860 JJ1=JJ1+JJD1
001135   034424      870 JJ2=JJ2+JJD2
001143   034432      880 JJ3 = JJ3+JJD3
001147   034436  890     IF(IFSET) 895,895,891
001151   034440      891 DO 892 I = 1,NX
001157   034446      892 A(2*I) = -A(2*I)
001165   034454      895 RETURN
001166   034455      900 MT=MAX0(M(1),M(2),M(3)) -2
001175   034464          IF(MT-1) 905,903,903
001177   034466  903     MT = MAX0(2,MT)
001203   034472      904 IF (MT-13)906,906,905
001206   034475      905 IFERR = 1
001207   034476          GO TO 895
001210   034477      906 IFERR=0
001211   034500          NT=2**MT
001214   034503          NTV2=NT/2
001215   034504          PFNT2=PI/FLOAT(2*NT)
001217   034506          DO 950 L=1,NT
001221   034510          S(L)=SIN(FLOAT(L)*PFNT2)
001231   034520      950 CONTINUE
001233   034522      960 MTLEXP=NTV2
001234   034523          LM1EXP=1
001235   034524          INV(1)=0
001237   034526          DO 980 L=1,MT
001240   034527          INV(LM1EXP+1) = MTLEXP
001242   034531          DO 970 J=2,LM1EXP
001250   034537          JJ=J+LM1EXP
001251   034540      970 INV(JJ)=INV(J)+MTLEXP
001254   034543          MTLEXP=MTLEXP/2
```

```
001260    034547        980 LM1Exp=LM1Exp*2
001264    034553        982 IF(IFSET)12,895,12
001266    034555            END
```

ACKNOWLEDGMENTS

I would first of all like to extend my sincere thanks to Dr. Shen for both his intelligent guidance as well as his patience and understanding through difficult times. I am also so grateful to my wife Lydia who has given me such love and support through these years. And how can I forget my good friends Nabil Amer and Arnold Schmidt who have been so understanding and helpful.

This work was done under the auspices of the U. S. Atomic Energy Commission.

TECHNICAL INFORMATION DIVISION
LAWRENCE BERKELEY LABORATORY
UNIVERSITY OF CALIFORNIA
BERKELEY, CALIFORNIA 94720